

## **Supplemental information for**

“Optical-chemical relationships for carbonaceous aerosols observed at Jeju Island, Korea with a 3-laser photoacoustic spectrometer”

B. A. Flowers, M. K. Dubey, C. Mazzoleni, E. Stone, J. Schauer, and S. W. Kim

## **Description**

The supplemental information for the above titled letter is comprised of a short description of the PASS-3 calibration method and operation, one table showing instrumental detection limits of the PASS-3, and back trajectory calculations for every deployment day during the CAPMEX field campaign. These are all 5-day back trajectories illustrating the path the air masses took to arrive at Cheju Island.

The back trajectories were calculated using the NOAA-HYSPLIT internet application,

Draxler, R. R. and Rolph, G. D. (2003), HYSPLIT (Hybrid Single-Particle Lagrangian Integrated Trajectory) Model access via NOAA ARL READY (<http://www.arl.noaa.gov/ready/hysplit4.html>). NOAA Air Resources Laboratory

### PASS-3 Performance Characteristics

Before the campaign the  $\beta_{\text{abs}}$ ,  $\beta_{\text{sca}}$ , and  $\beta_{\text{ext}}$  ( $\beta_{\text{abs}} + \beta_{\text{sca}}$ ) signals were calibrated using highly absorbing aerosols and non-absorbing (highly scattering) aerosols. The  $\beta_{\text{ext}}$  signal was calibrated using non-absorbing aerosols (from smoldering cardboard) and the laser power at 405, 532, and 781 nm and using  $\beta_{\text{ext}} = \frac{-1}{0.2486} \ln \frac{I}{I_0} \times 10^6$  [ $\text{Mm}^{-1}$ ]. Here, 0.2486 is the pathlength of the cavity in meters,  $I$  and  $I_0$  refer to the interpolated laser power over the sampling period using the laser power measured immediately before the aerosols were sampled and immediately after completely flushing the cavity with filtered air. Because  $\beta_{\text{ext}}$  for non-absorbing aerosols equals  $\beta_{\text{sca}}$ , the slope of the linear regression line for the signal measured by the scattering sensor vs.  $\beta_{\text{ext}}$  is used as a calibration factor for the  $\beta_{\text{sca}}$  measurement. The absorption coefficient ( $\beta_{\text{abs}}$ ) is calibrated in a similar manner using kerosene soot. The slope of the linear regression line for a plot of the photoacoustic absorption signal vs. ( $\beta_{\text{ext}} - \beta_{\text{sca}}$ ) is used as the calibration factor for  $\beta_{\text{abs}}$ . Further, absolute calibration of  $\beta_{\text{abs}}$  was performed using gaseous  $\text{NO}_2$  absorption at 405 and 532 nm. Nitrogen dioxide was measured independently with a commercial  $\text{NO}_x$  measurement instrument (2B Technologies, Boulder, CO.). Between 200 and 0 ppb  $\text{NO}_2$ , we measured a linear photoacoustic response at both wavelengths. The relative and absolute  $\beta_{\text{abs}}$  calibrations agree within 4% at 405 and 3% at 532 nm. The error introduced to  $\beta_{\text{sca}}$  by truncation of the scattering detection angle is found to be minimal. We compared the PASS-3  $\beta_{\text{sca}}$  to nephelometer data from ambient measurements and find linear response in all laser channels ( $m_{405} = 0.93$ ,  $R^2 = 0.97$ ;  $m_{532} = 1.01$ ,  $R^2 = 0.99$ ;  $m_{781} = 1.18$ ,  $R^2 = 0.96$ ). A manuscript describing the calibration of the instrument and its performance characteristics is in preparation (Flowers, B. A., Mazzoleni, C., Dubey, M. K., and Walker, J., *manuscript in preparation*, 2010). In the interim, details about the calibration and performance of the PASS-3 instrument can be obtained through contact with the LANL and MTU author(s).

The instrumental noise was determined by measuring  $\beta_{\text{abs}}$  and  $\beta_{\text{sca}}$  for particle free dry air at three-second intervals over several hours. Because of low  $\text{NO}_2$  and  $\text{O}_3$  concentrations in the lab and because the background absorption and scattering signals are continuously and automatically subtracted, there should be negligible absorption and scattering signals from gases, so the standard deviation of the  $\beta_{\text{abs}}$  and  $\beta_{\text{sca}}$  signals for a given signal integration time arise solely from instrumental noise sources.

Table 1. Absorption and Scattering standard deviation and integration time values obtained for particle free and absorber-free air. The values at 600 sec integration time are the instrumental noise for the  $\beta_{\text{abs}}$  and  $\beta_{\text{sca}}$  discussed in the text.

Integration time / sec.	$\lambda$ / nm	$\beta_{\text{abs}}$ / $\text{Mm}^{-1}$	$\beta_{\text{sca}}$ / $\text{Mm}^{-1}$
	405		
10		4.2	6.1
100		1.8	2.6
600		1.3	1.8
	532		
10		4.5	4.7
100		2.3	3.0
600		1.8	2.7
	781		
10		0.31	2.5
100		0.15	1.4
600		0.13	1.0

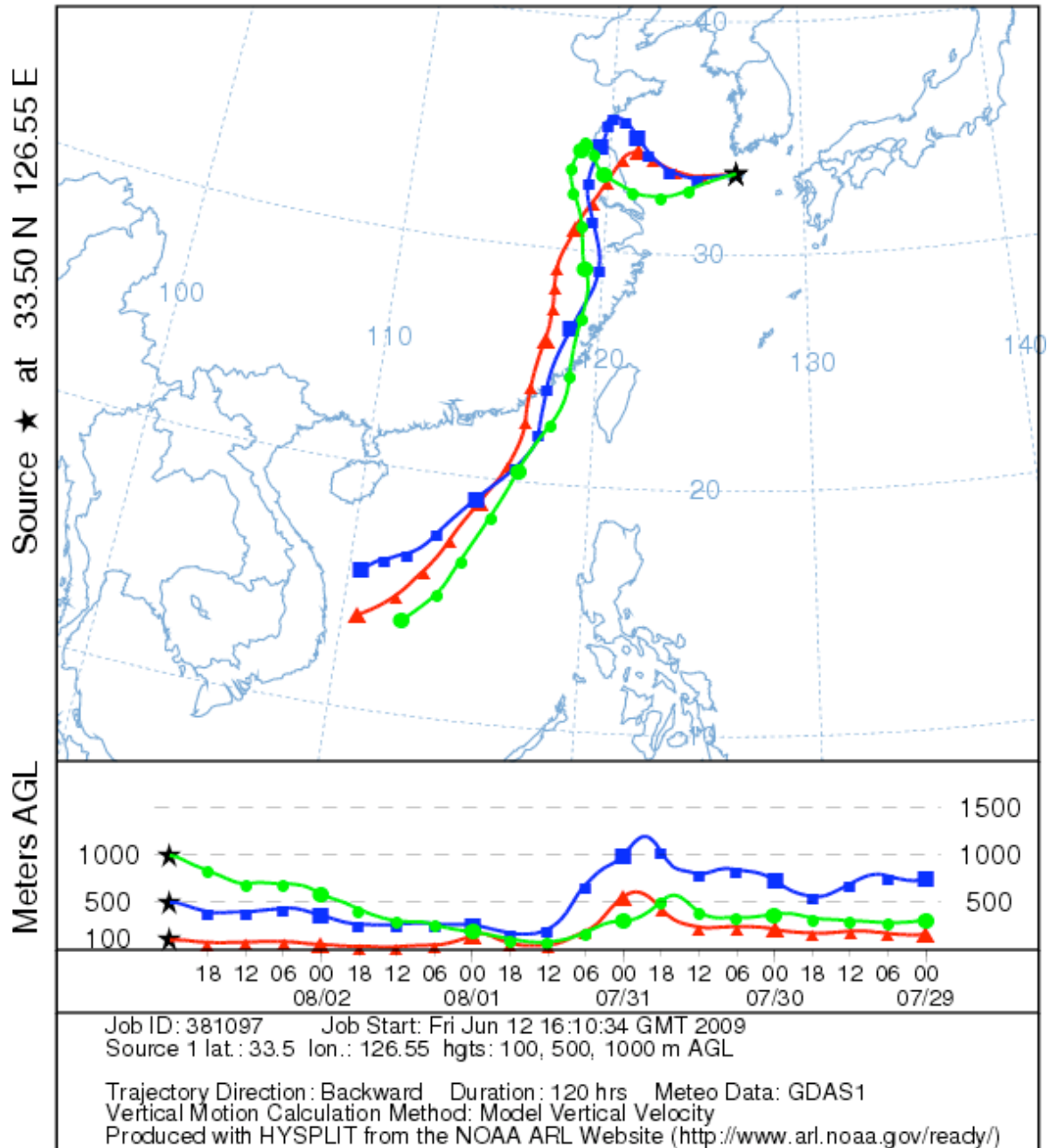
### **PASS-3 Operational Details**

The 3-laser photoacoustic soot spectrometer (PASS-3, Droplet Measurement Technologies, Inc., Boulder, CO) was used to measure aerosol absorption and scattering coefficients ( $\beta_{\text{abs}}$  and  $\beta_{\text{sca}}$ ) at Jeju. The PASS-3 uses 405, 532, and 781 nm diode lasers aligned in an acoustic resonator cavity ( $l = 2.6$  m) and measures  $\beta_{\text{abs}}$  using the photoacoustic effect and  $\beta_{\text{sca}}$  with a spherical integrating nephelometer. The lasers are modulated at three different frequencies within the acoustic resonance bandwidth and a microphone measures the acoustic signal generated from aerosol light absorption. A Lambertian diffuser mounted at the center of the acoustic resonator is used to measure light scattering integrated from  $5^\circ$ - $175^\circ$  with a cosine square weighting. As mentioned previously, the scattering angle truncation error is negligible.

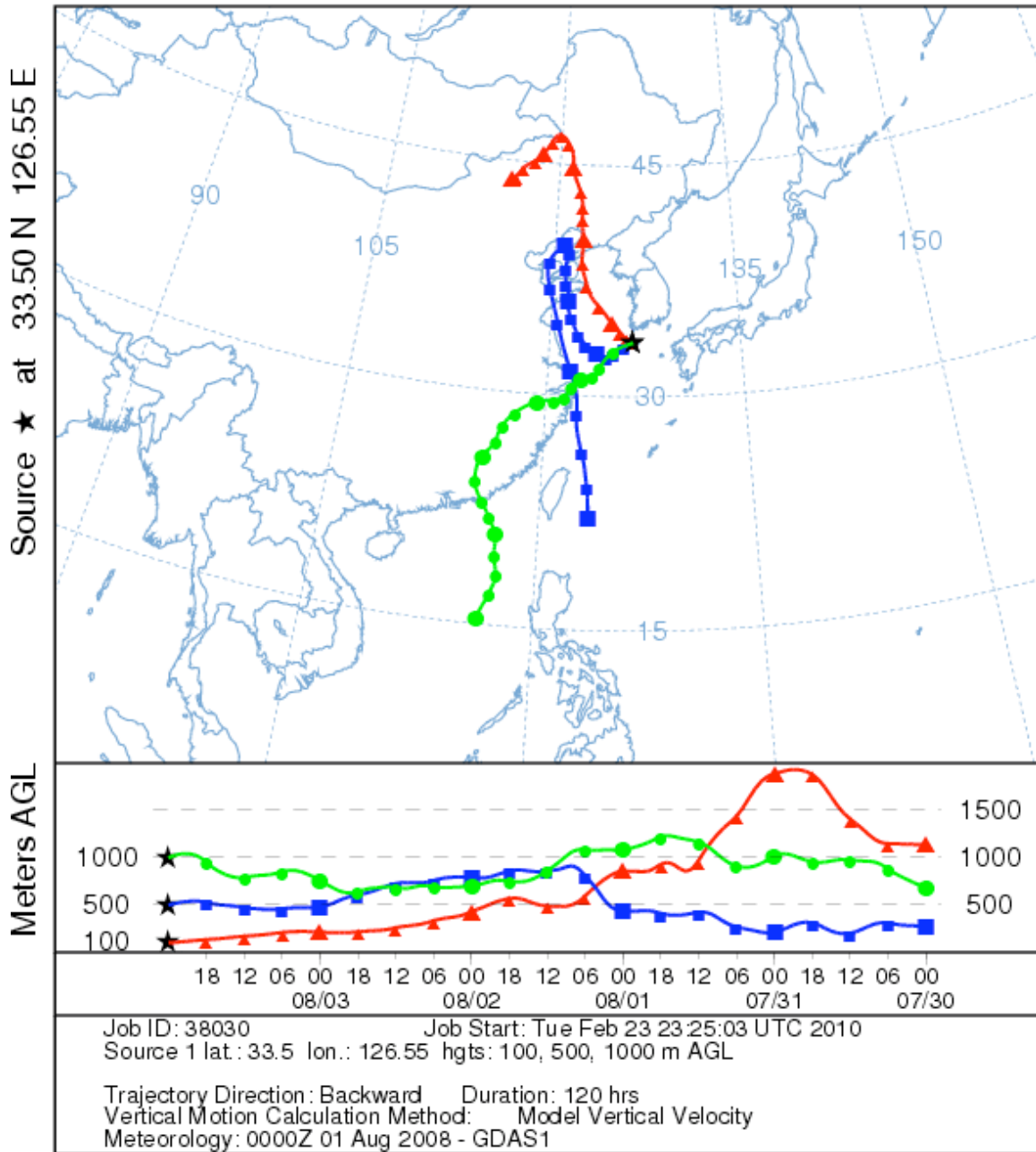
We measure *dry* aerosols sampled at  $< 25\%$  relative humidity inside the instrument. Particle-free “zeros” are taken with a duty cycle of 0.72 and interpolation of the acoustic background signal is performed between zero periods to correct for background drifts. In conjunction with “zero” measurements, an acoustic calibration is also routinely performed to lock the laser modulation to the acoustic resonance. Laser powers are continuously monitored to normalize the data. For this ground-based deployment, the background subtracted  $\beta_{\text{abs}}$  and  $\beta_{\text{sca}}$  signals were averaged into 10-minute segments, to increase the signal to noise ratio.

**Episode 1, 3 August 2008.**

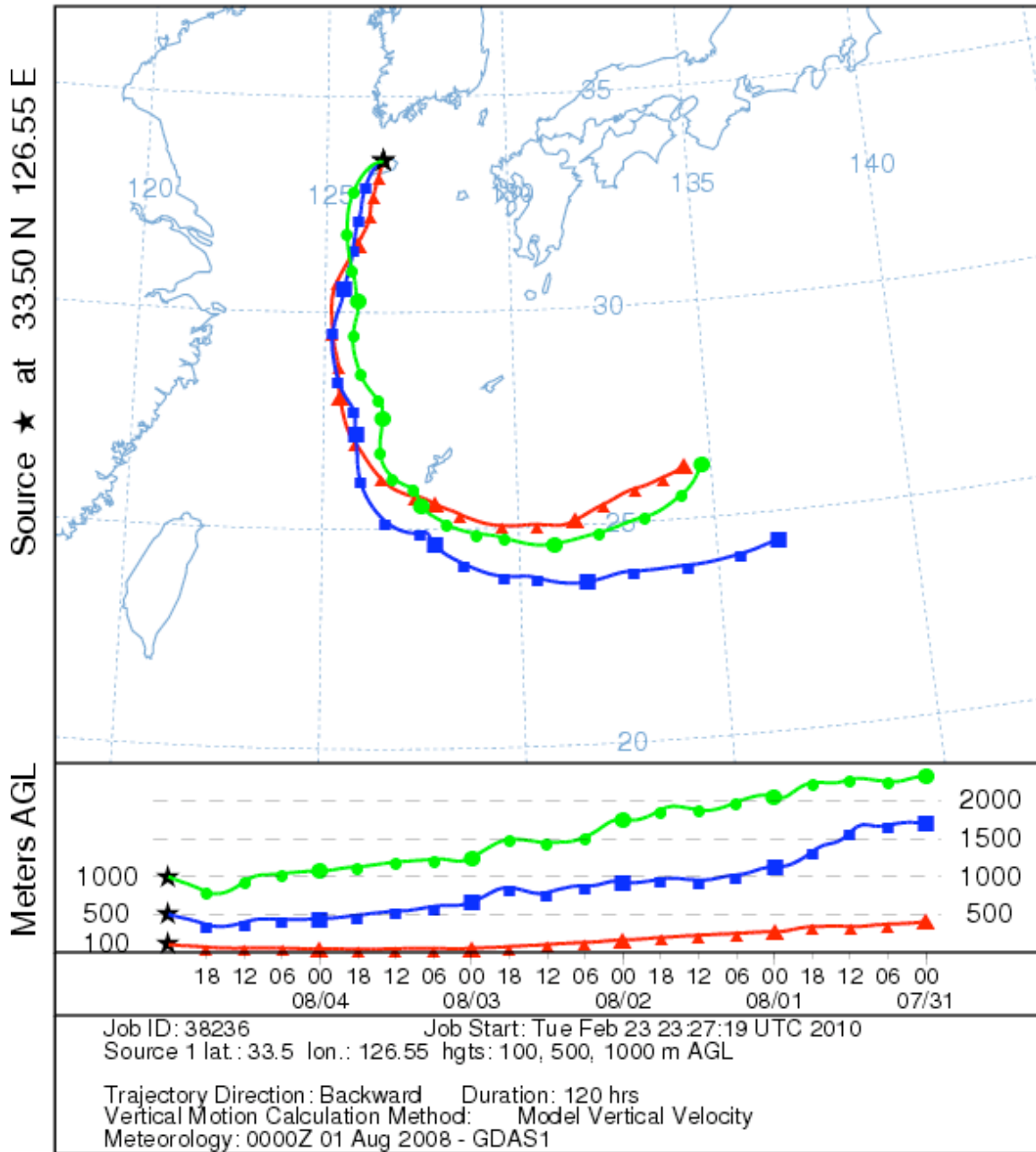
NOAA HYSPLIT MODEL  
Backward trajectories ending at 0000 UTC 03 Aug 08  
GDAS Meteorological Data



NOAA HYSPLIT MODEL  
 Backward trajectories ending at 0000 UTC 04 Aug 08  
 GDAS Meteorological Data



NOAA HYSPLIT MODEL  
 Backward trajectories ending at 0000 UTC 05 Aug 08  
 GDAS Meteorological Data

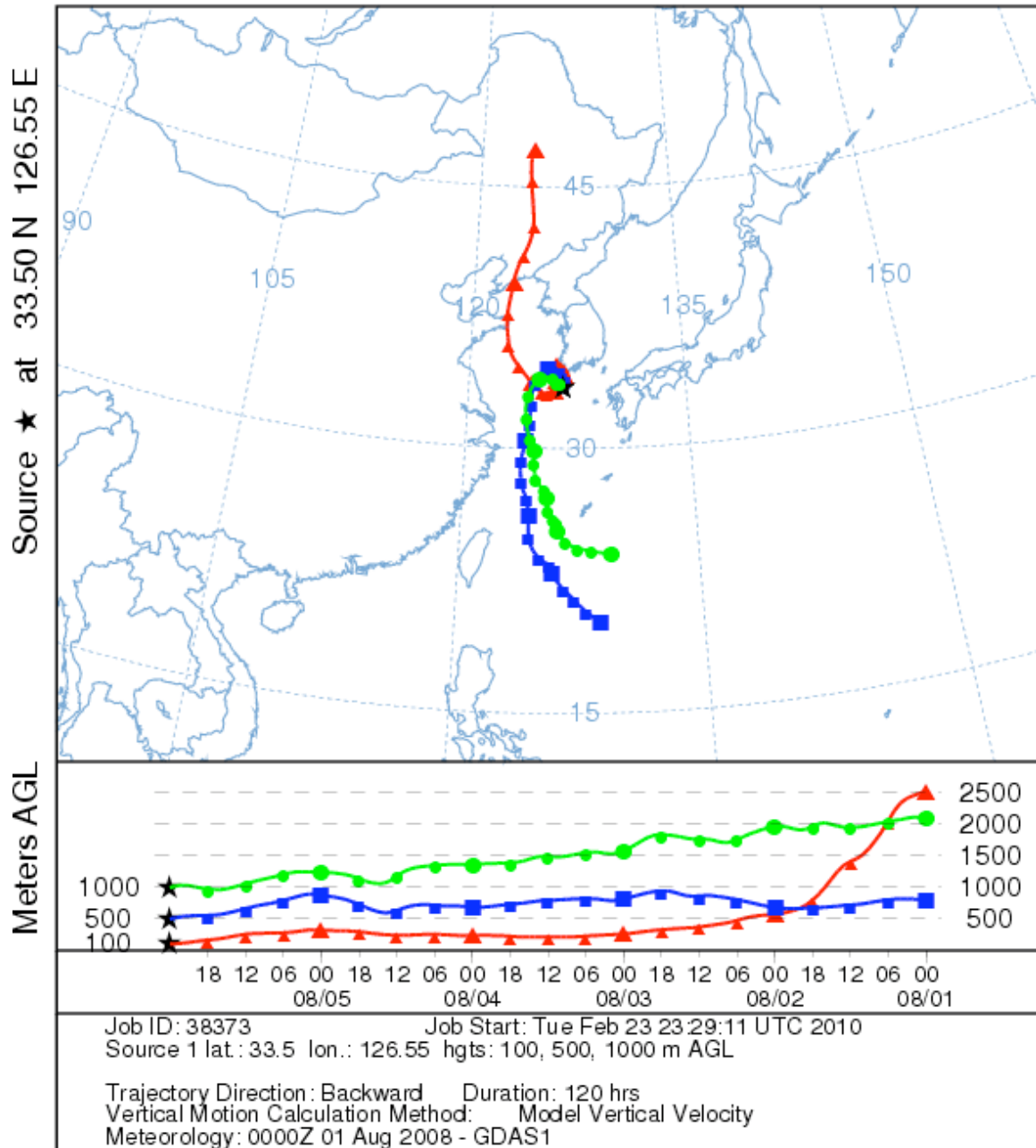


**Episode 2, 06-08 August 2008.**

NOAA HYSPLIT MODEL

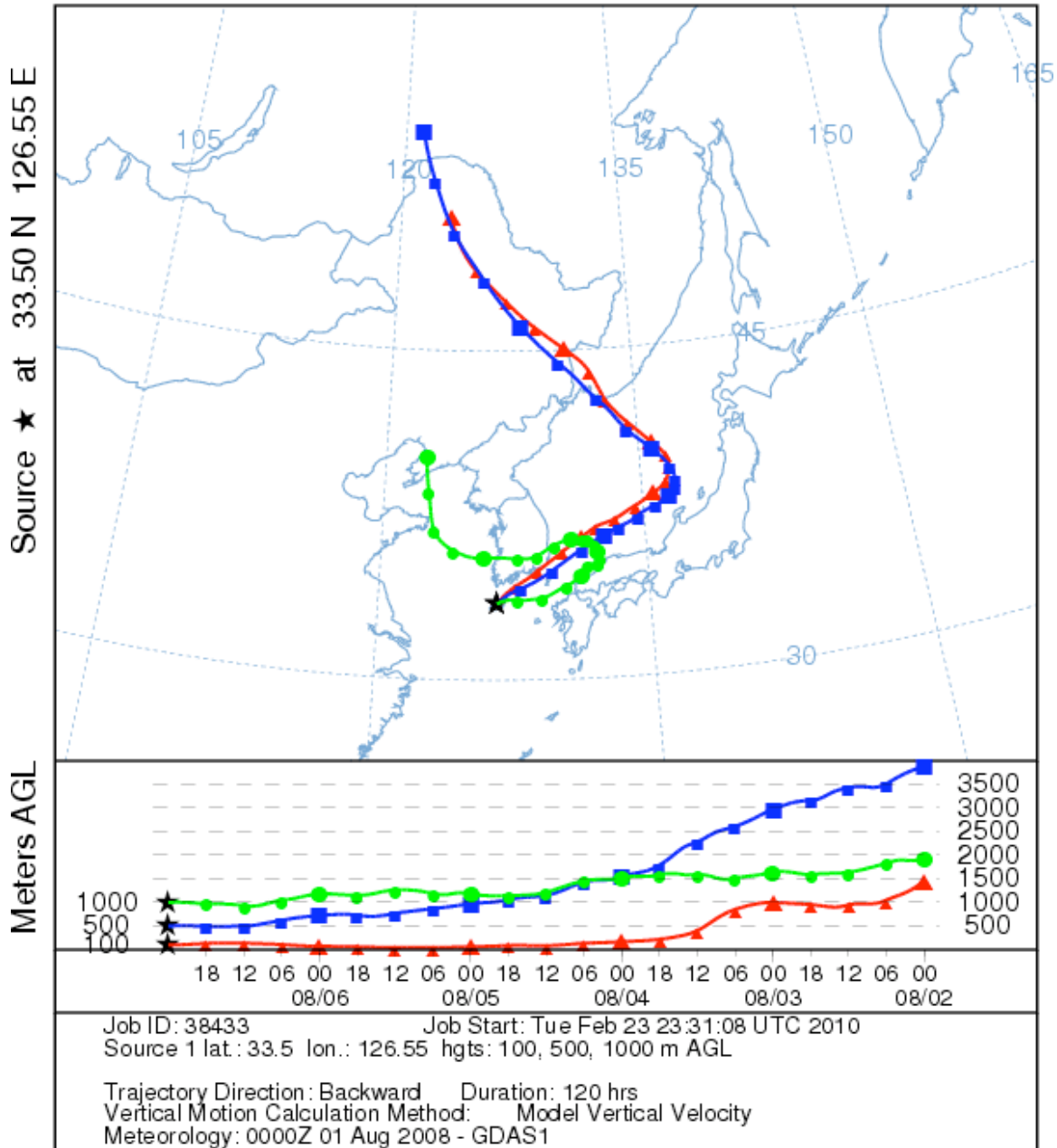
Backward trajectories ending at 0000 UTC 06 Aug 08

GDAS Meteorological Data

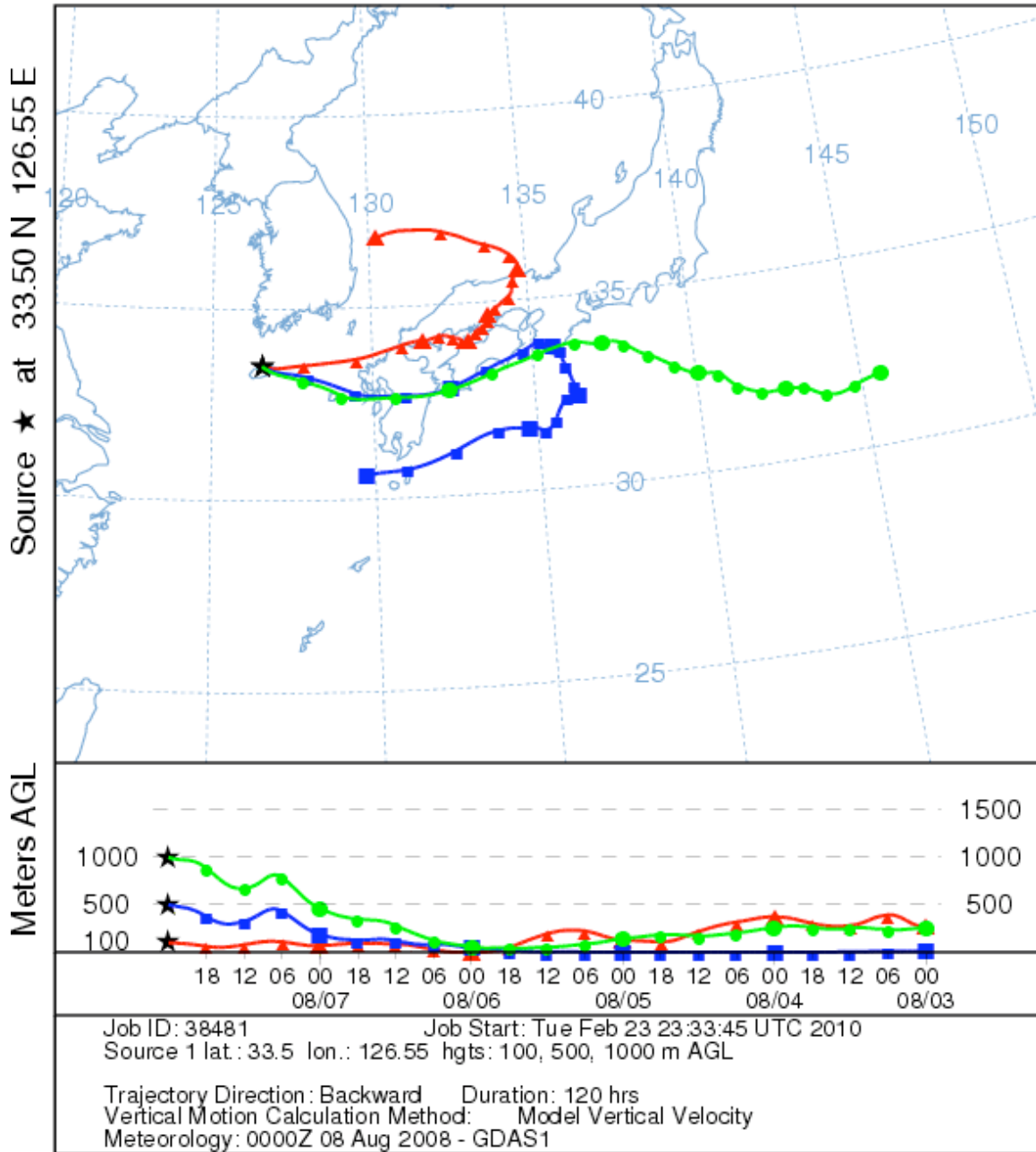




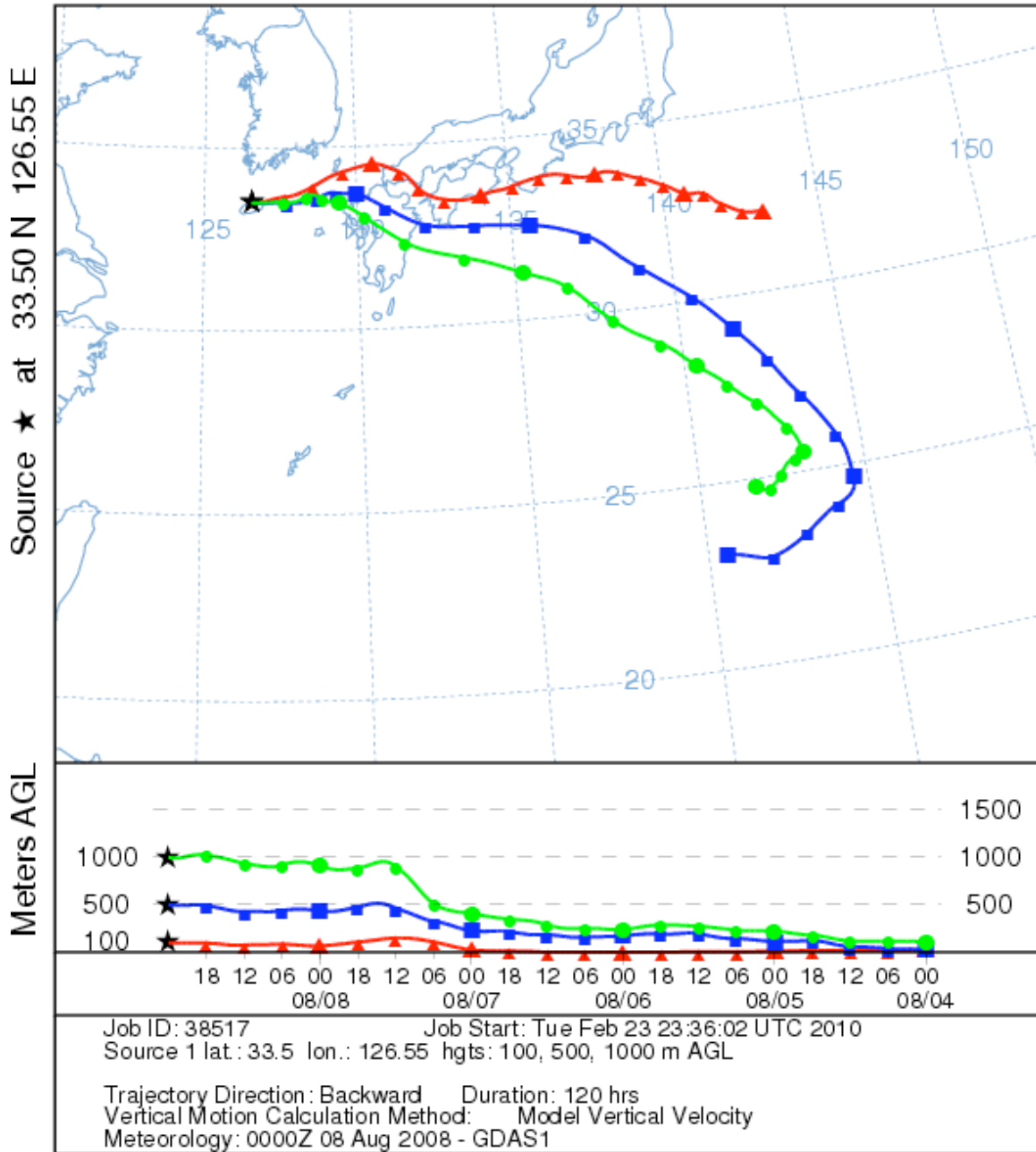
NOAA HYSPLIT MODEL  
 Backward trajectories ending at 0000 UTC 07 Aug 08  
 GDAS Meteorological Data



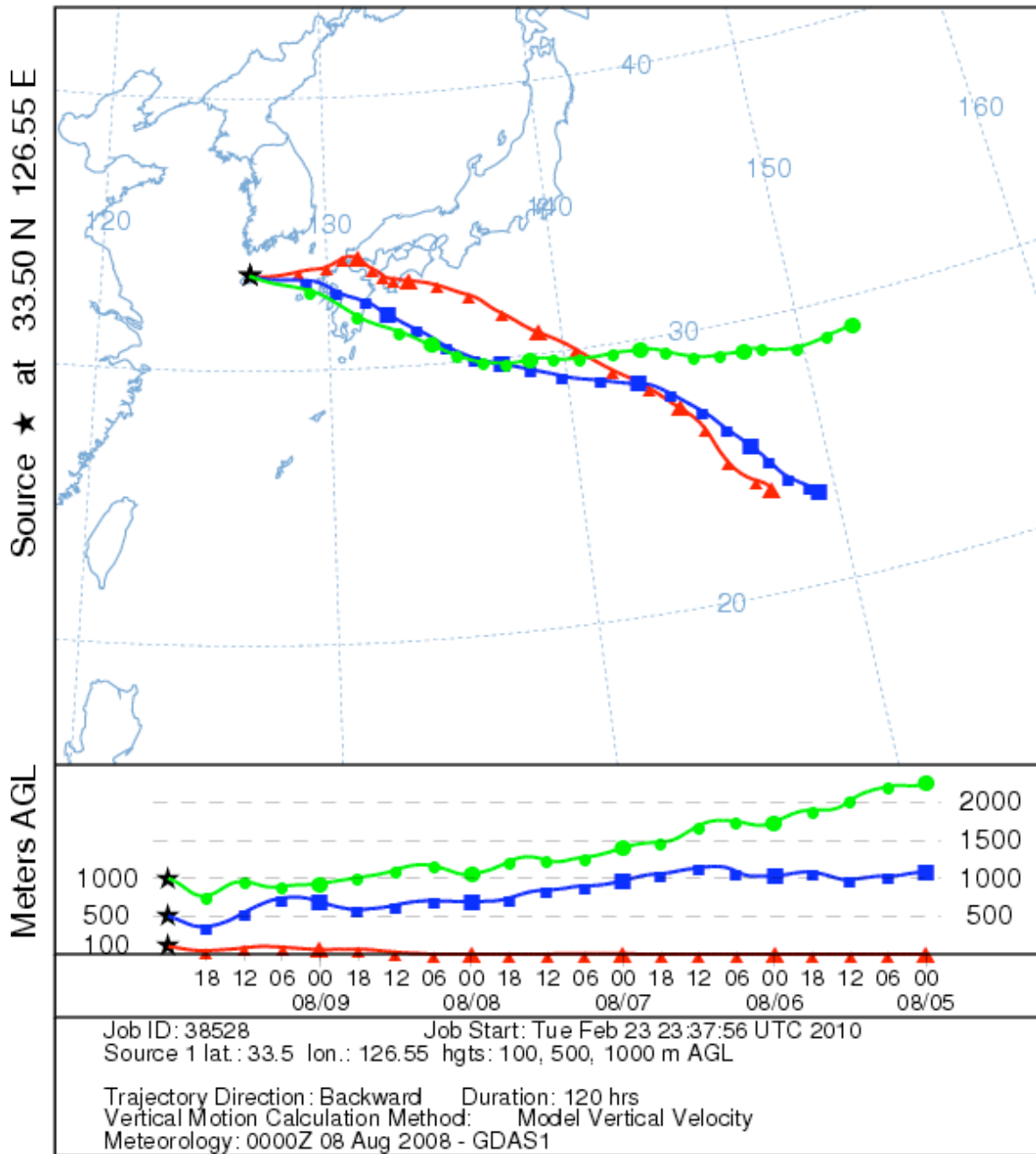
NOAA HYSPLIT MODEL  
 Backward trajectories ending at 0000 UTC 08 Aug 08  
 GDAS Meteorological Data



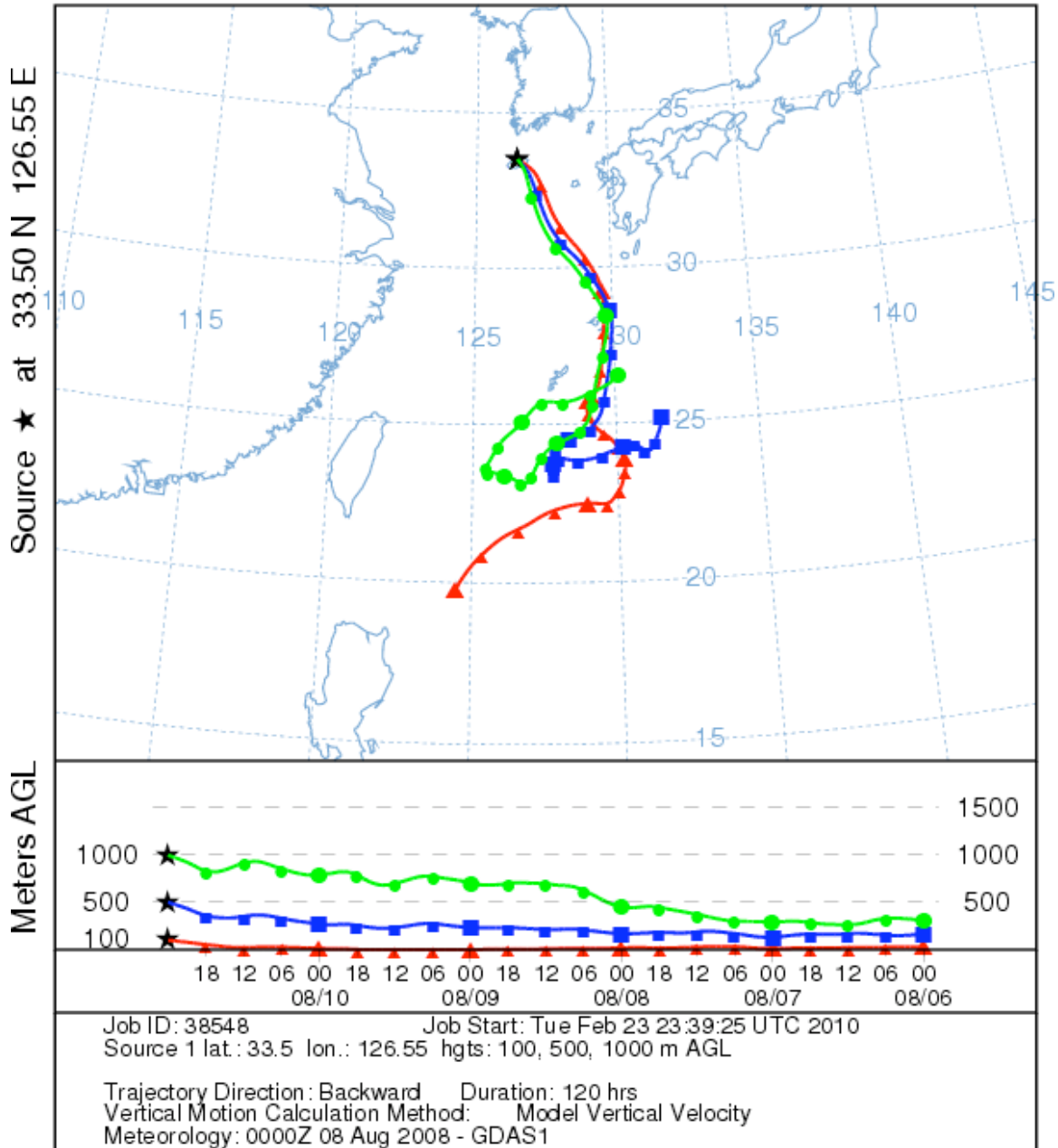
NOAA HYSPLIT MODEL  
 Backward trajectories ending at 0000 UTC 09 Aug 08  
 GDAS Meteorological Data



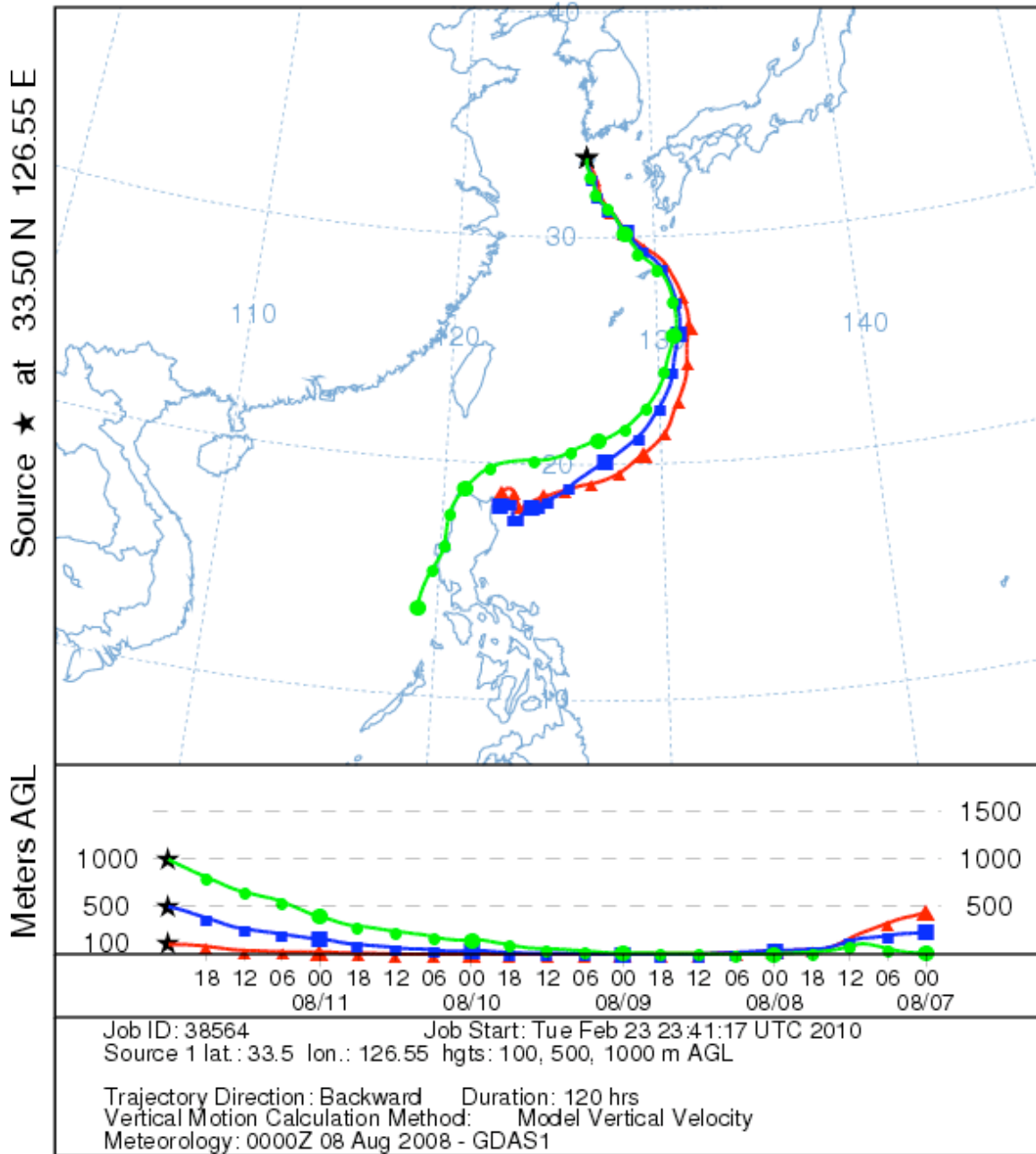
NOAA HYSPLIT MODEL  
 Backward trajectories ending at 0000 UTC 10 Aug 08  
 GDAS Meteorological Data



NOAA HYSPLIT MODEL  
 Backward trajectories ending at 0000 UTC 11 Aug 08  
 GDAS Meteorological Data

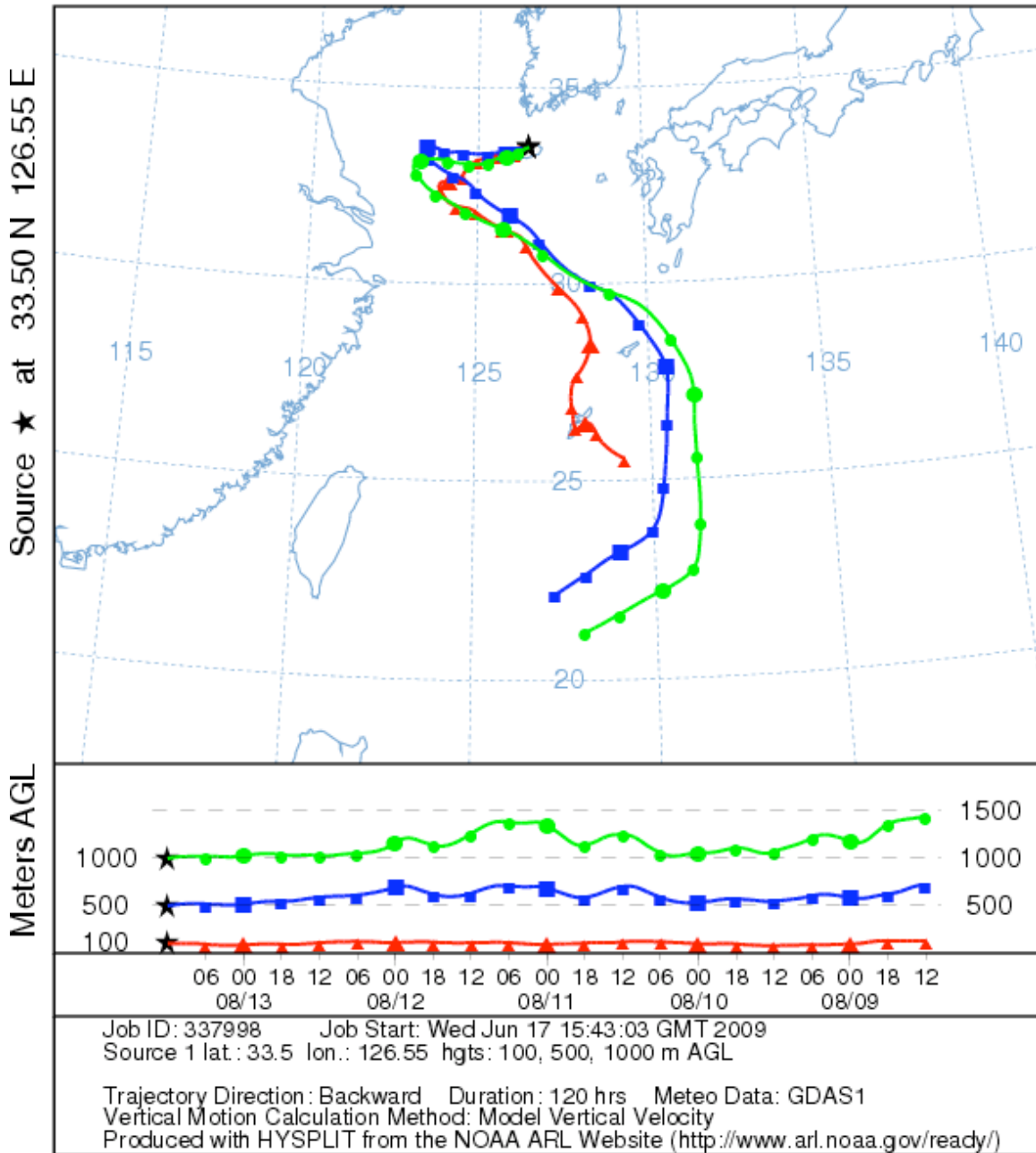


NOAA HYSPLIT MODEL  
 Backward trajectories ending at 0000 UTC 12 Aug 08  
 GDAS Meteorological Data



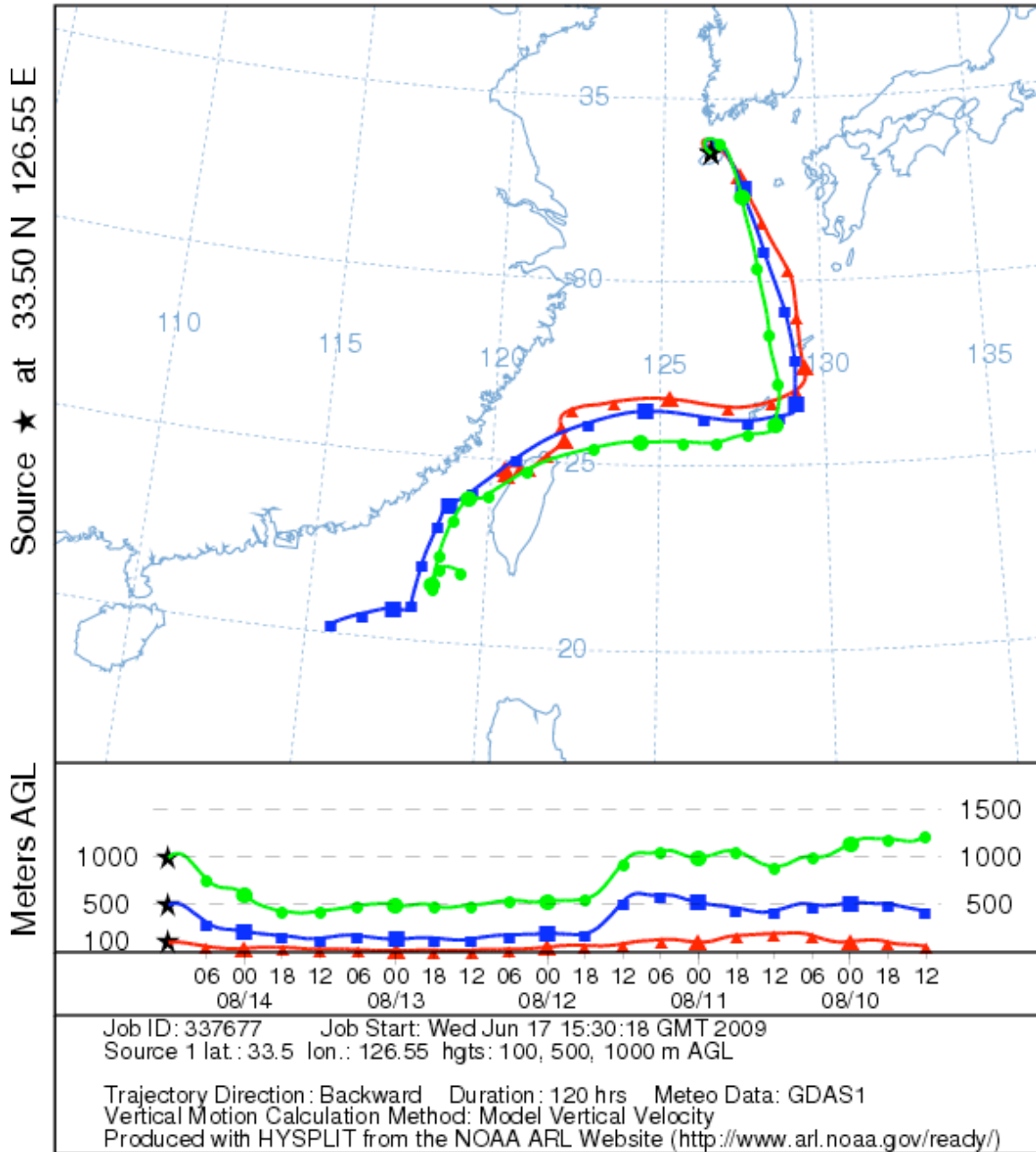
**Episode 3, 13-23 August 2008.**

NOAA HYSPLIT MODEL  
Backward trajectories ending at 1200 UTC 13 Aug 08  
GDAS Meteorological Data



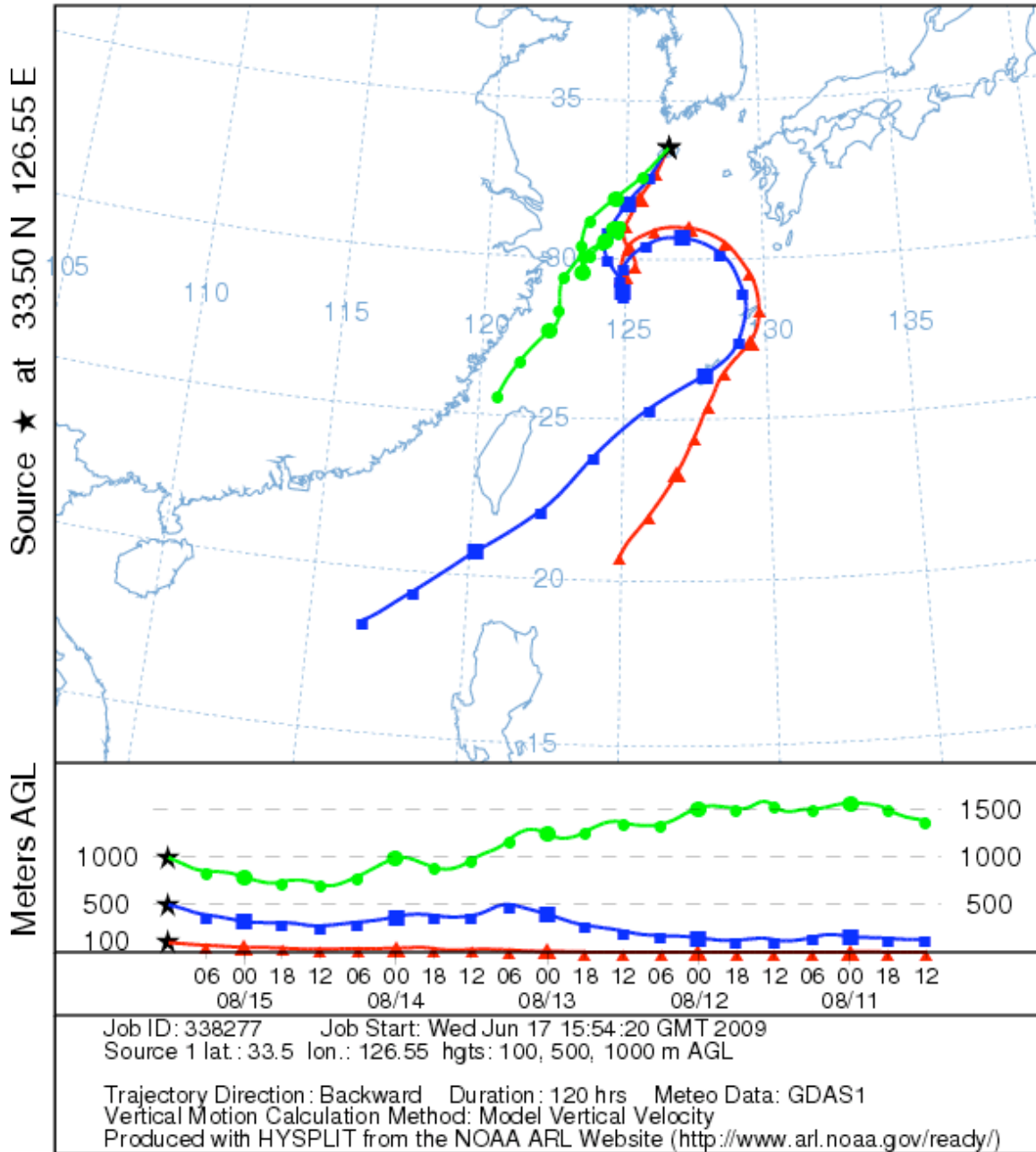


NOAA HYSPLIT MODEL  
 Backward trajectories ending at 1200 UTC 14 Aug 08  
 GDAS Meteorological Data

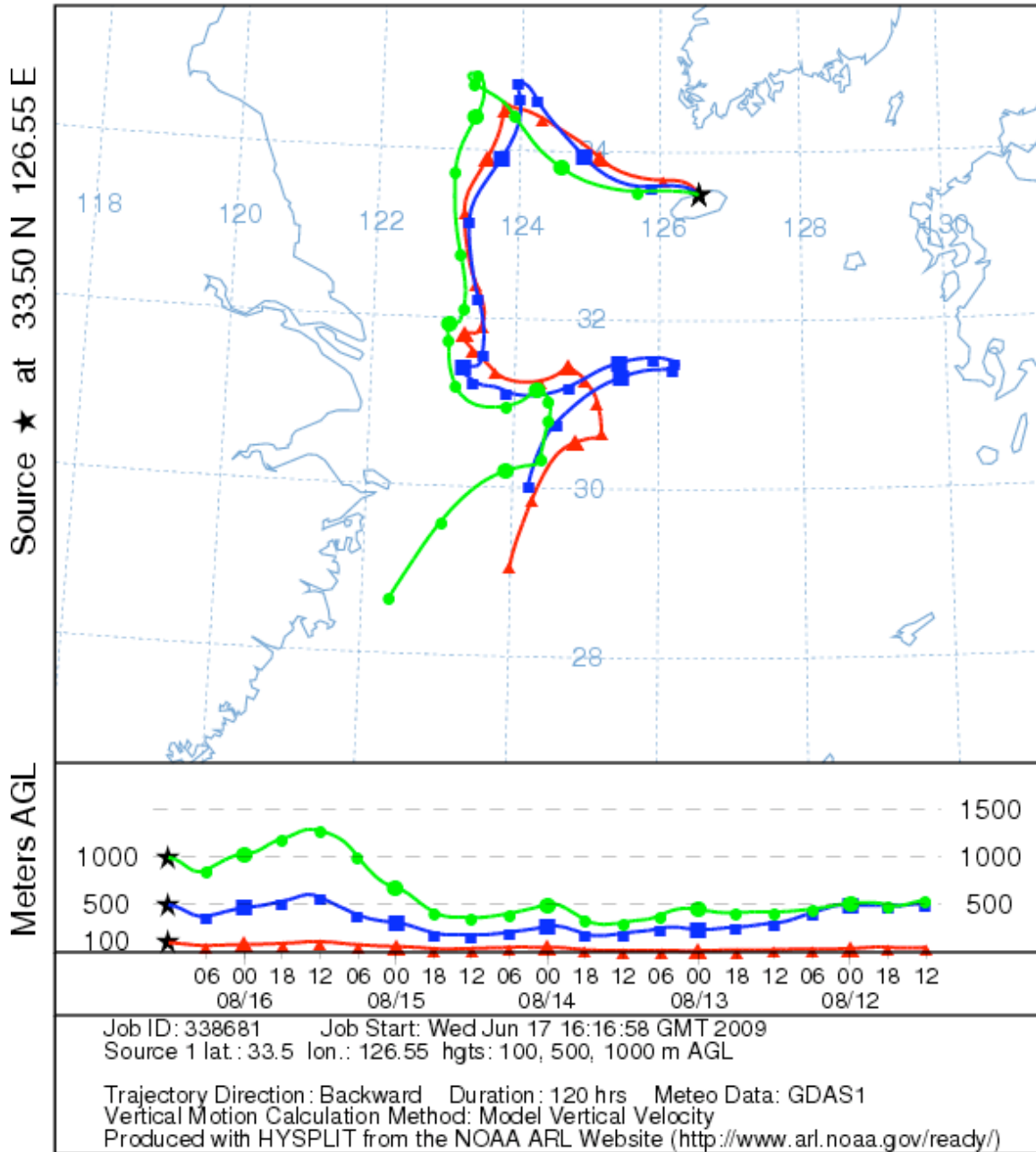




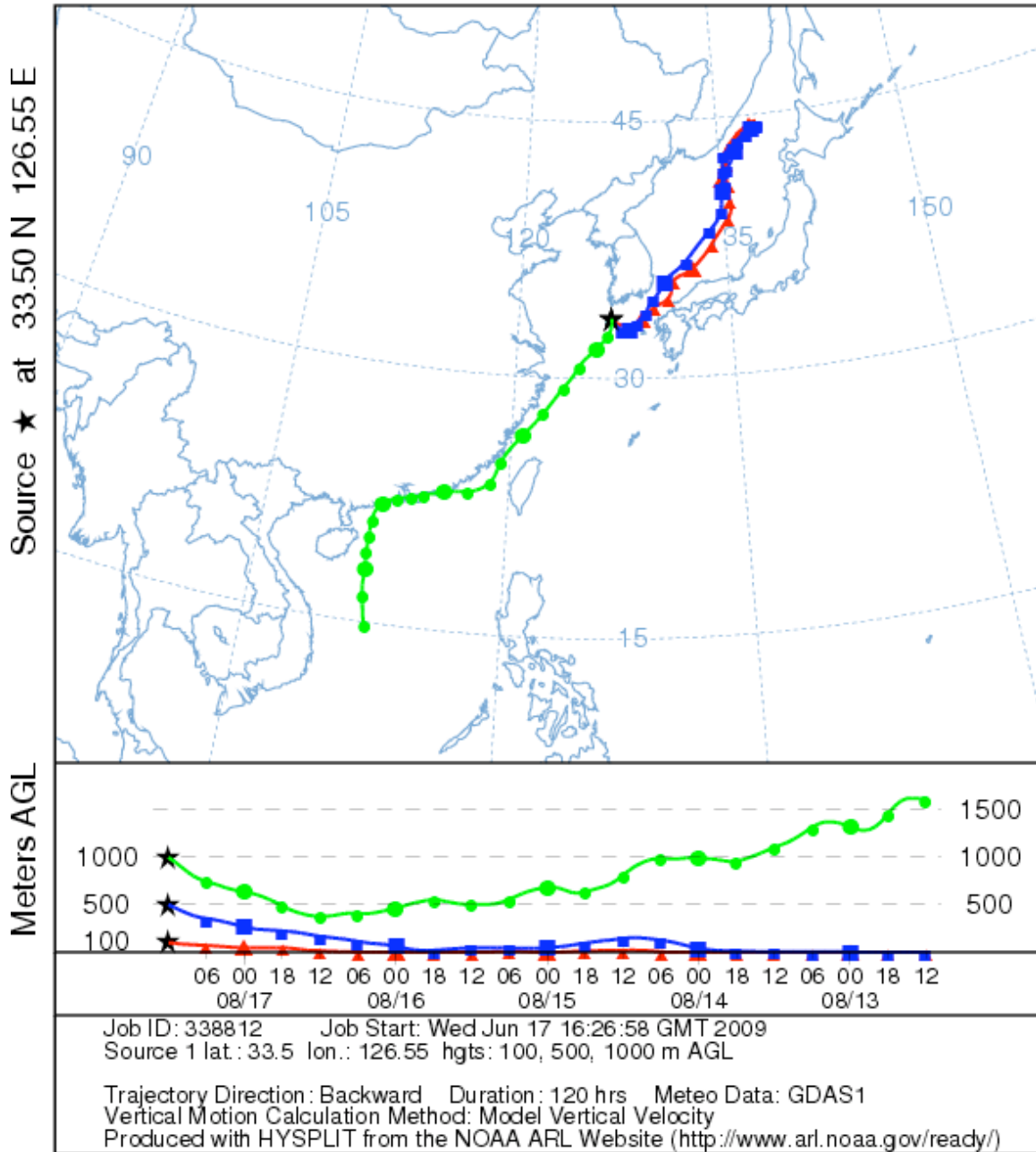
NOAA HYSPLIT MODEL  
 Backward trajectories ending at 1200 UTC 15 Aug 08  
 GDAS Meteorological Data



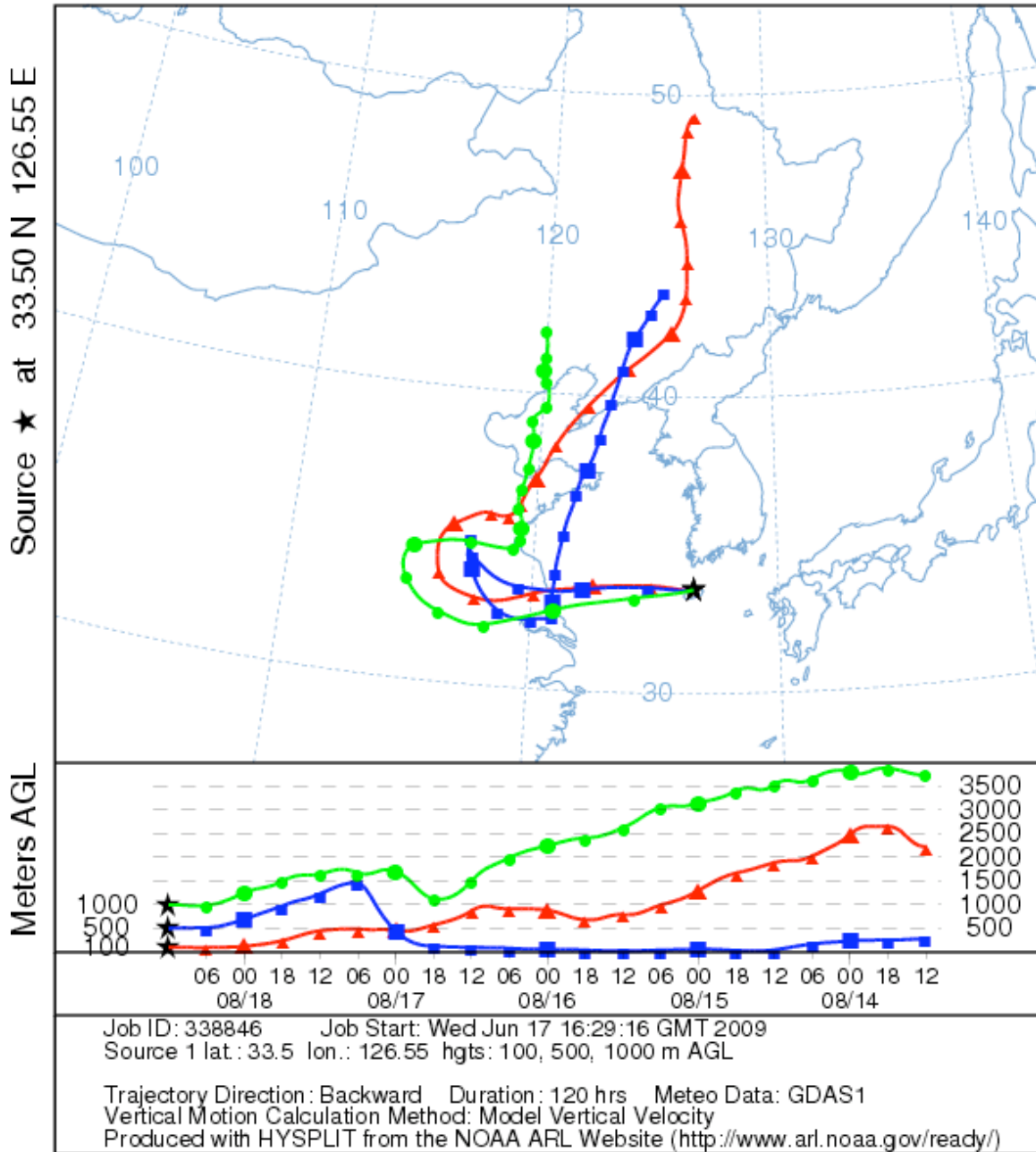
NOAA HYSPLIT MODEL  
 Backward trajectories ending at 1200 UTC 16 Aug 08  
 GDAS Meteorological Data



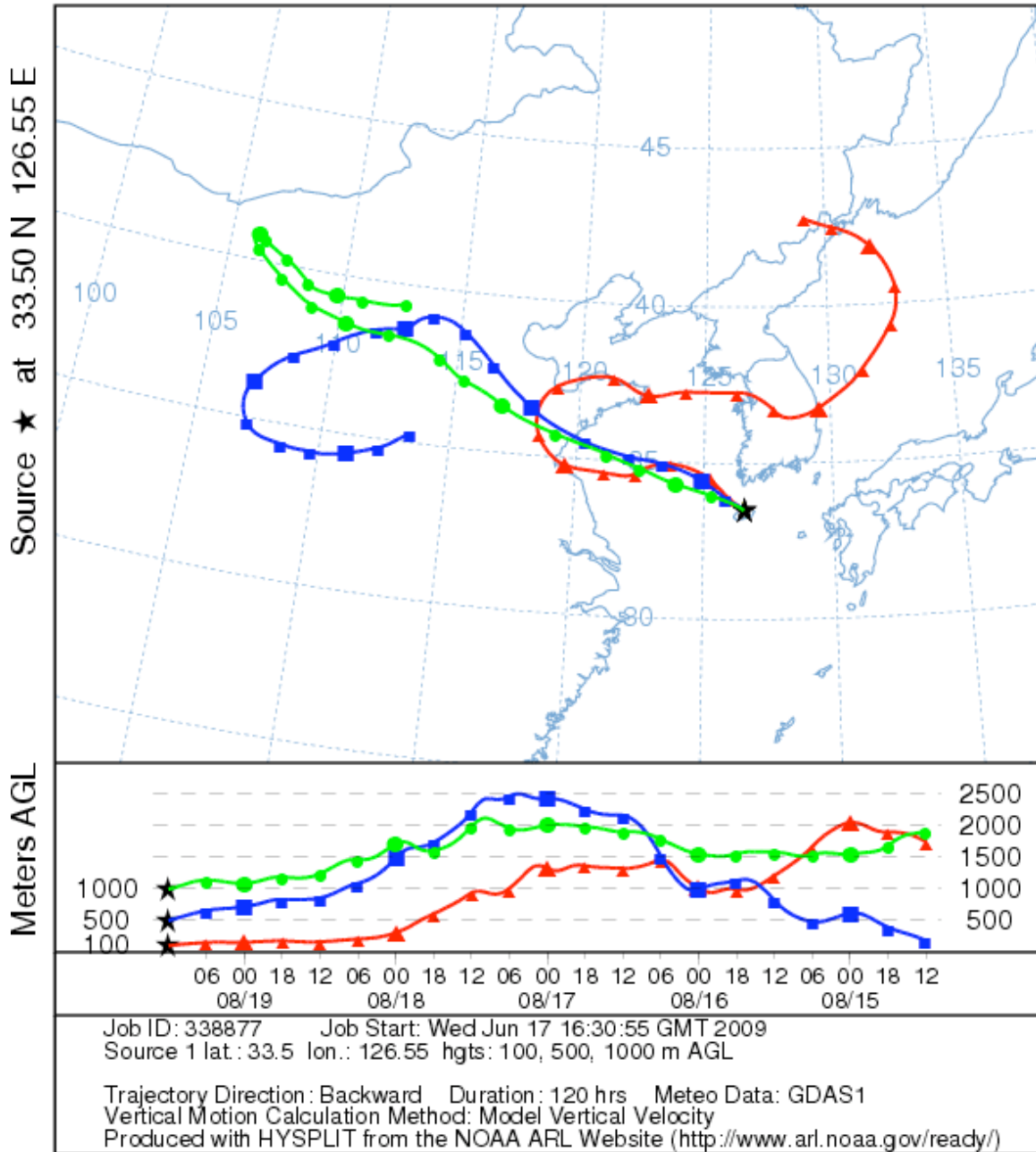
NOAA HYSPLIT MODEL  
 Backward trajectories ending at 1200 UTC 17 Aug 08  
 GDAS Meteorological Data



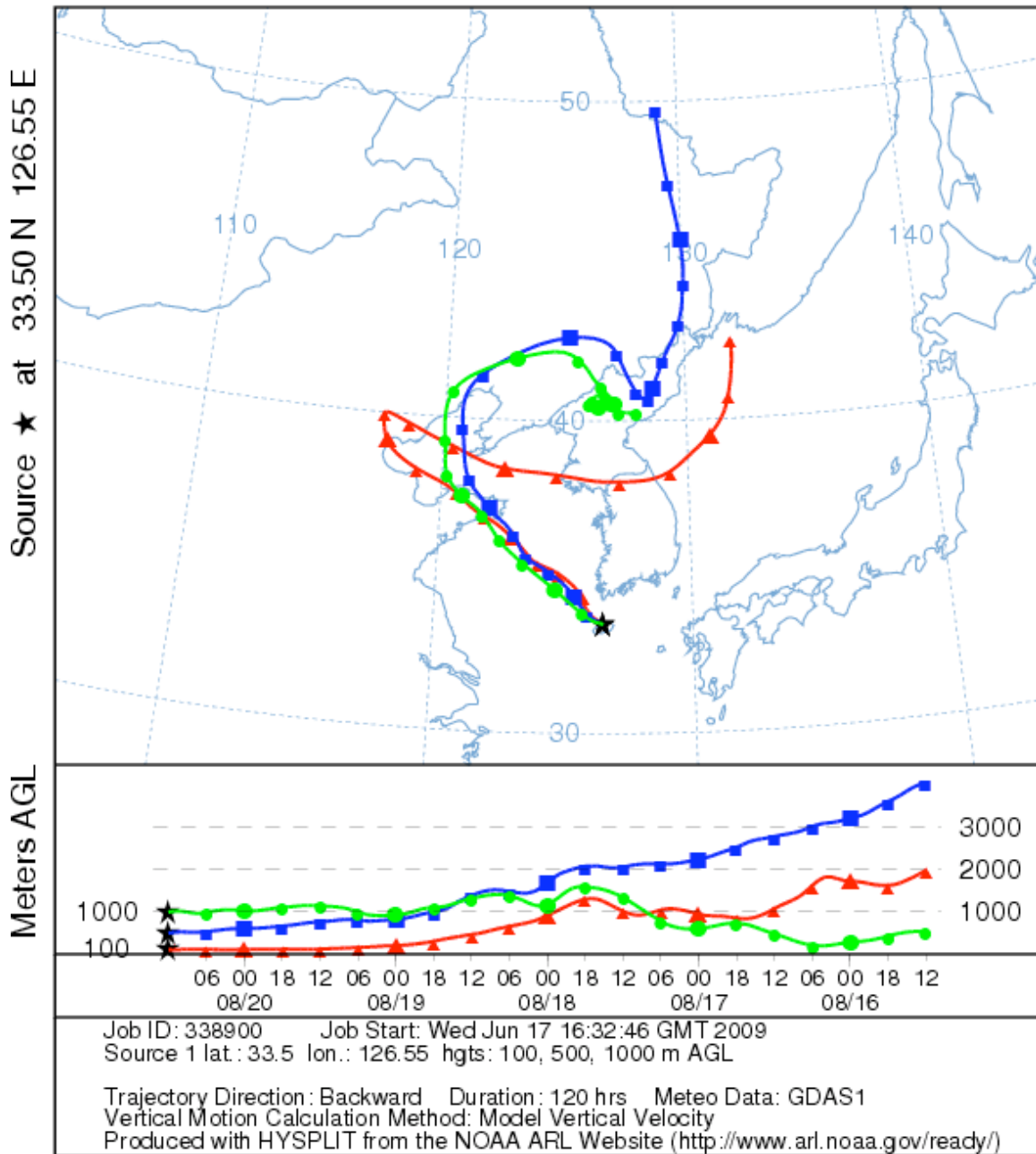
NOAA HYSPLIT MODEL  
 Backward trajectories ending at 1200 UTC 18 Aug 08  
 GDAS Meteorological Data



NOAA HYSPLIT MODEL  
 Backward trajectories ending at 1200 UTC 19 Aug 08  
 GDAS Meteorological Data

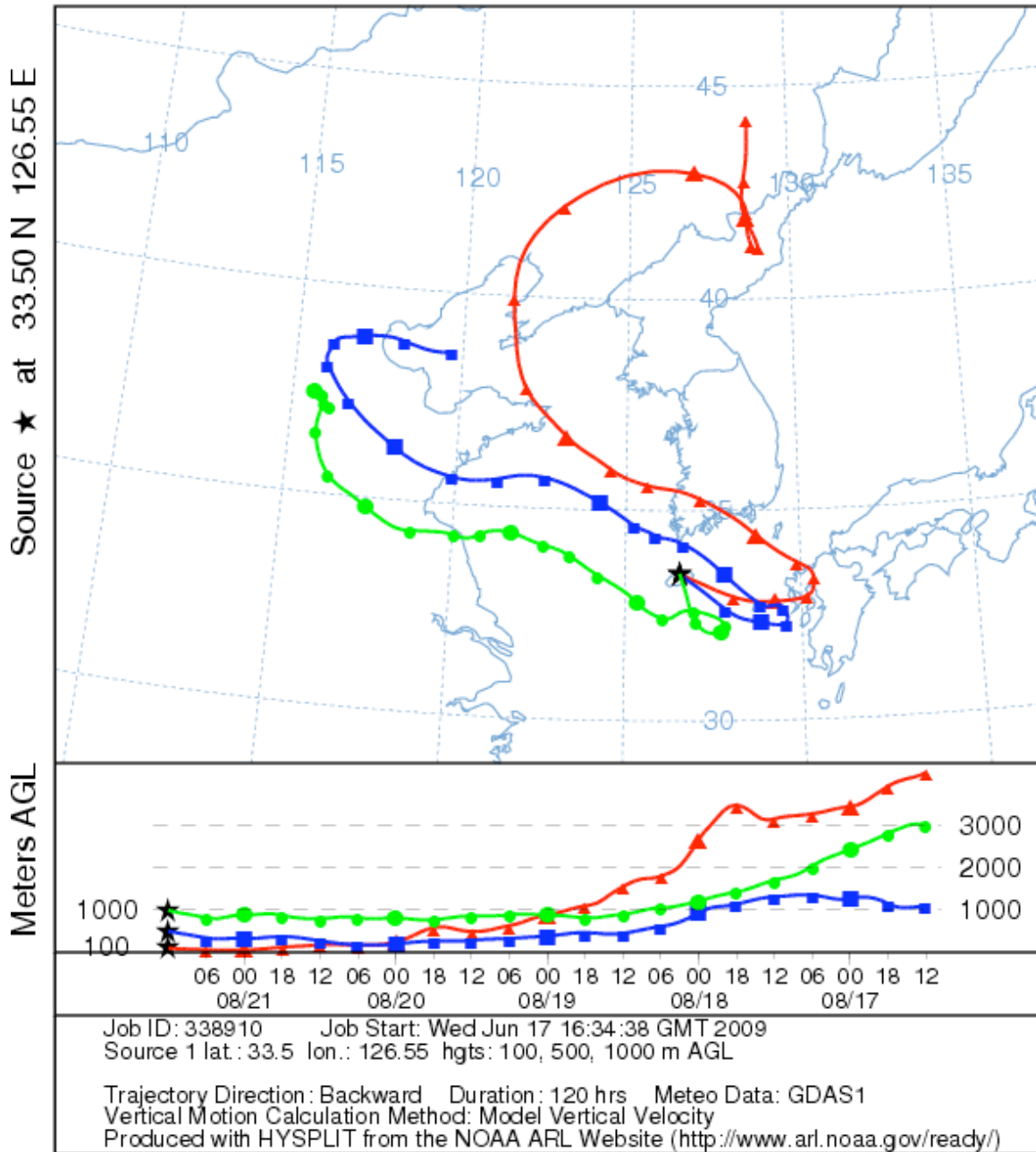


NOAA HYSPLIT MODEL  
 Backward trajectories ending at 1200 UTC 20 Aug 08  
 GDAS Meteorological Data



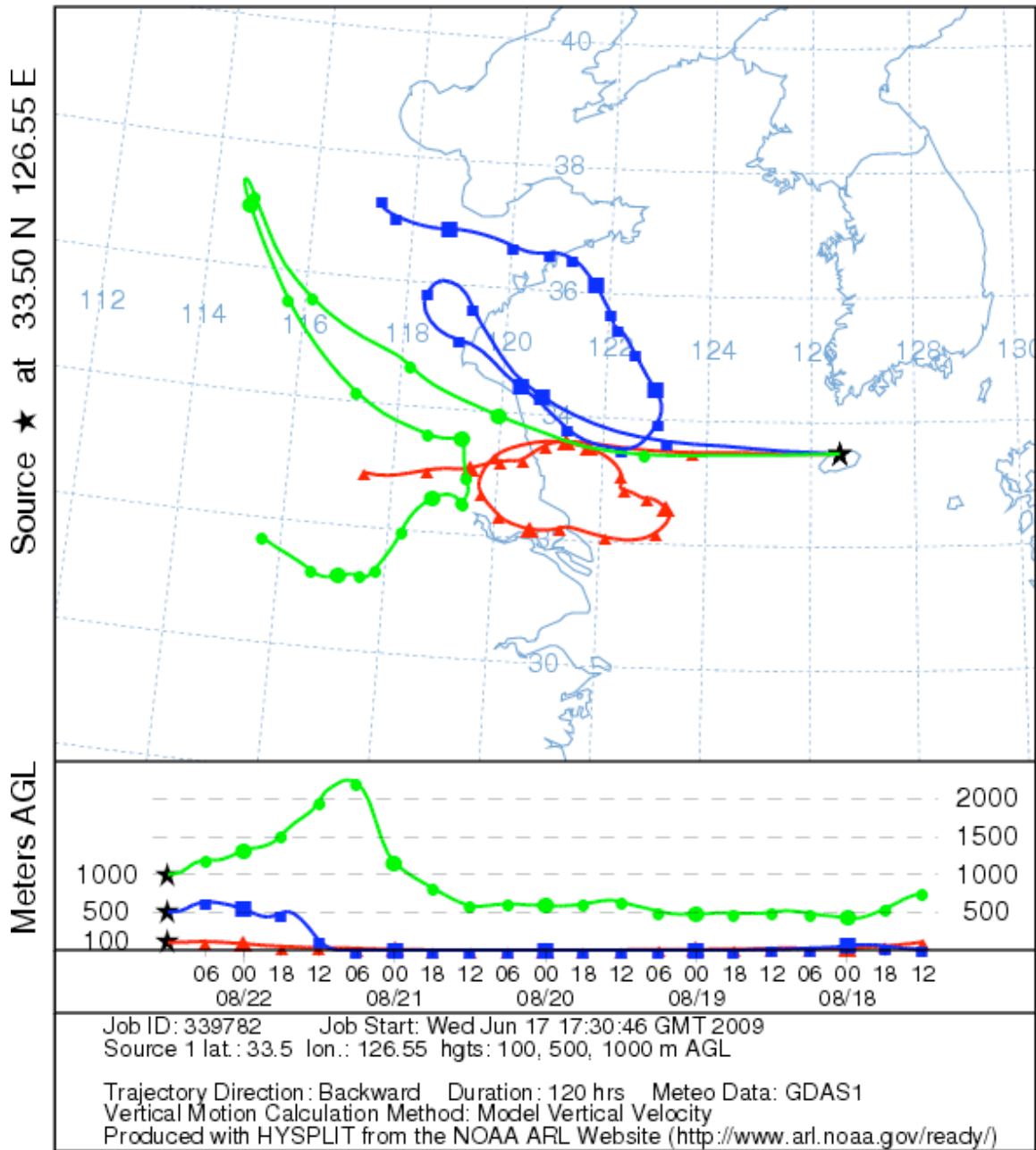
Episode 3 13-23 August 2008.

NOAA HYSPLIT MODEL  
Backward trajectories ending at 1200 UTC 21 Aug 08  
GDAS Meteorological Data



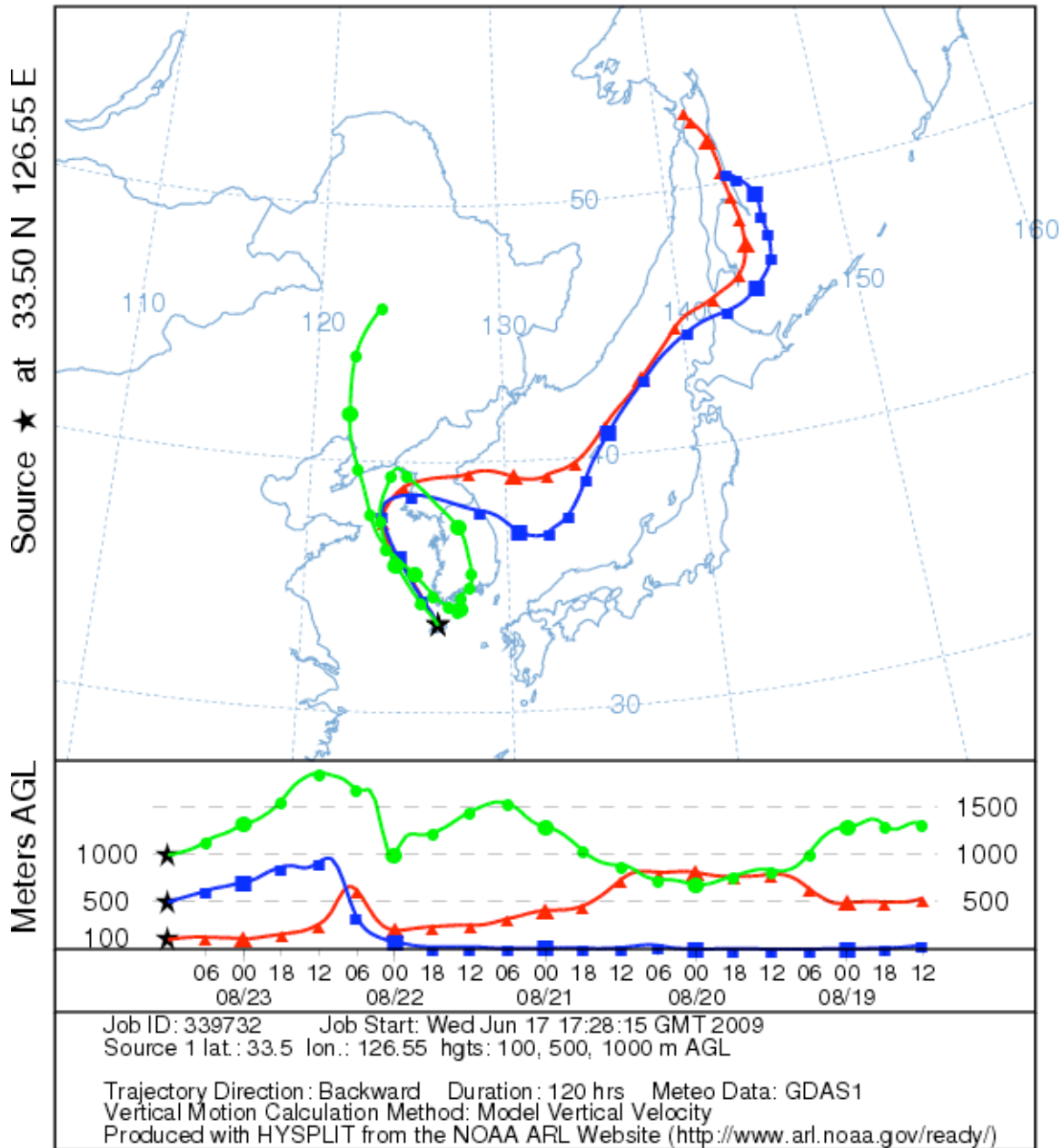


NOAA HYSPLIT MODEL  
 Backward trajectories ending at 1200 UTC 22 Aug 08  
 GDAS Meteorological Data

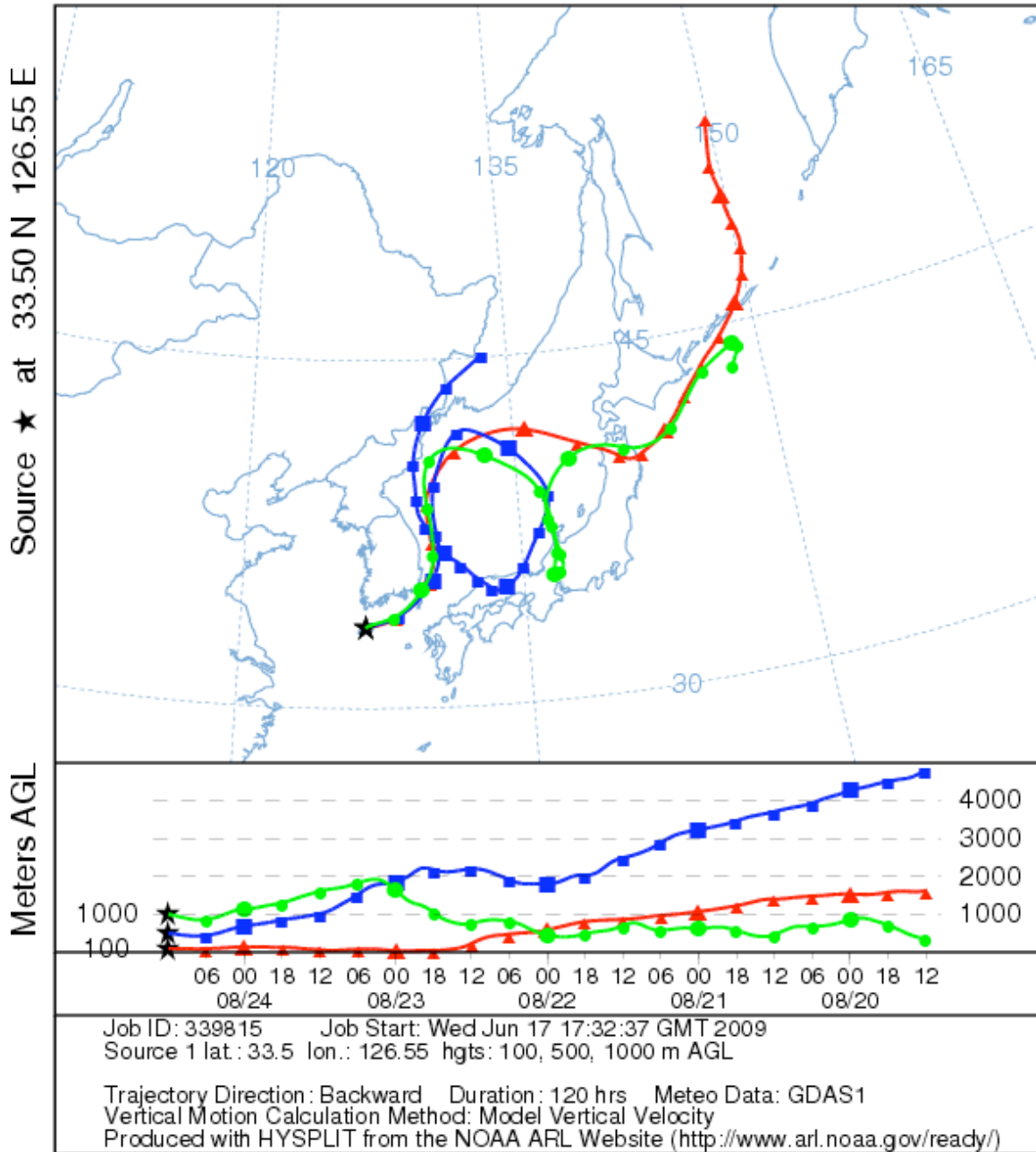




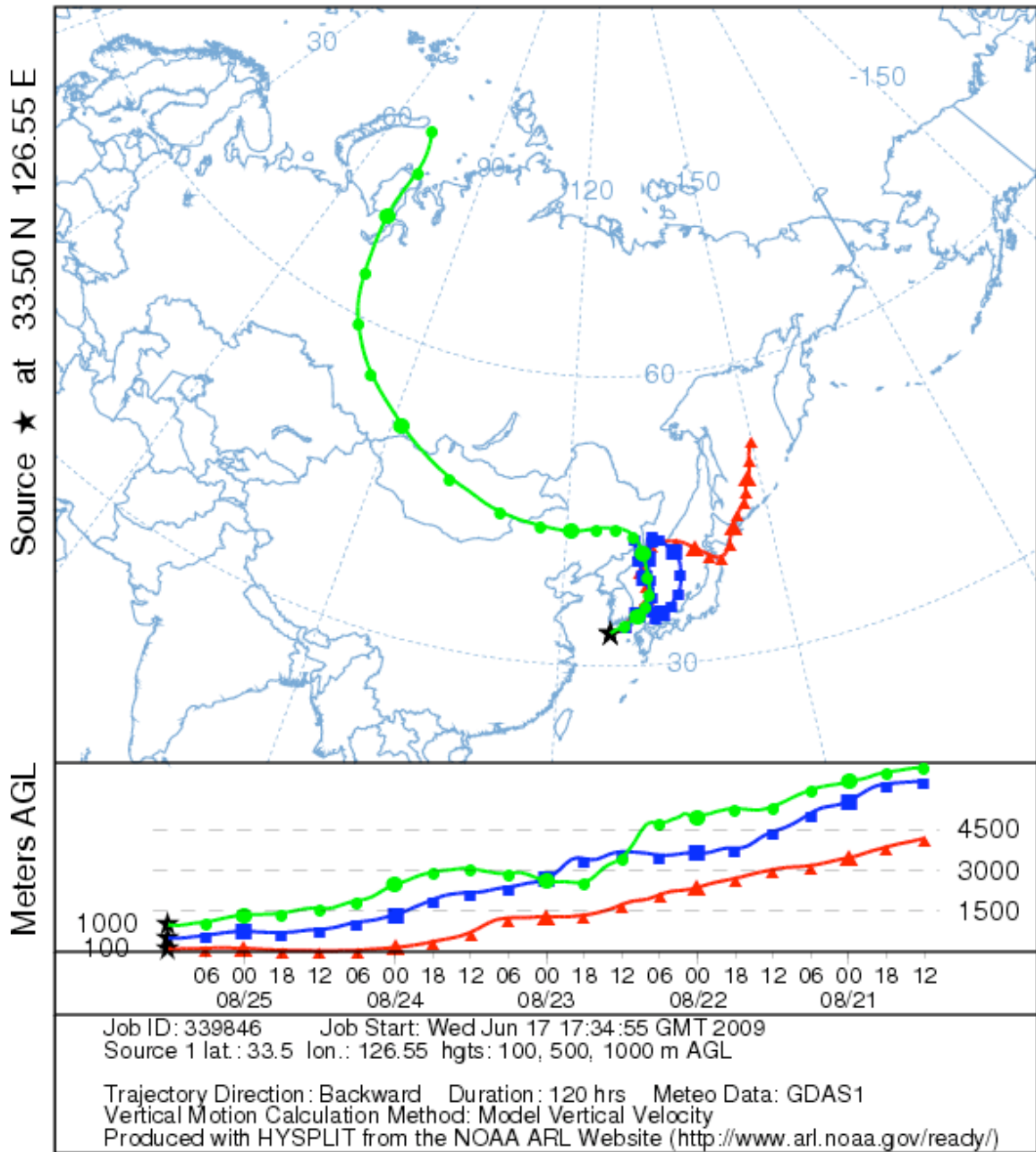
NOAA HYSPLIT MODEL  
 Backward trajectories ending at 1200 UTC 23 Aug 08  
 GDAS Meteorological Data



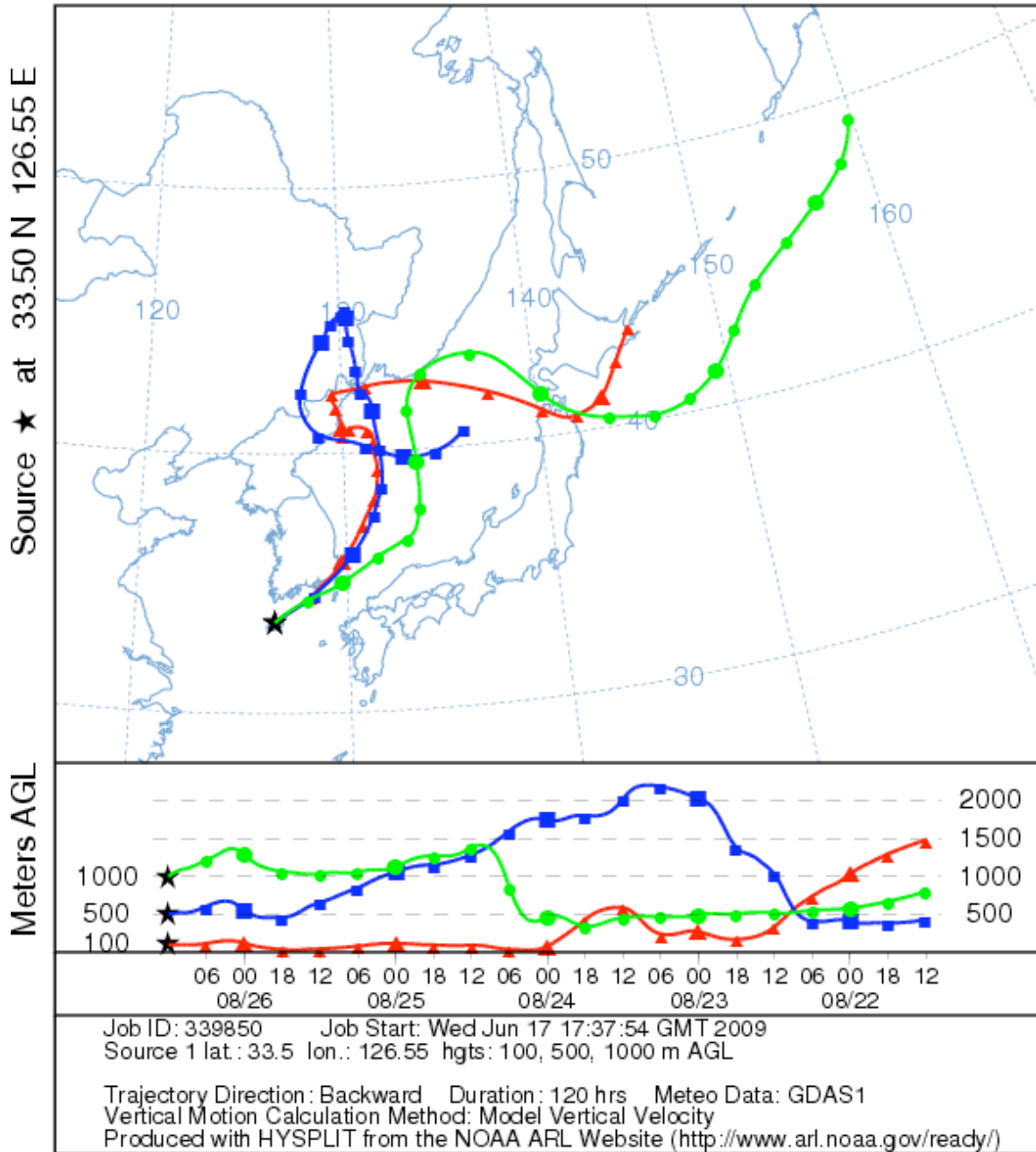
NOAA HYSPLIT MODEL  
 Backward trajectories ending at 1200 UTC 24 Aug 08  
 GDAS Meteorological Data



NOAA HYSPLIT MODEL  
 Backward trajectories ending at 1200 UTC 25 Aug 08  
 GDAS Meteorological Data



NOAA HYSPLIT MODEL  
 Backward trajectories ending at 1200 UTC 26 Aug 08  
 GDAS Meteorological Data

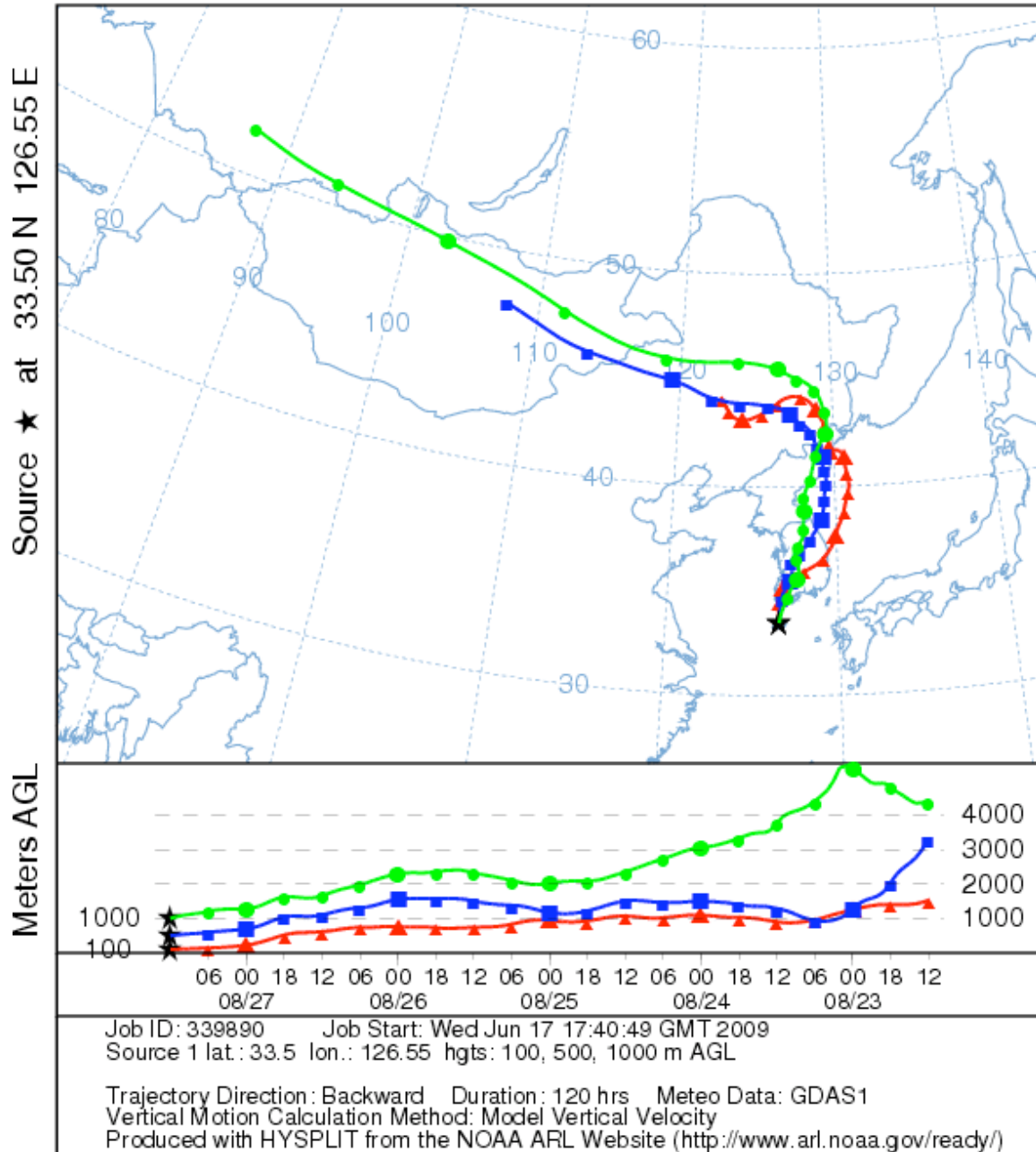


**Episode 4, 27 - 31 August 2008.**

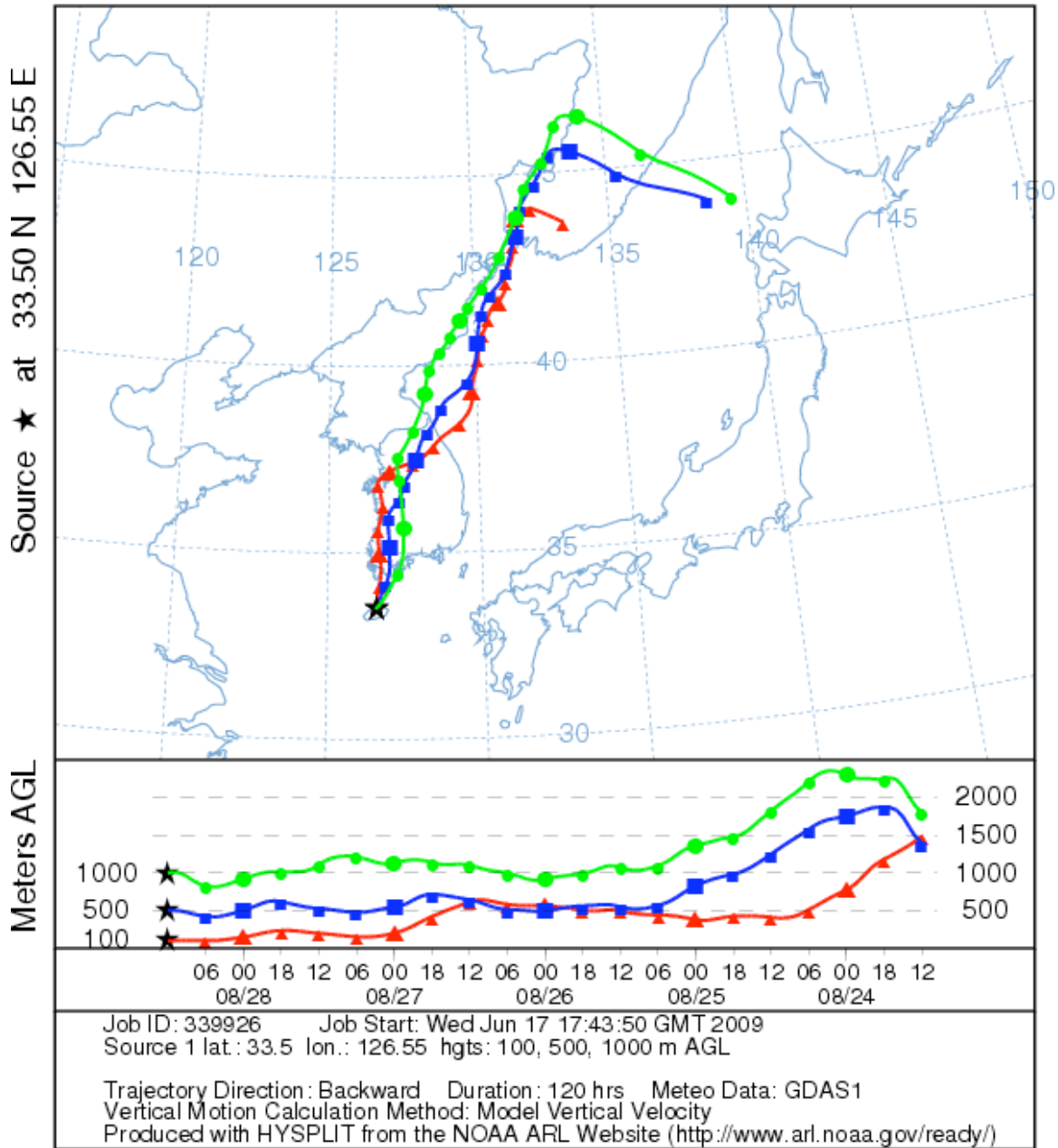
NOAA HYSPLIT MODEL

Backward trajectories ending at 1200 UTC 27 Aug 08

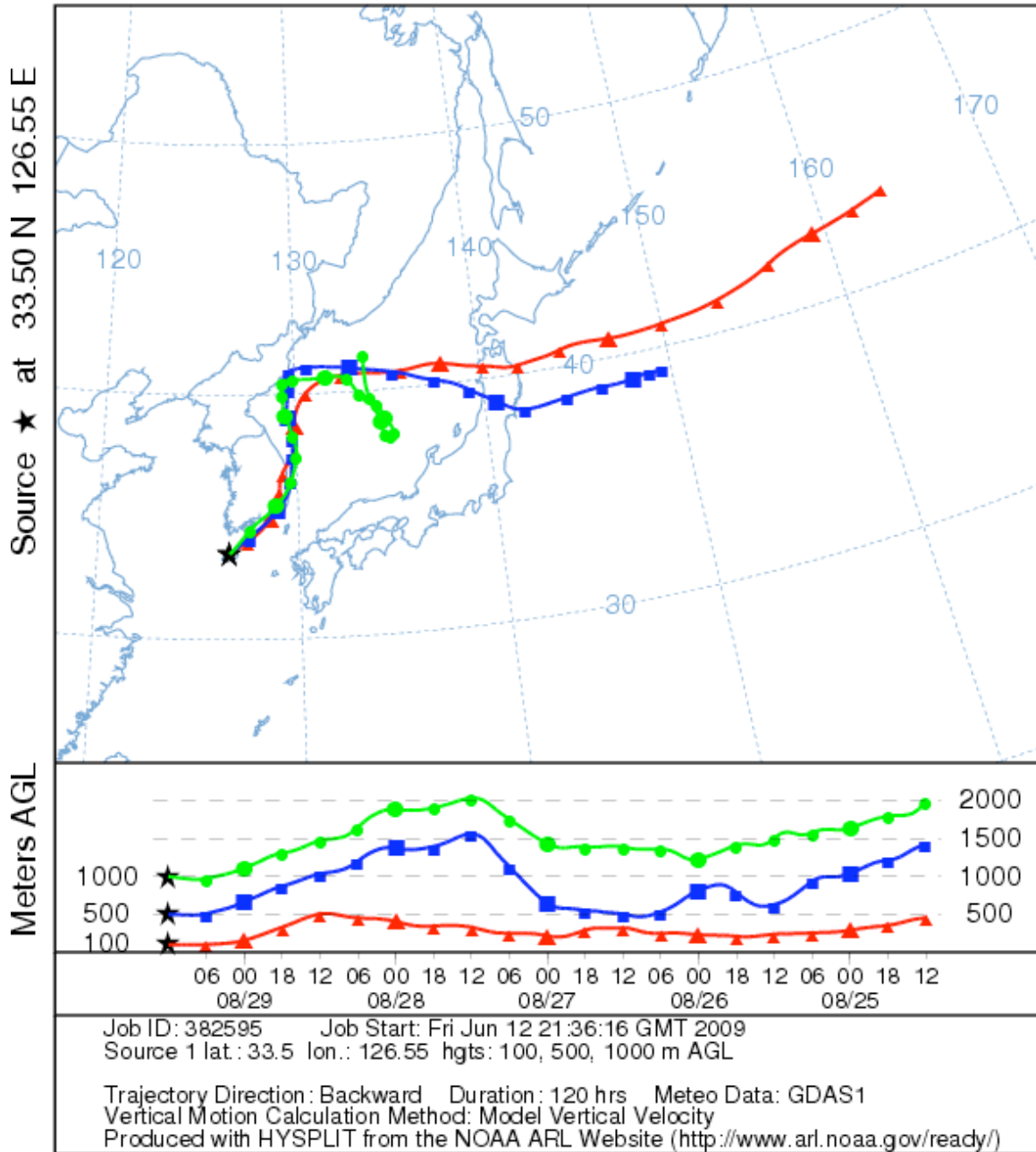
GDAS Meteorological Data



NOAA HYSPLIT MODEL  
 Backward trajectories ending at 1200 UTC 28 Aug 08  
 GDAS Meteorological Data

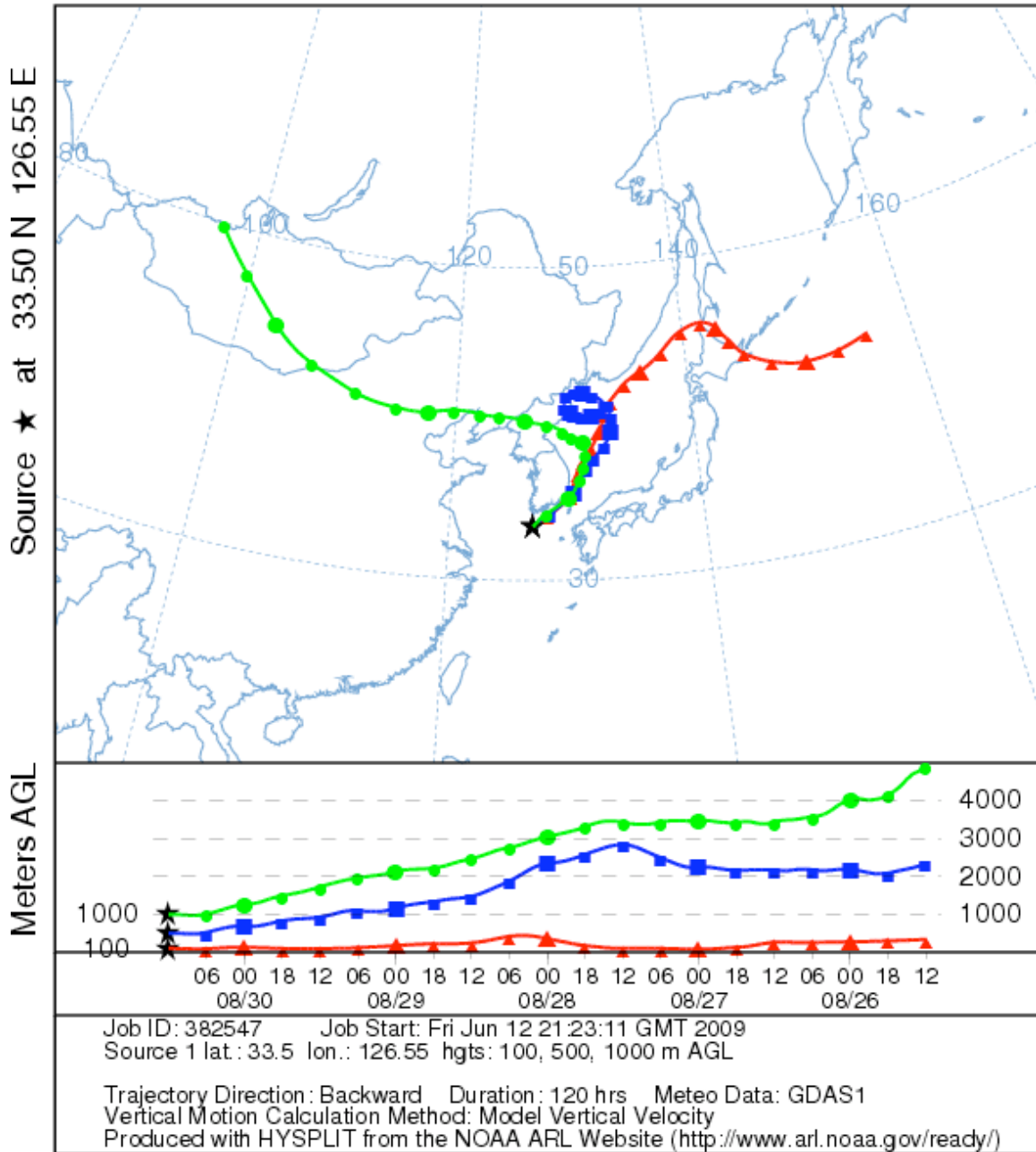


NOAA HYSPLIT MODEL  
 Backward trajectories ending at 1200 UTC 29 Aug 08  
 GDAS Meteorological Data



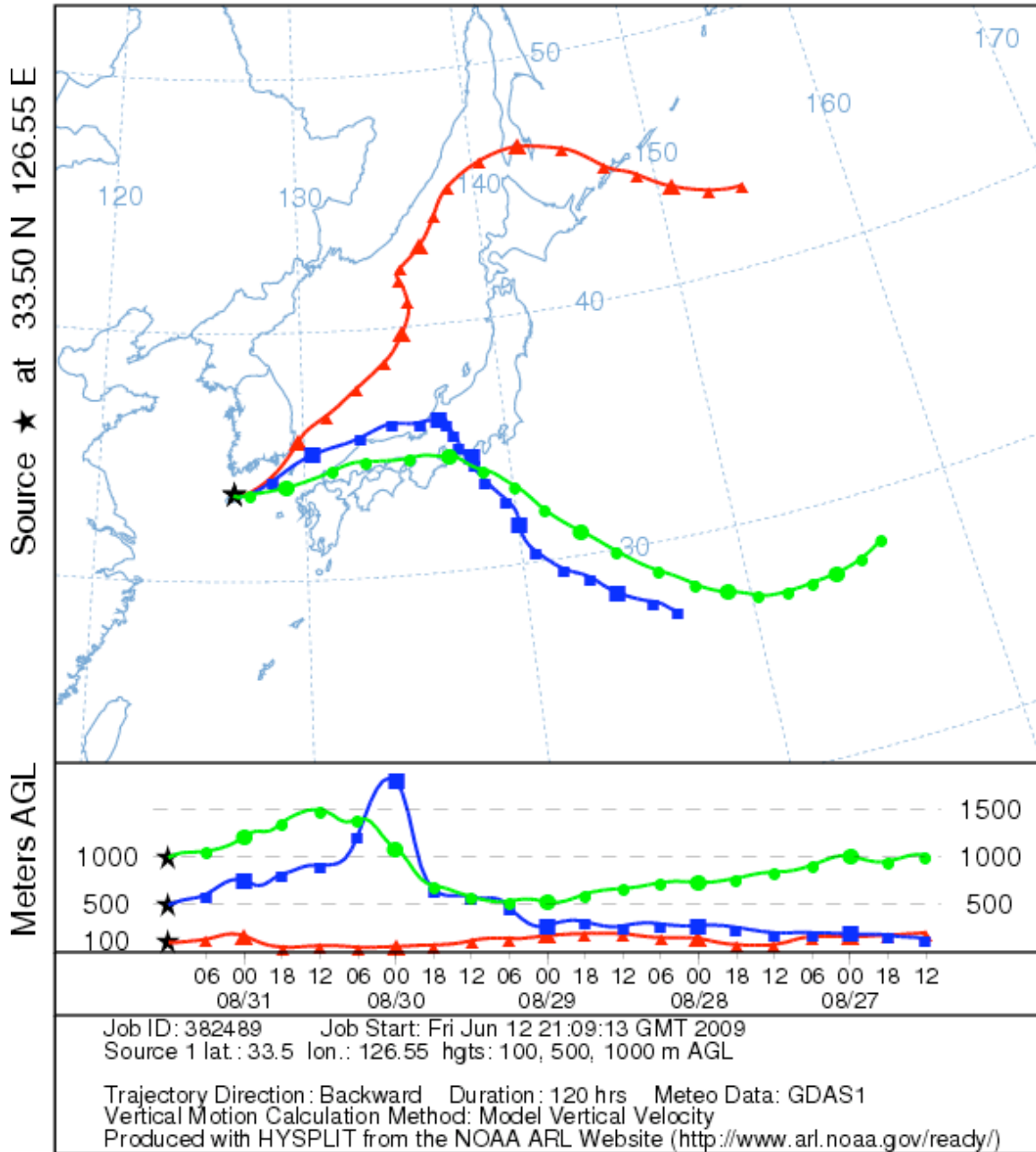


NOAA HYSPLIT MODEL  
 Backward trajectories ending at 1200 UTC 30 Aug 08  
 GDAS Meteorological Data

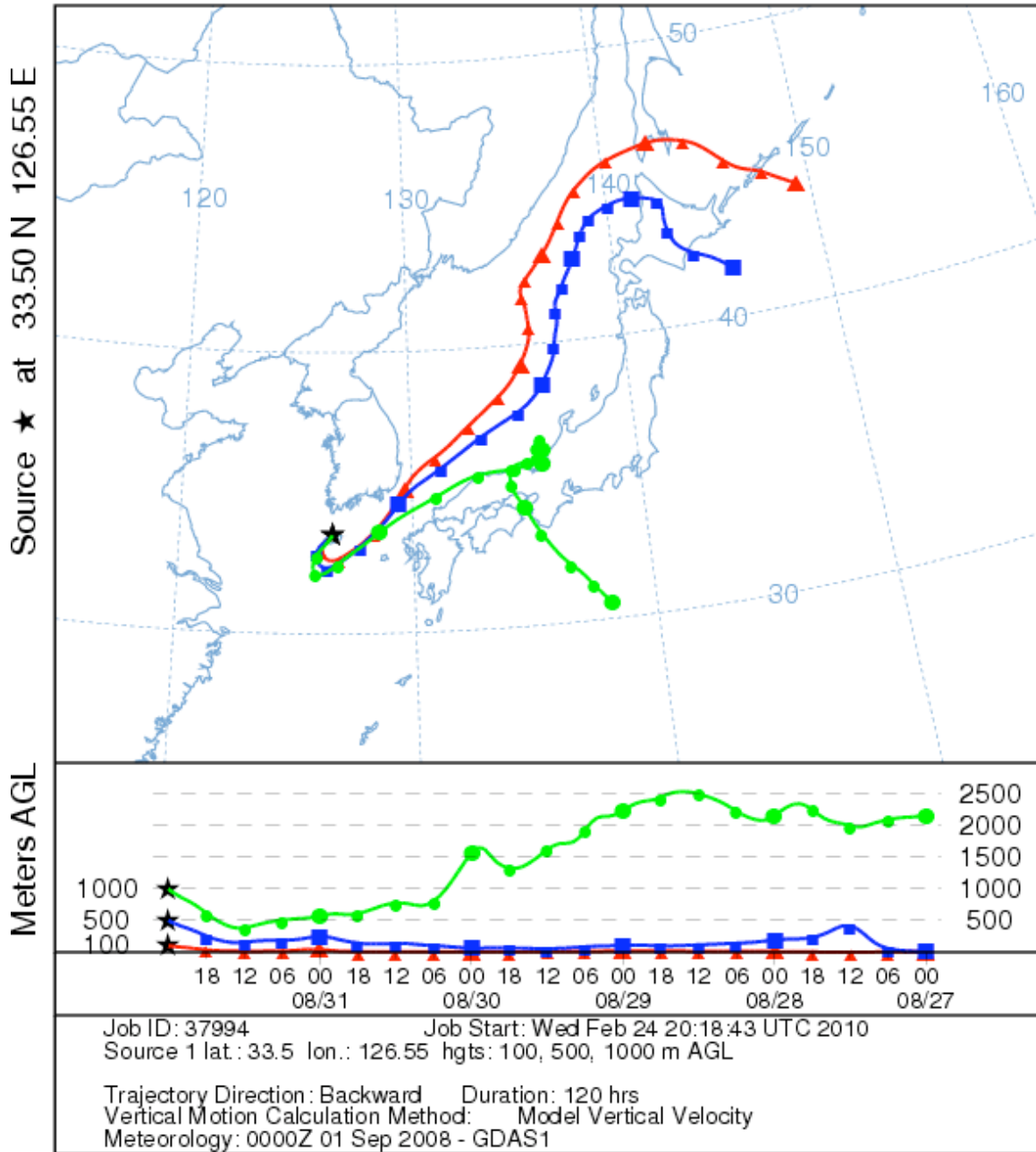




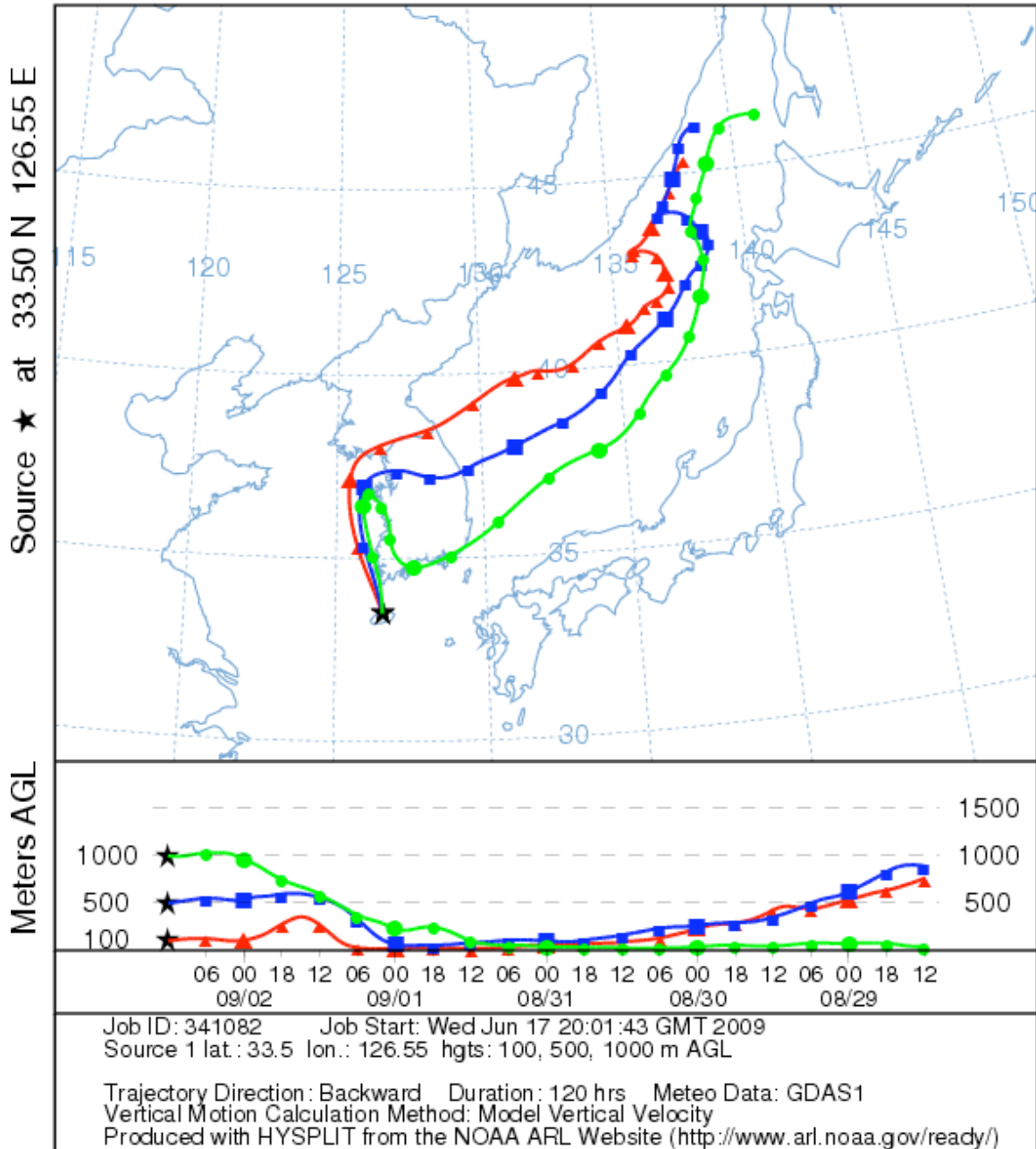
NOAA HYSPLIT MODEL  
 Backward trajectories ending at 1200 UTC 31 Aug 08  
 GDAS Meteorological Data



NOAA HYSPLIT MODEL  
 Backward trajectories ending at 0000 UTC 01 Sep 08  
 GDAS Meteorological Data



NOAA HYSPLIT MODEL  
 Backward trajectories ending at 1200 UTC 02 Sep 08  
 GDAS Meteorological Data

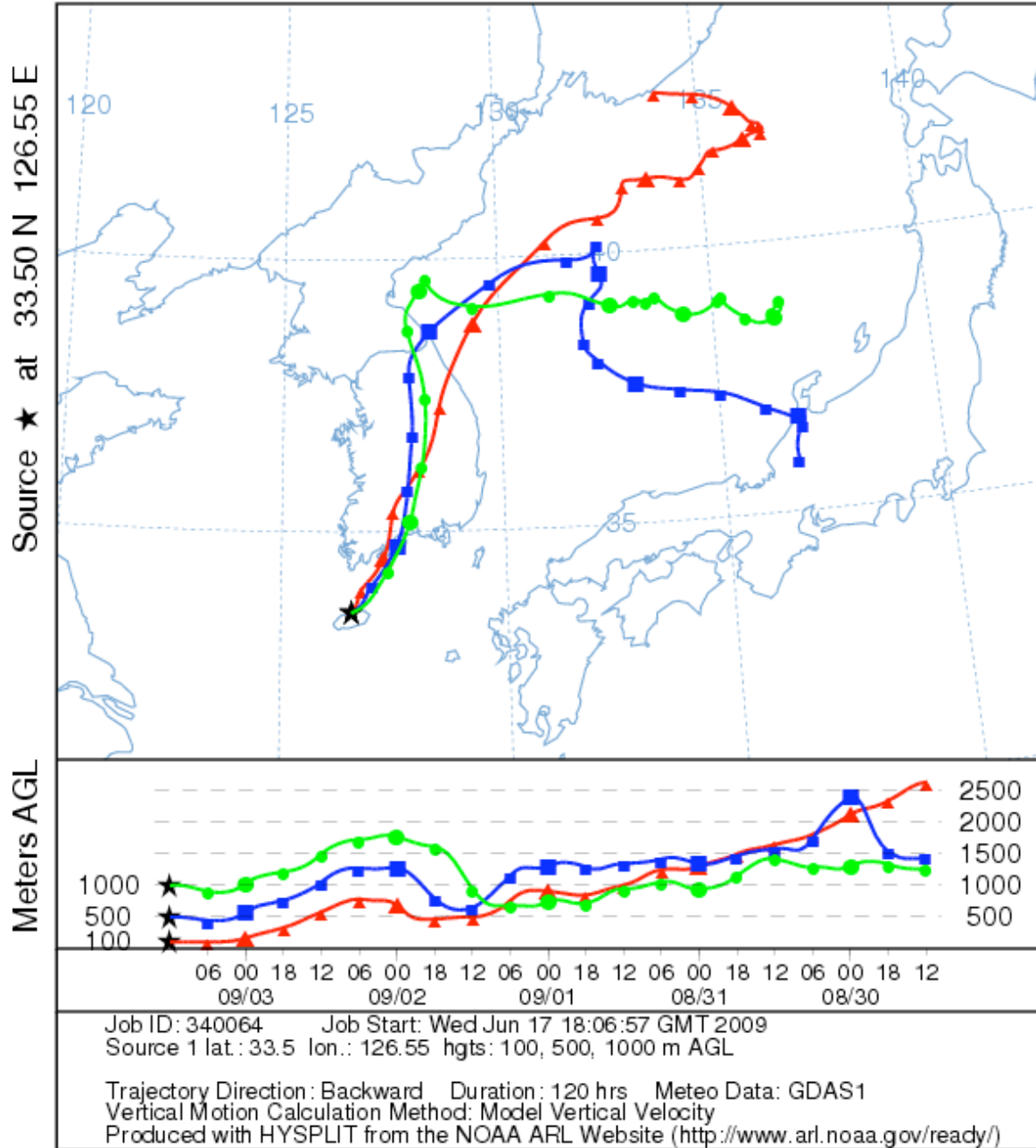


**Episode 5, 3 - 12 September 2008.**

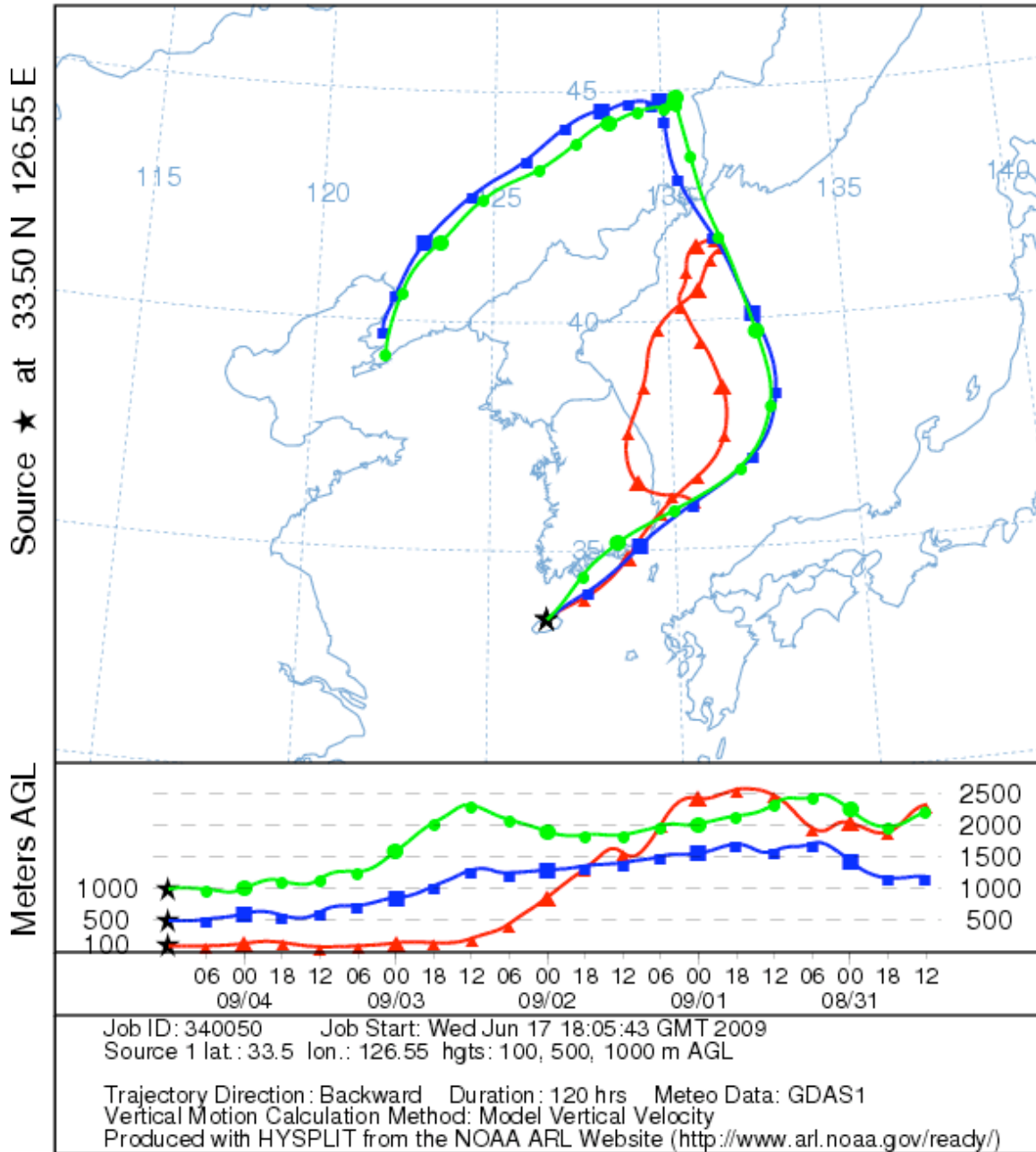
NOAA HYSPLIT MODEL

Backward trajectories ending at 1200 UTC 03 Sep 08

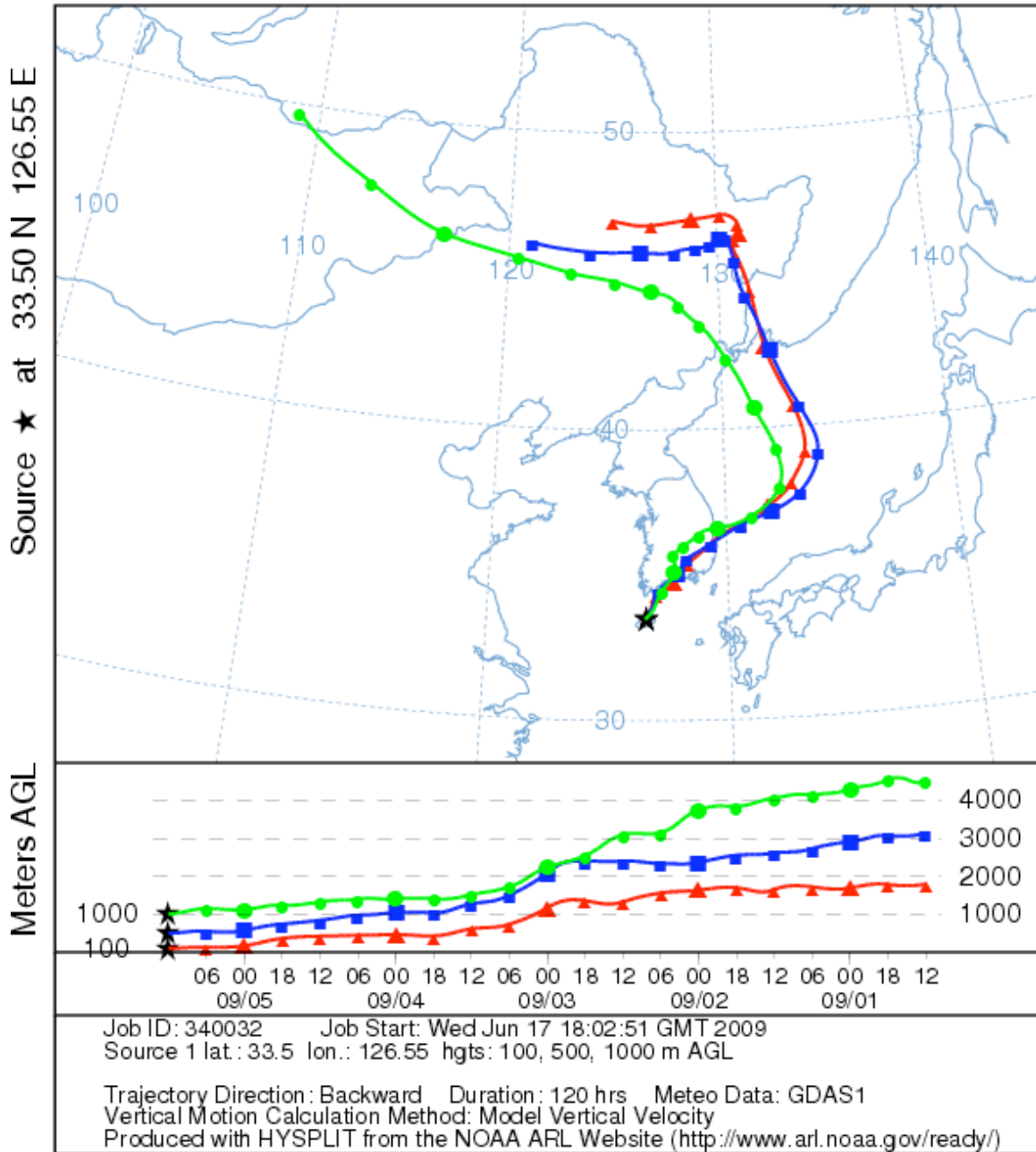
GDAS Meteorological Data



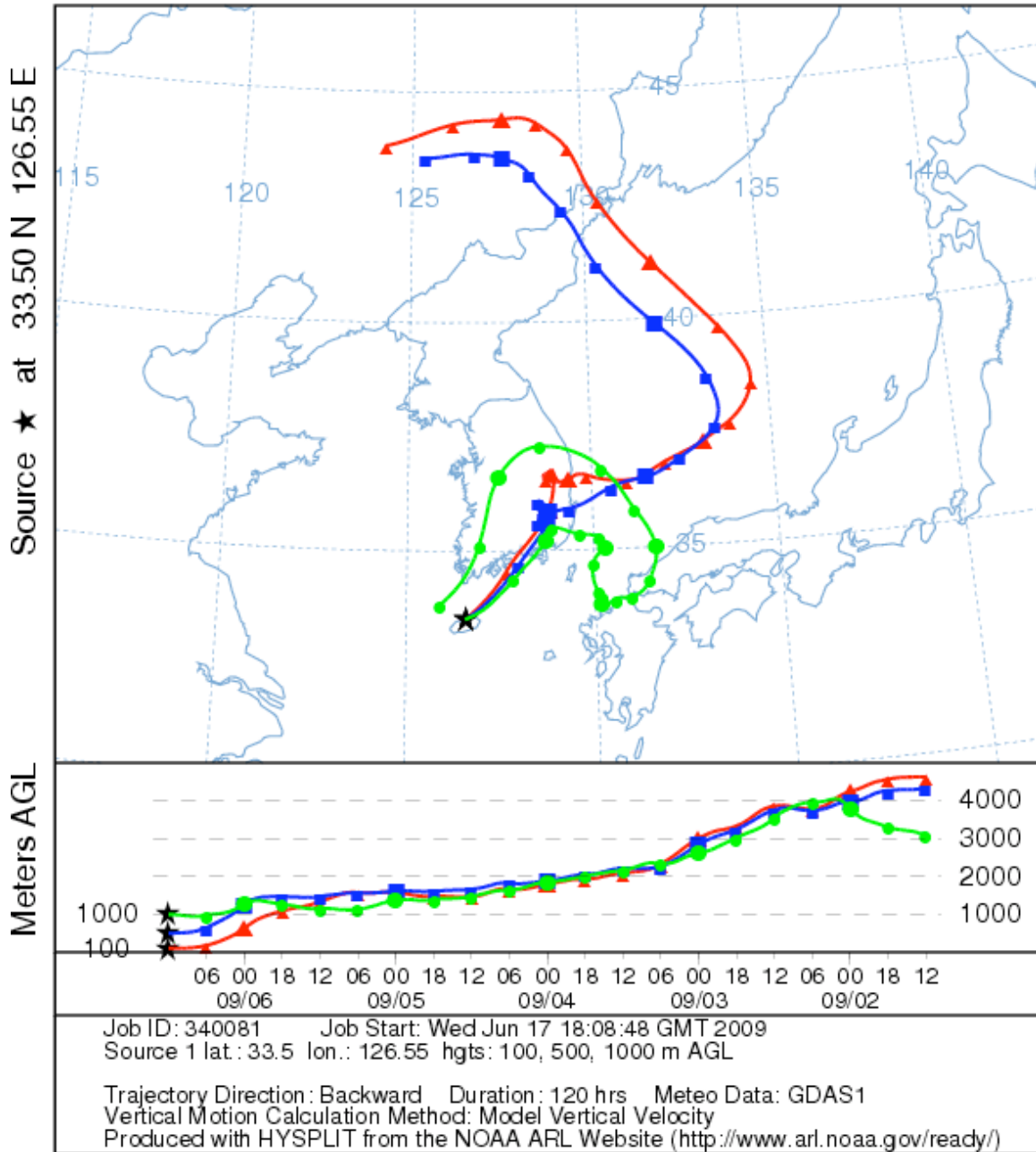
NOAA HYSPLIT MODEL  
 Backward trajectories ending at 1200 UTC 04 Sep 08  
 GDAS Meteorological Data



NOAA HYSPLIT MODEL  
 Backward trajectories ending at 1200 UTC 05 Sep 08  
 GDAS Meteorological Data

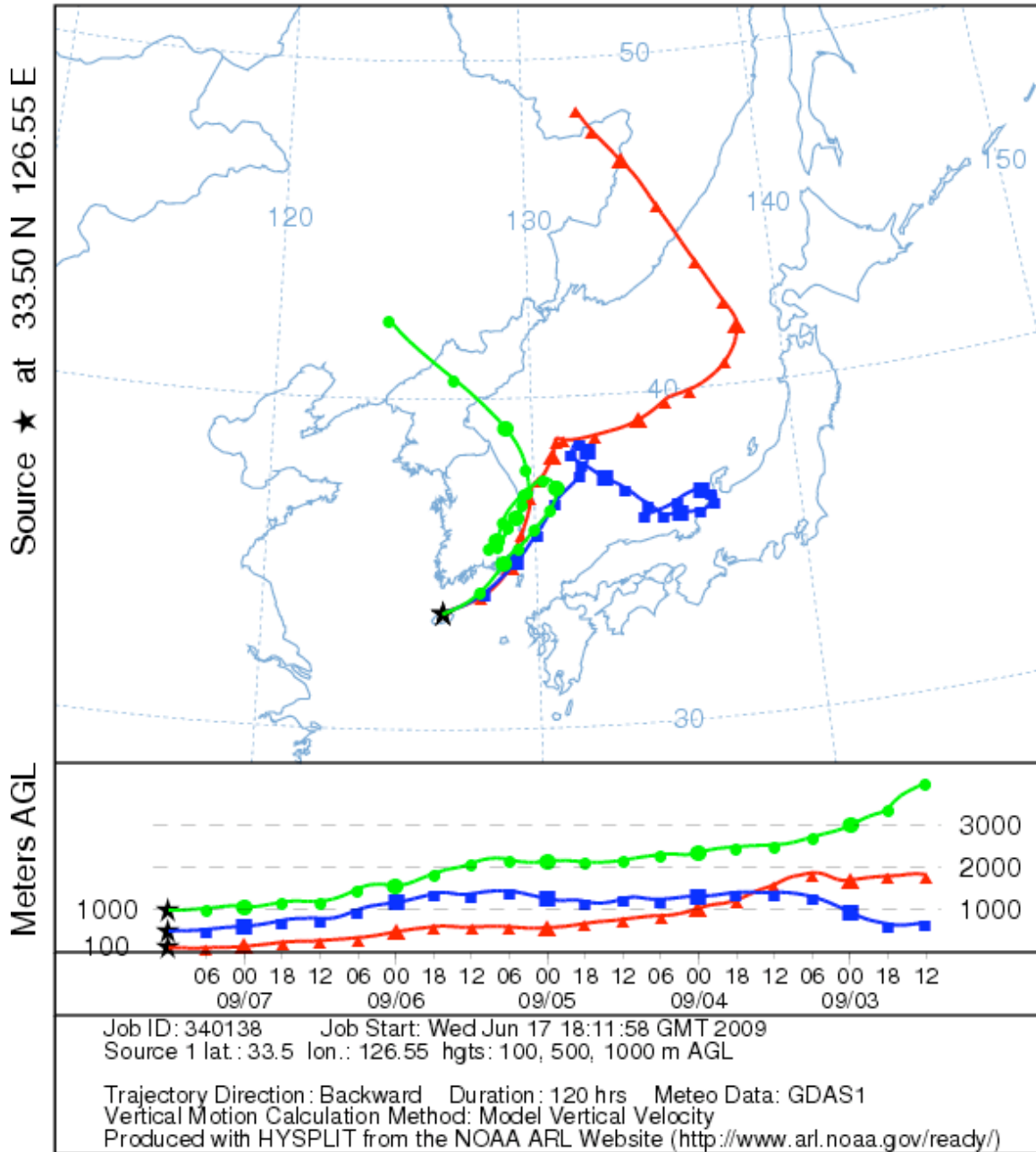


NOAA HYSPLIT MODEL  
 Backward trajectories ending at 1200 UTC 06 Sep 08  
 GDAS Meteorological Data





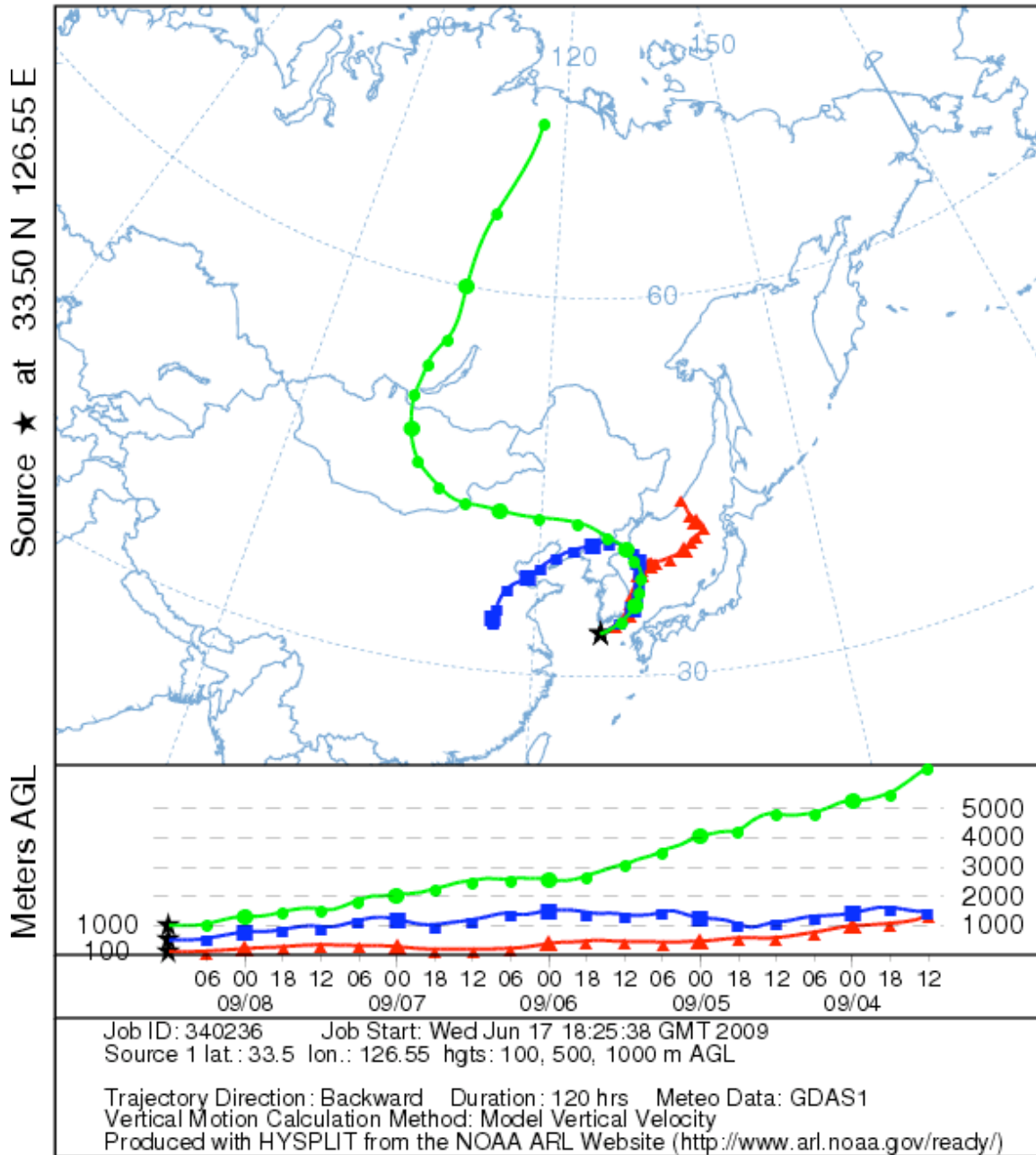
NOAA HYSPLIT MODEL  
 Backward trajectories ending at 1200 UTC 07 Sep 08  
 GDAS Meteorological Data



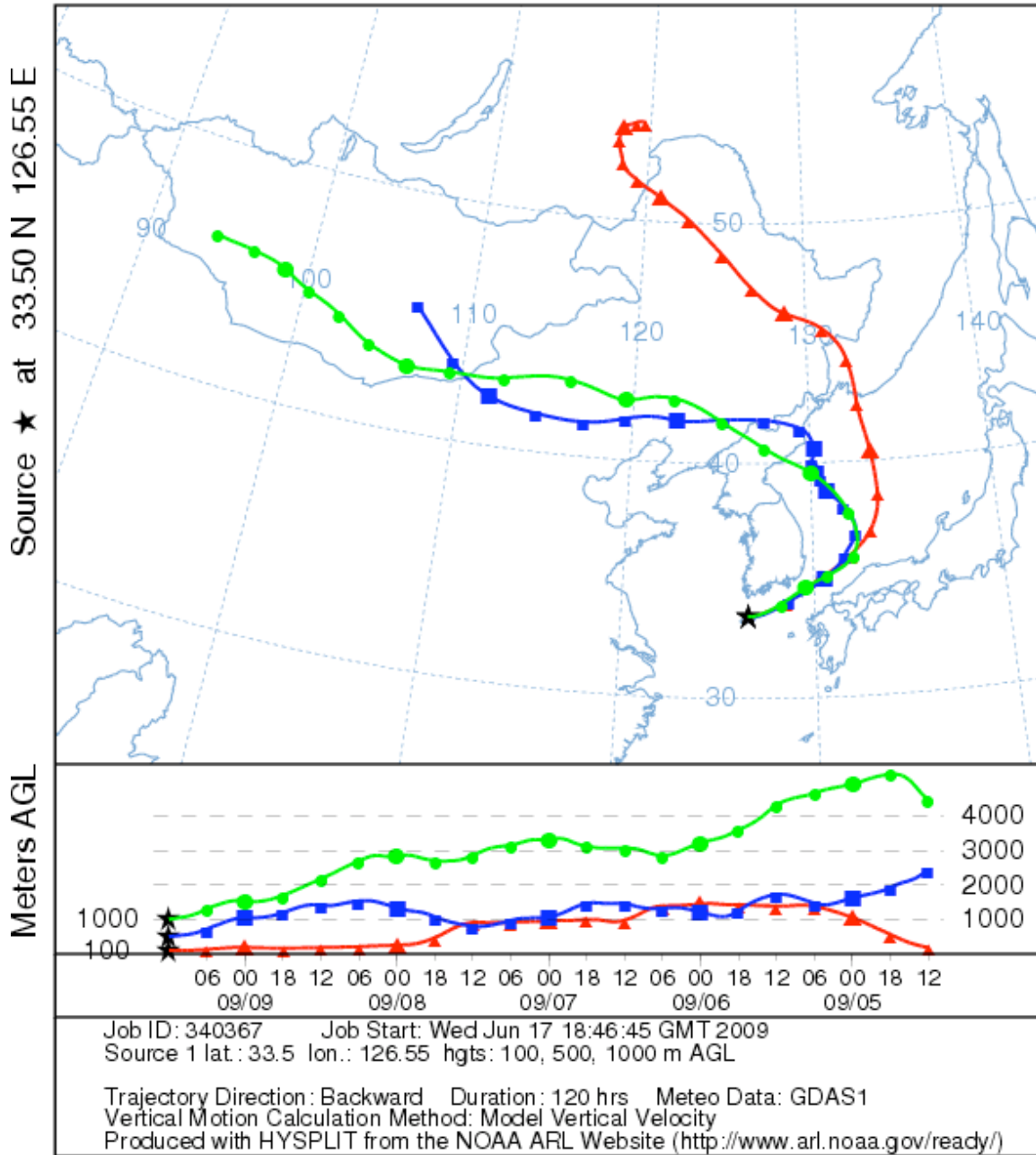


Episode 5, 3-14 September 2008.

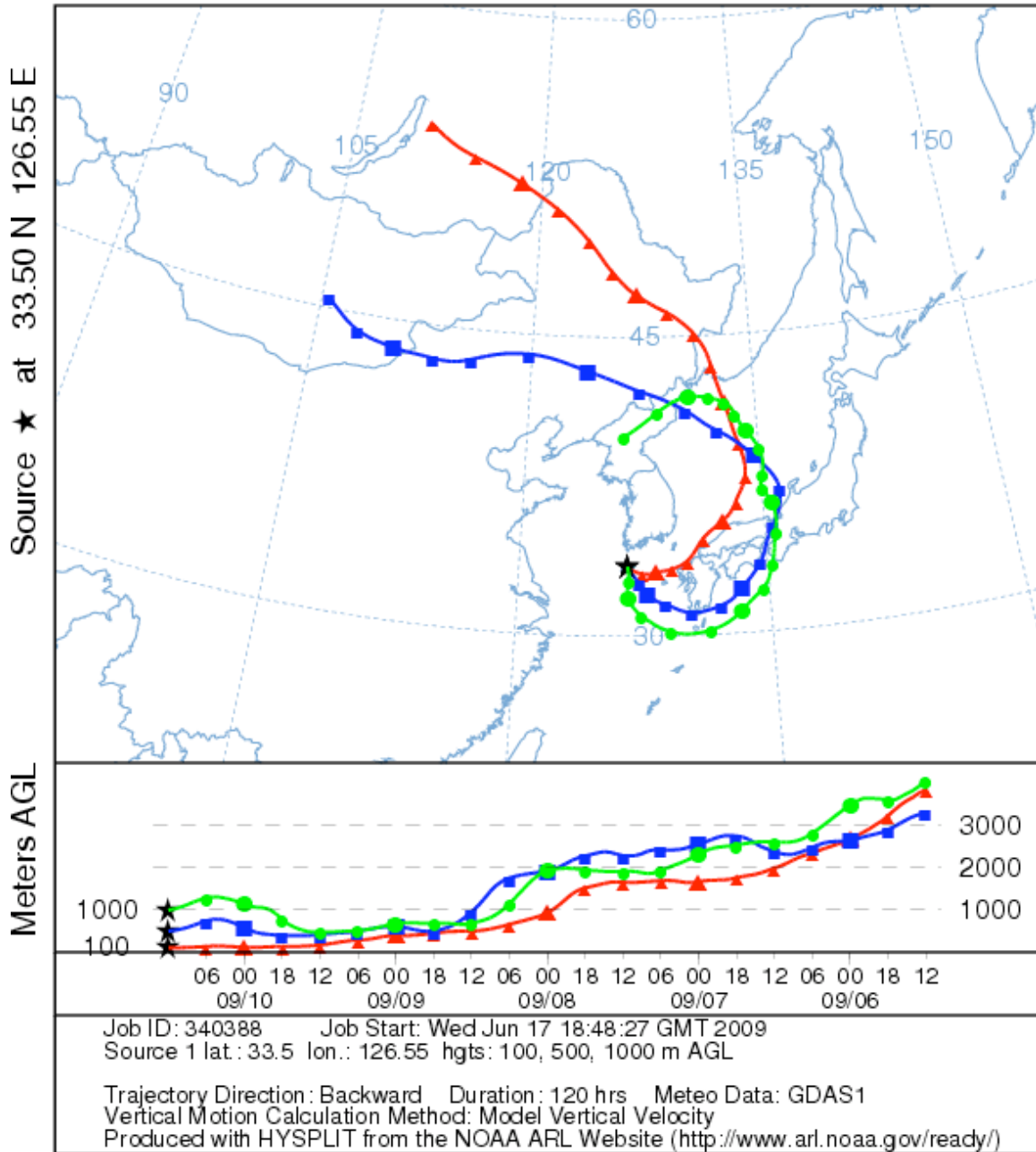
NOAA HYSPLIT MODEL  
Backward trajectories ending at 1200 UTC 08 Sep 08  
GDAS Meteorological Data



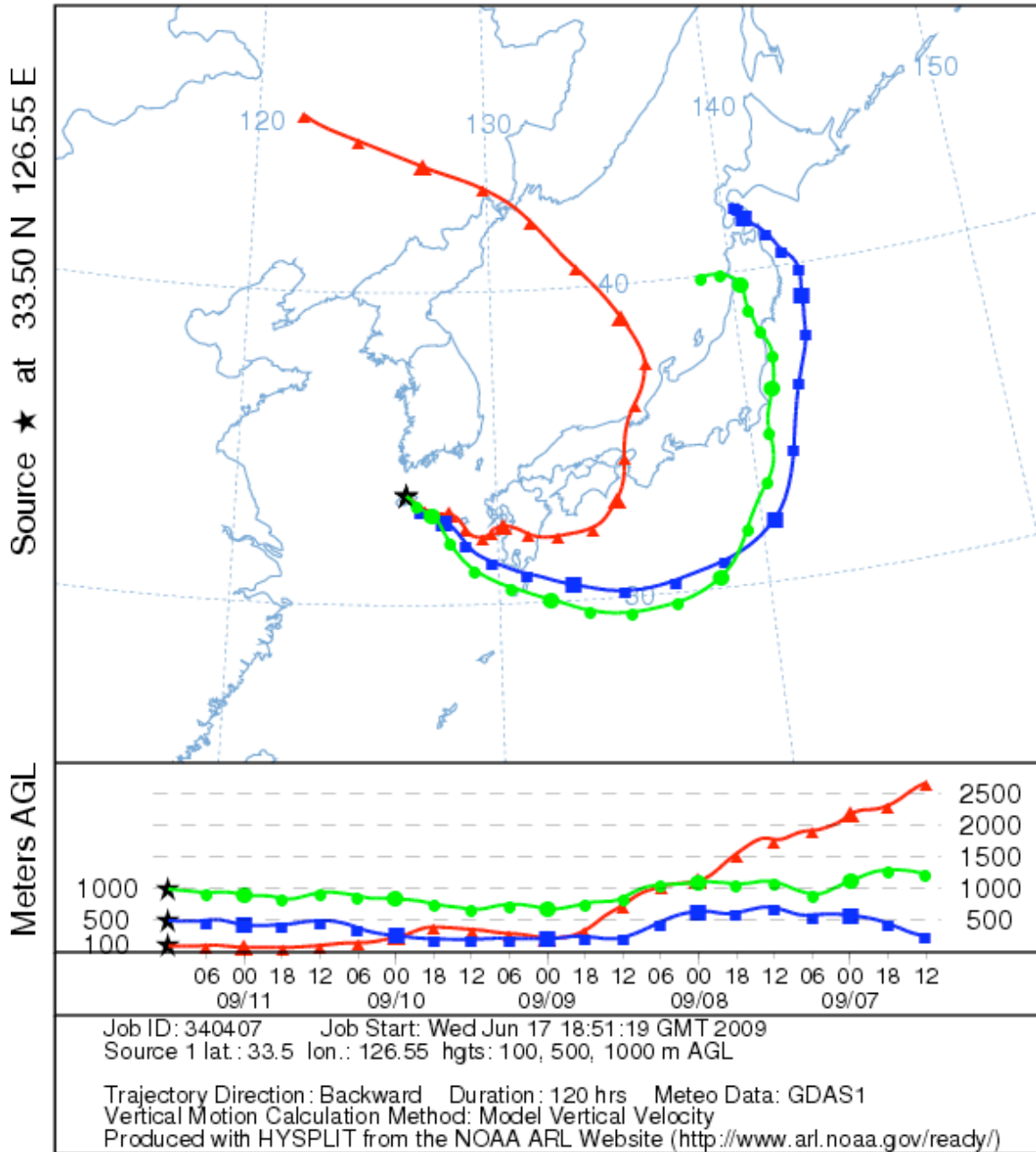
NOAA HYSPLIT MODEL  
 Backward trajectories ending at 1200 UTC 09 Sep 08  
 GDAS Meteorological Data



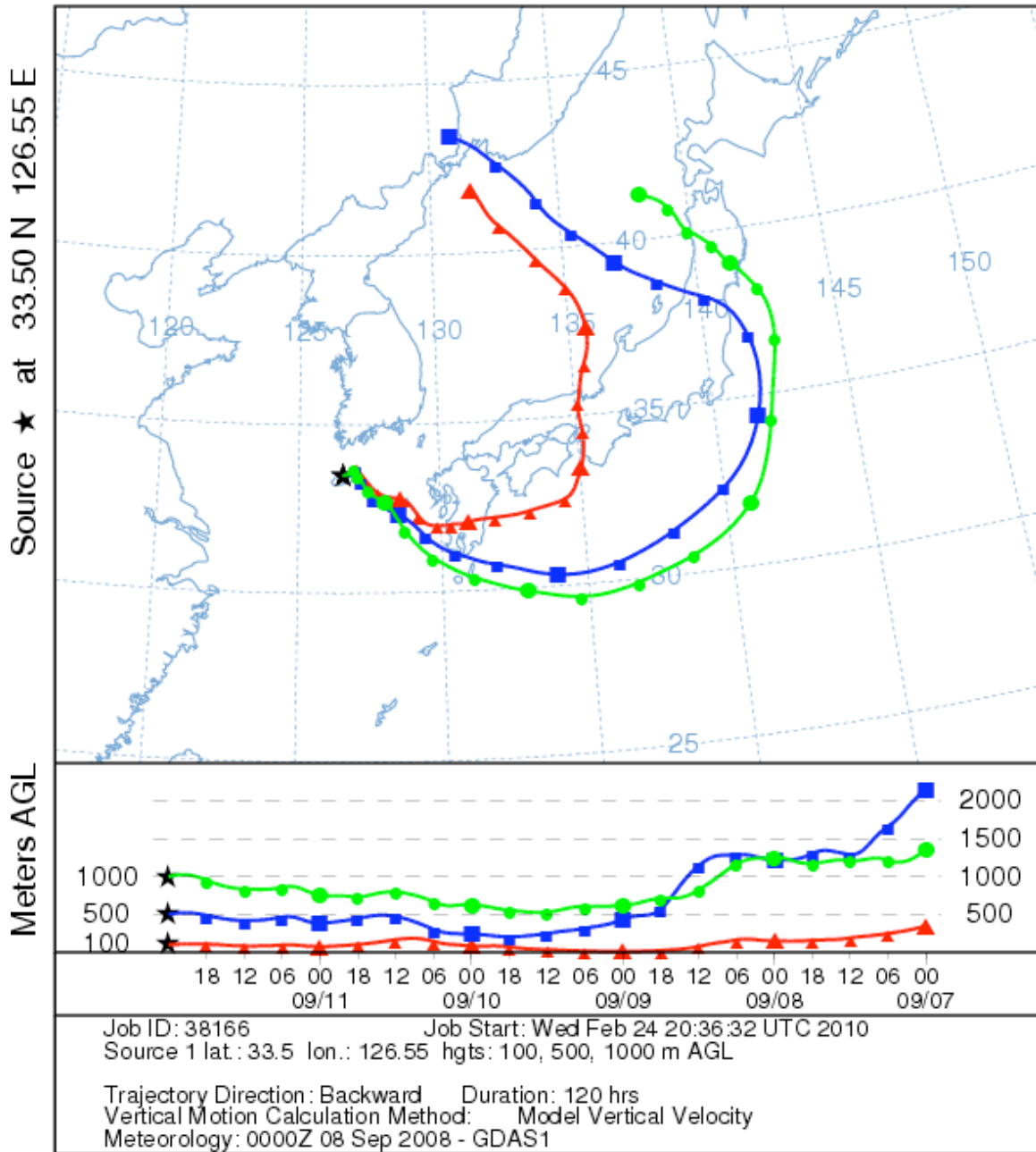
NOAA HYSPLIT MODEL  
 Backward trajectories ending at 1200 UTC 10 Sep 08  
 GDAS Meteorological Data



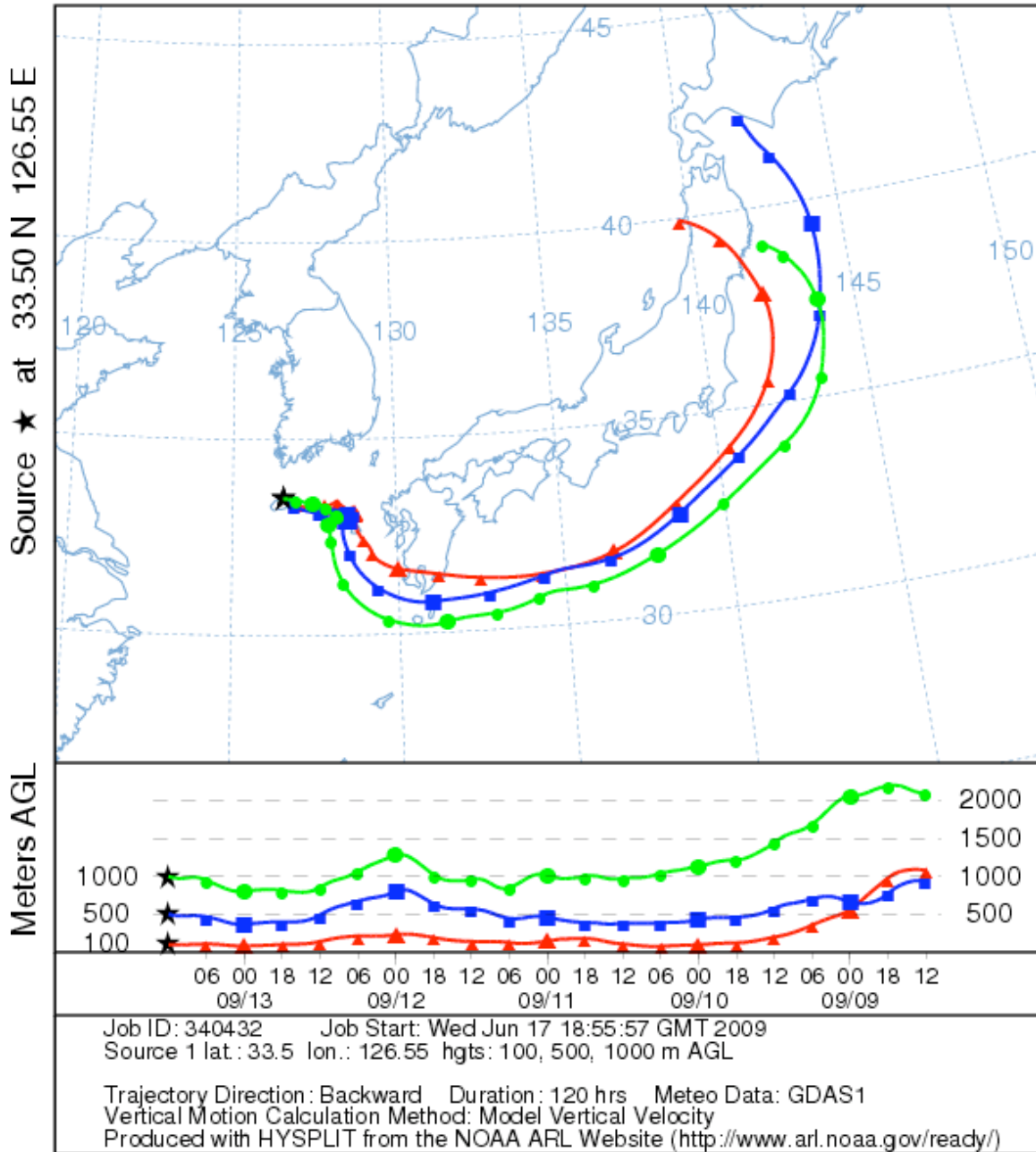
NOAA HYSPLIT MODEL  
 Backward trajectories ending at 1200 UTC 11 Sep 08  
 GDAS Meteorological Data



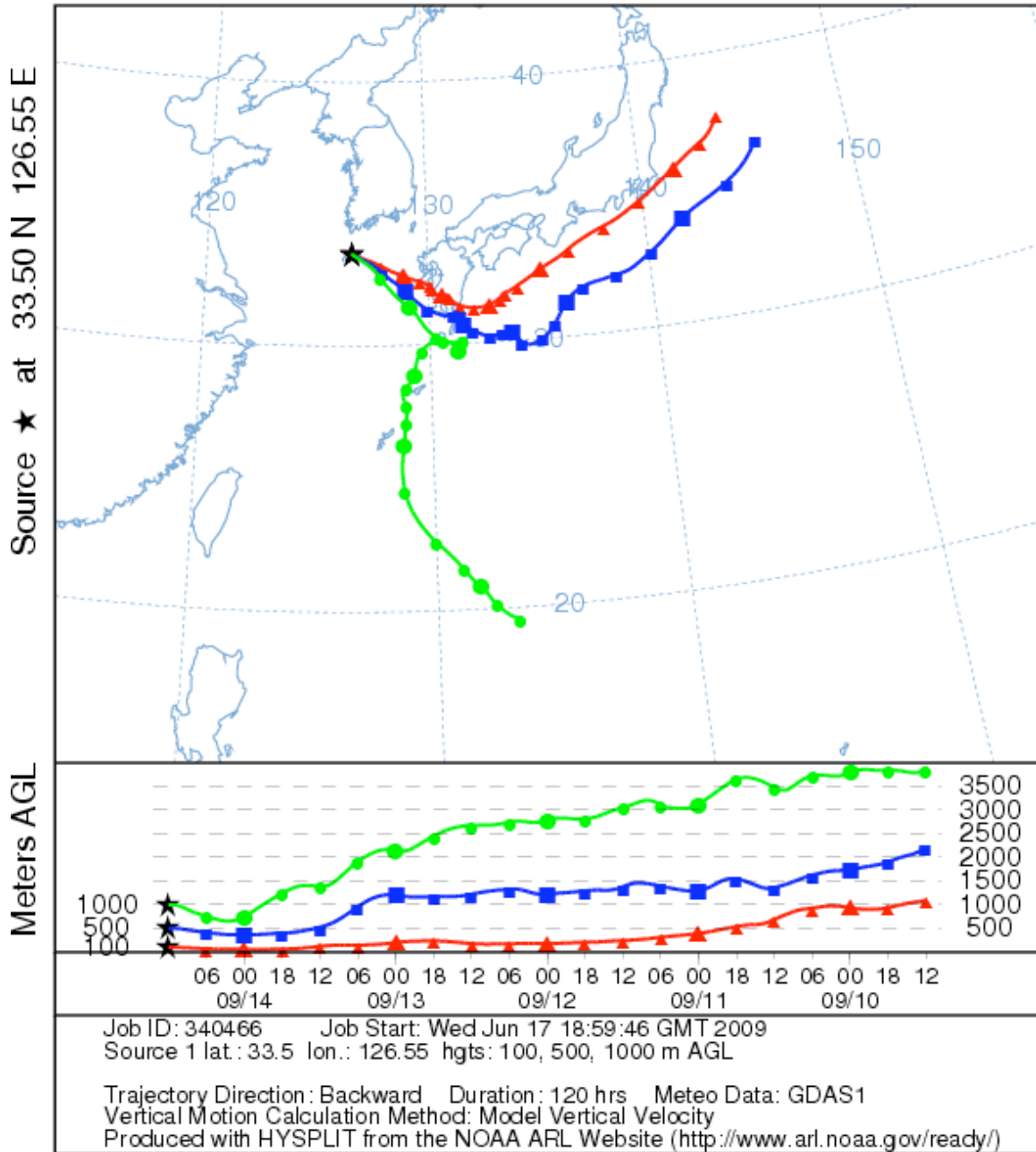
NOAA HYSPLIT MODEL  
 Backward trajectories ending at 0000 UTC 12 Sep 08  
 GDAS Meteorological Data



NOAA HYSPLIT MODEL  
 Backward trajectories ending at 1200 UTC 13 Sep 08  
 GDAS Meteorological Data

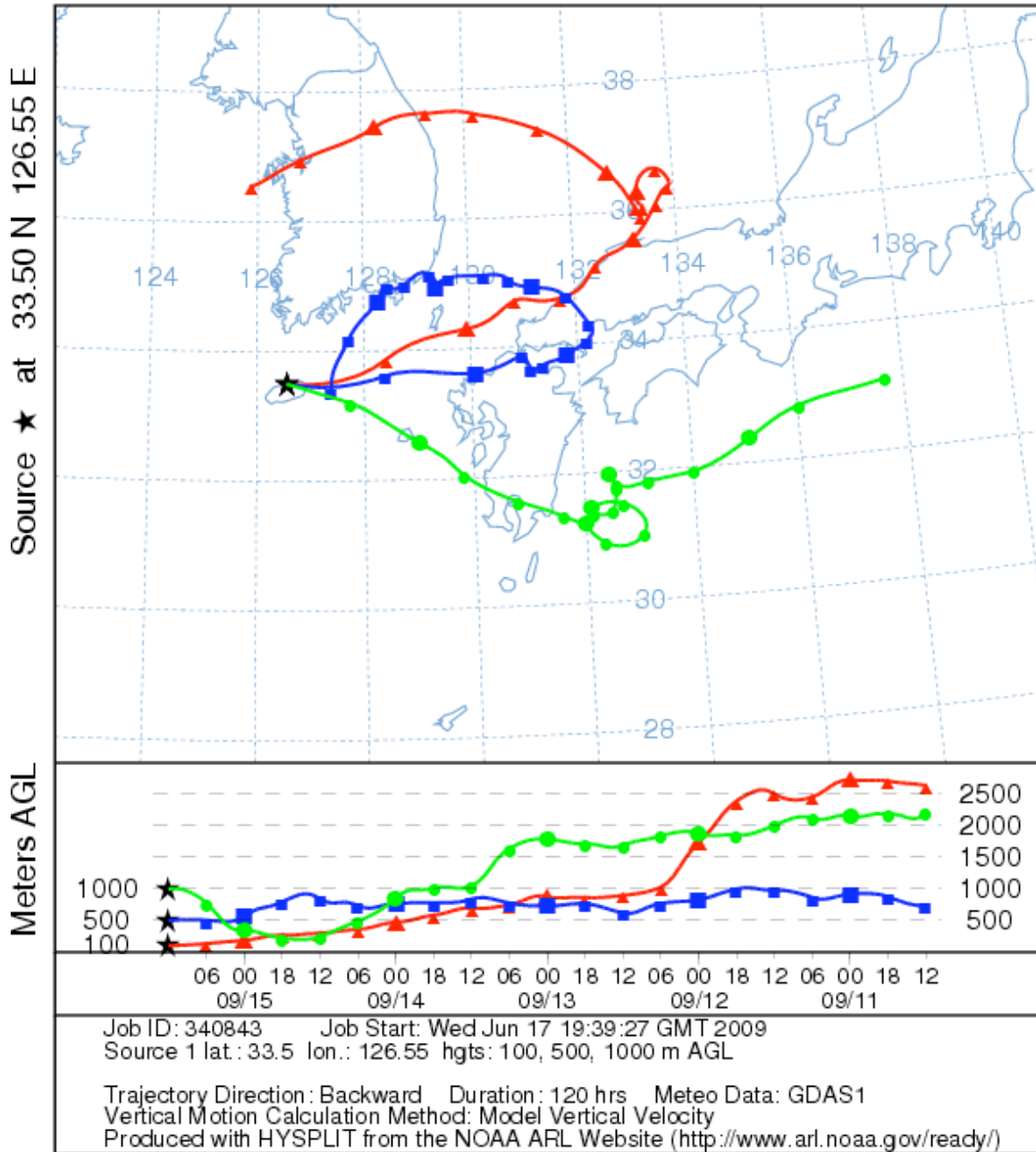


NOAA HYSPLIT MODEL  
 Backward trajectories ending at 1200 UTC 14 Sep 08  
 GDAS Meteorological Data



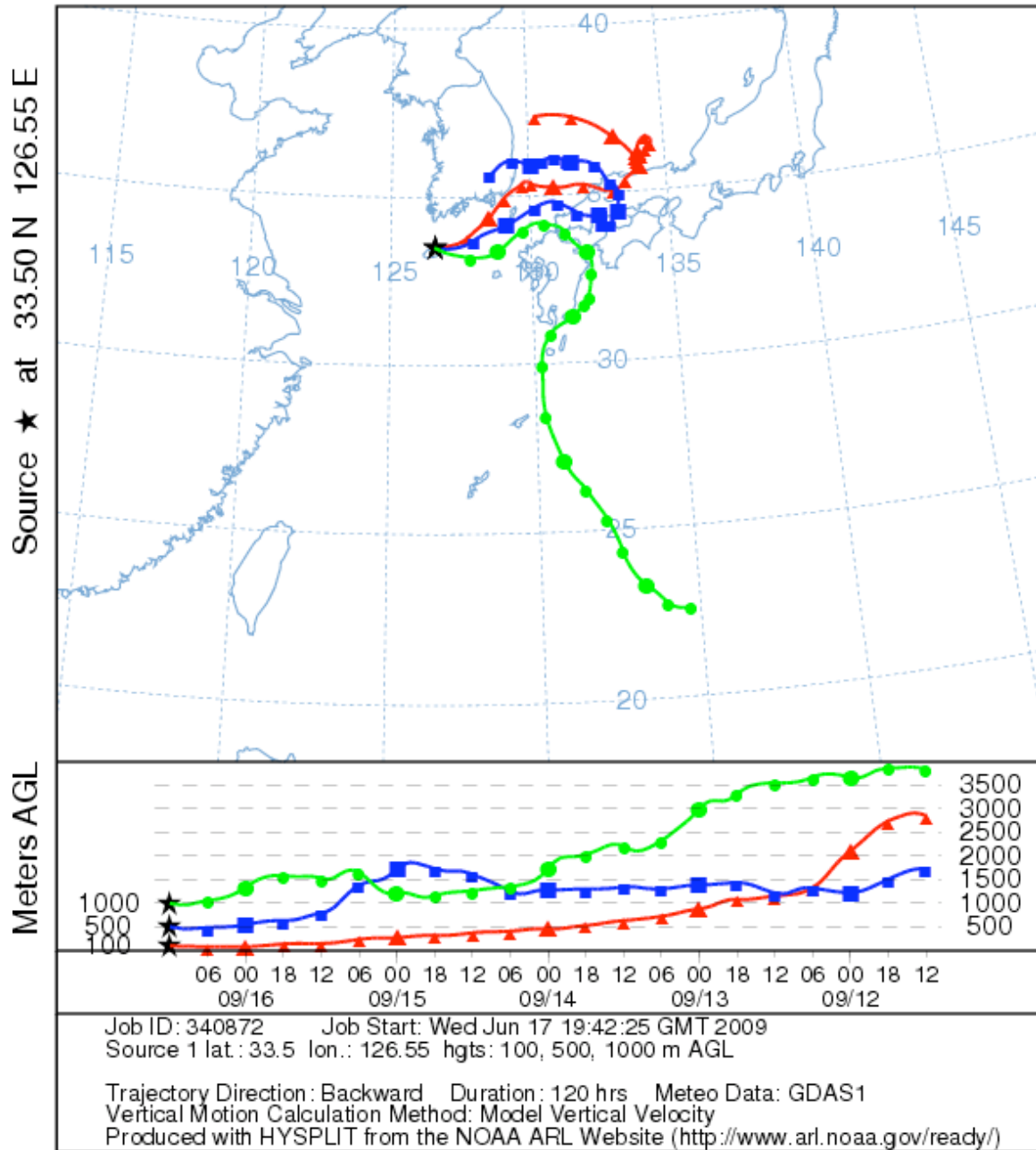


NOAA HYSPLIT MODEL  
 Backward trajectories ending at 1200 UTC 15 Sep 08  
 GDAS Meteorological Data

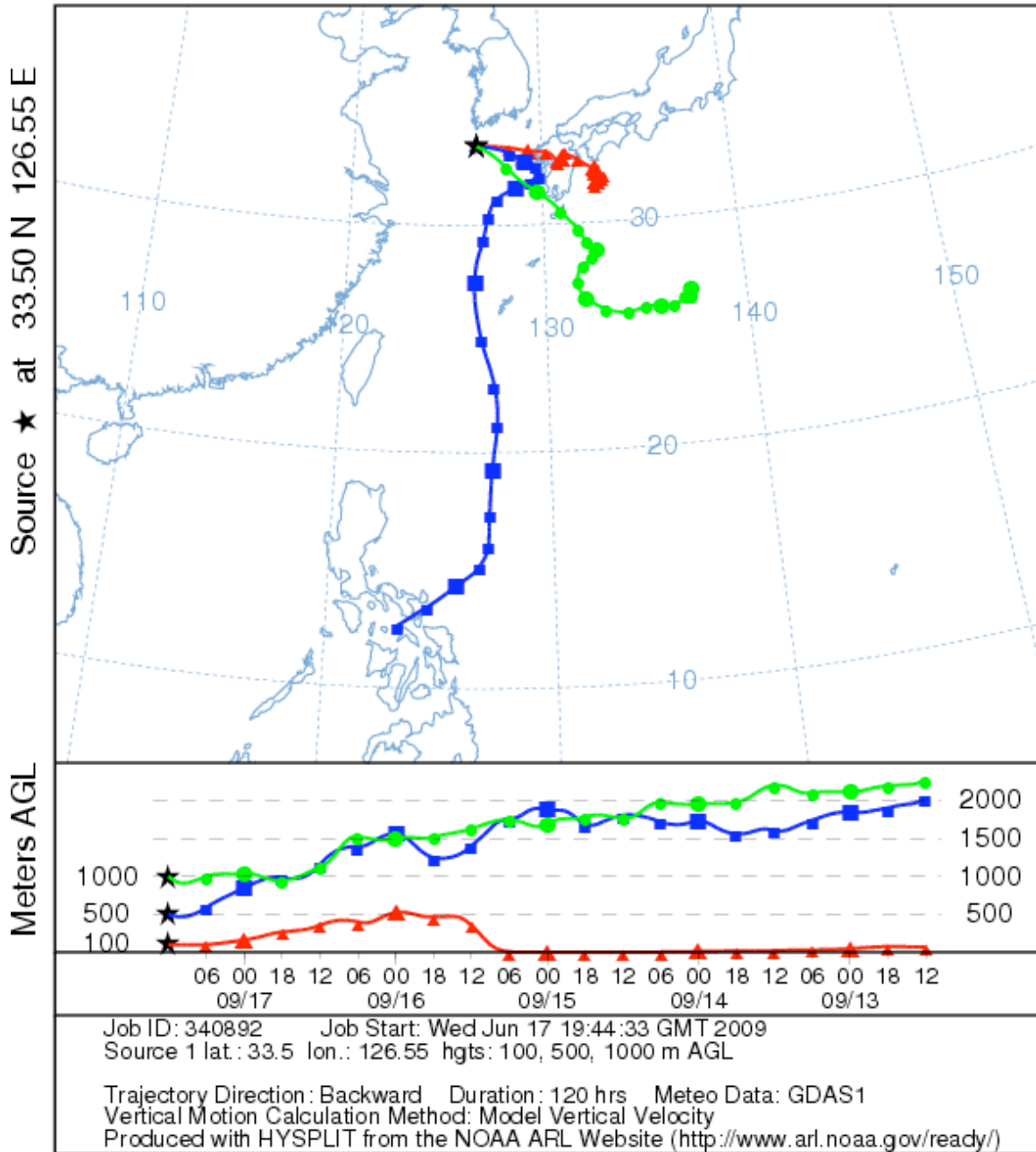


**Episode 6, 16 – 20 September 2008.**

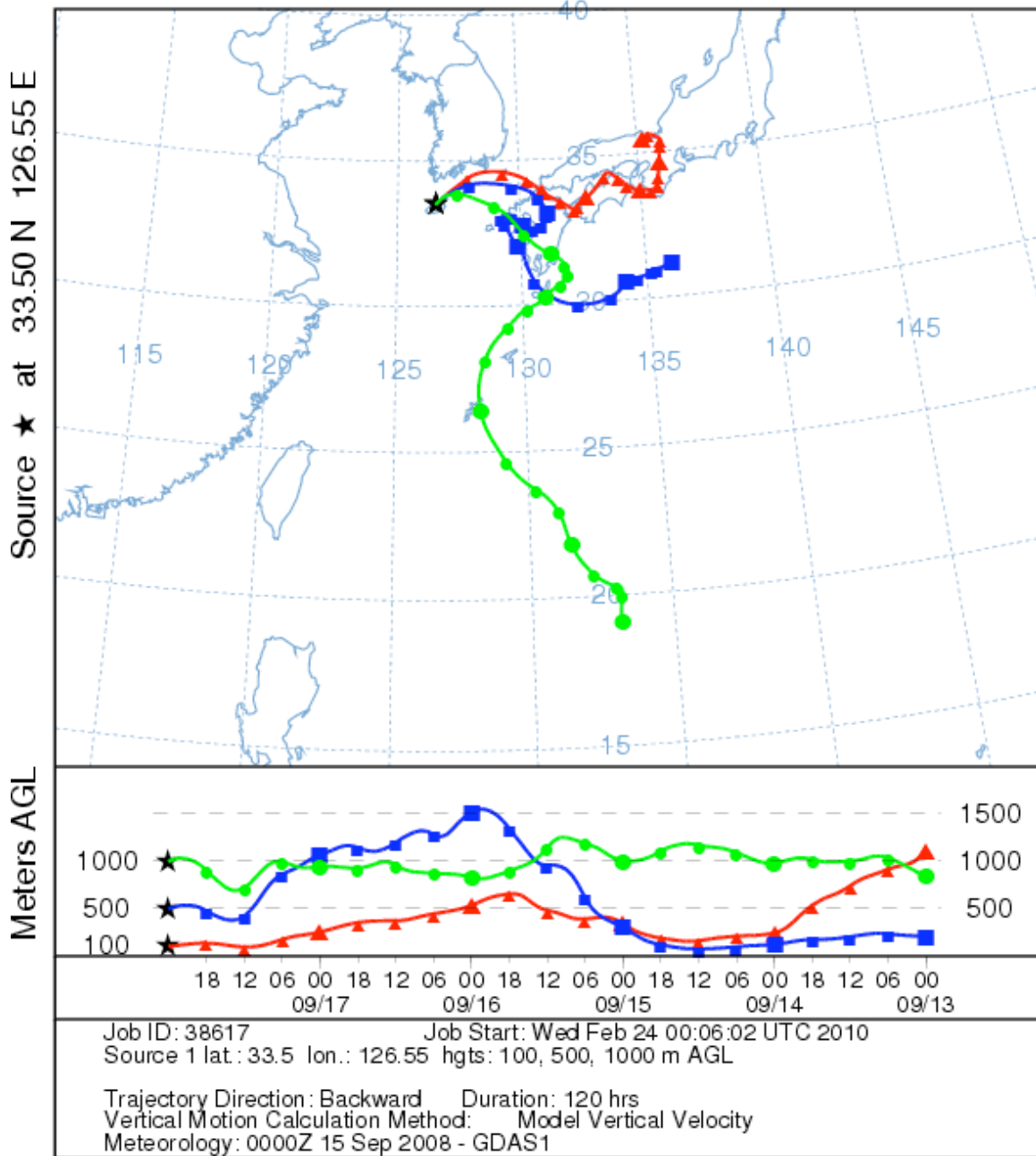
NOAA HYSPLIT MODEL  
Backward trajectories ending at 1200 UTC 16 Sep 08  
GDAS Meteorological Data



NOAA HYSPLIT MODEL  
 Backward trajectories ending at 1200 UTC 17 Sep 08  
 GDAS Meteorological Data

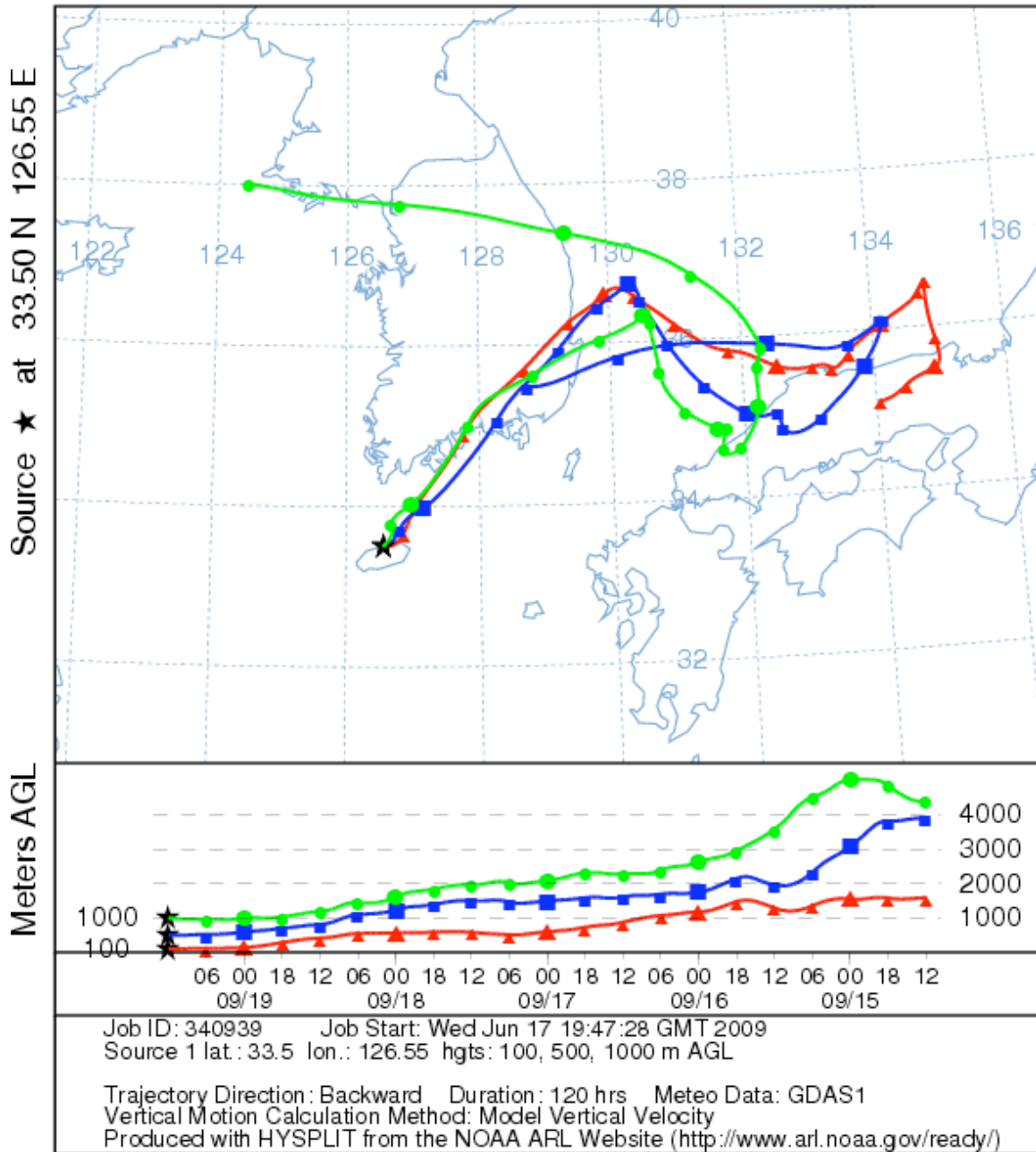


NOAA HYSPLIT MODEL  
 Backward trajectories ending at 0000 UTC 18 Sep 08  
 GDAS Meteorological Data

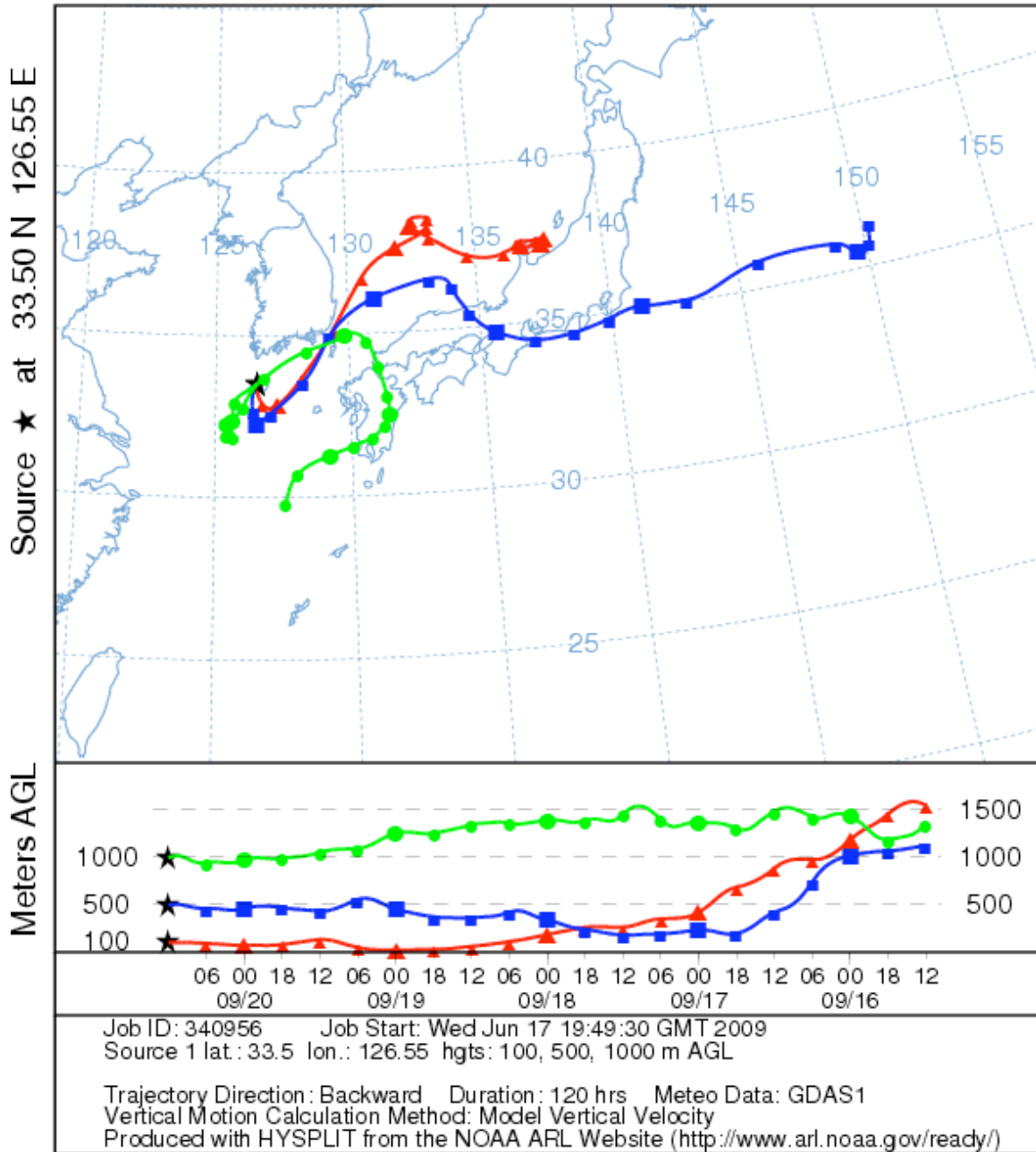


Episode 6, 17-21 September 2008.

NOAA HYSPLIT MODEL  
Backward trajectories ending at 1200 UTC 19 Sep 08  
GDAS Meteorological Data

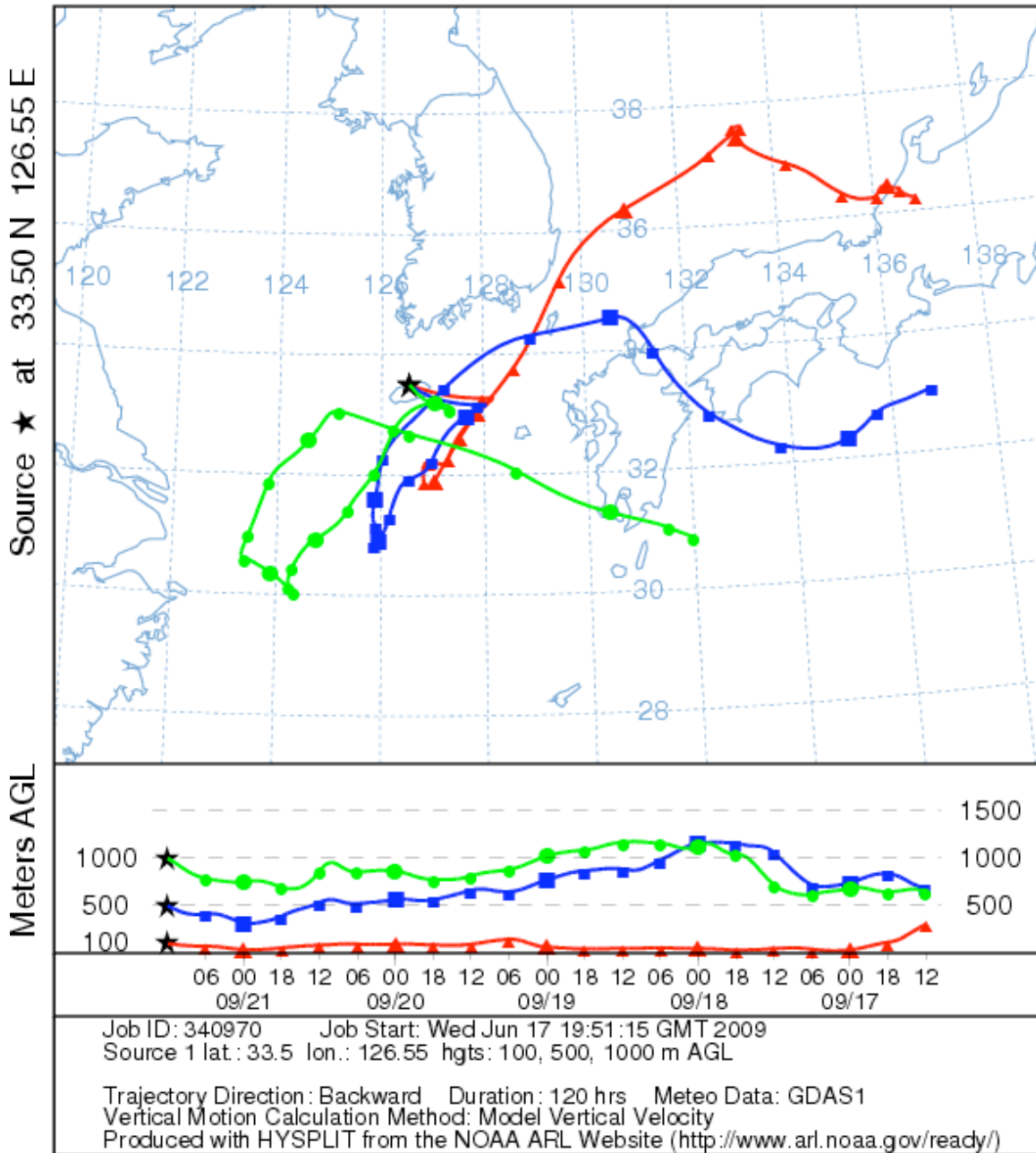


NOAA HYSPLIT MODEL  
 Backward trajectories ending at 1200 UTC 20 Sep 08  
 GDAS Meteorological Data



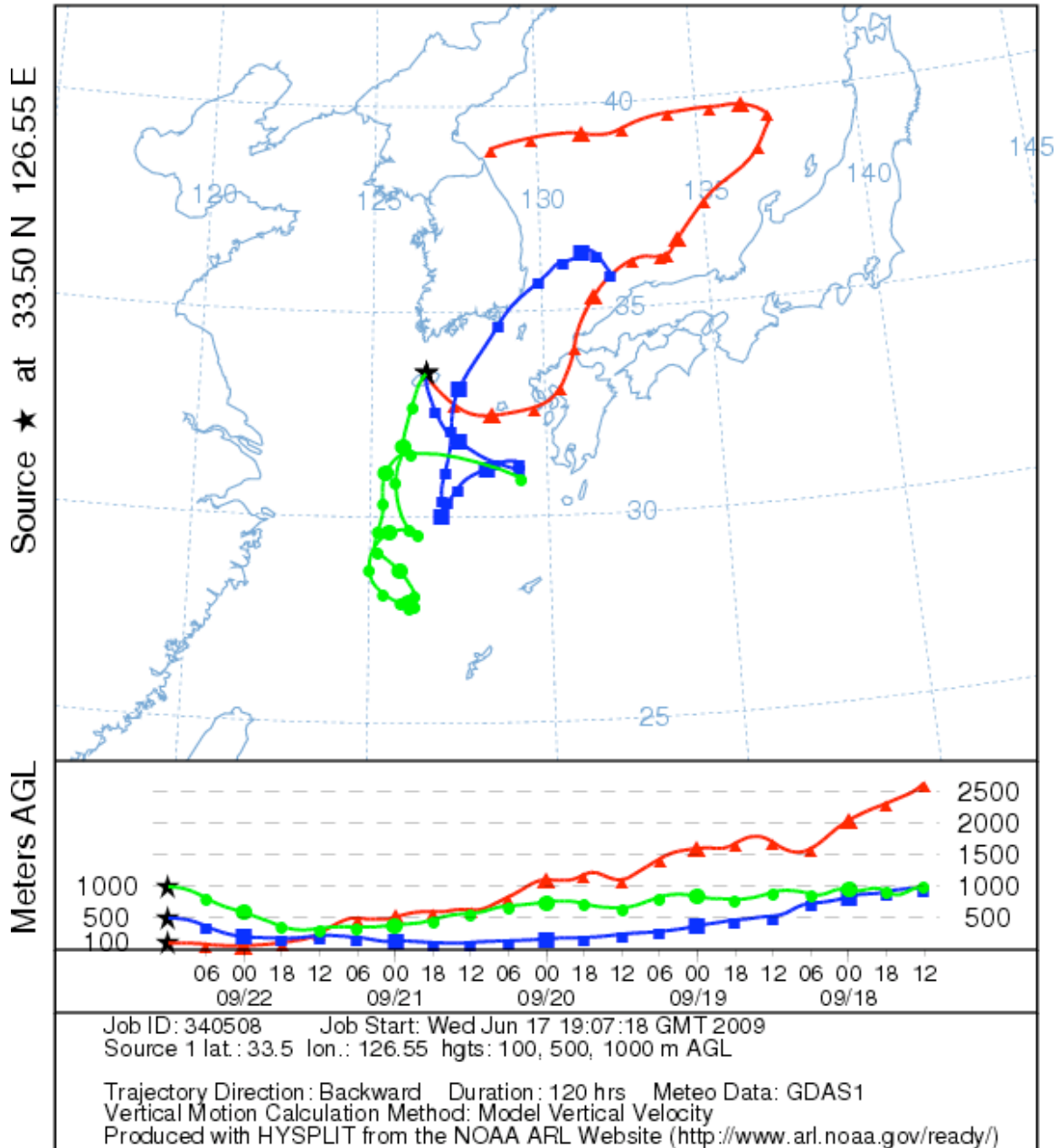
**Episode 7, 21 - 25 September 2008.**

NOAA HYSPLIT MODEL  
Backward trajectories ending at 1200 UTC 21 Sep 08  
GDAS Meteorological Data

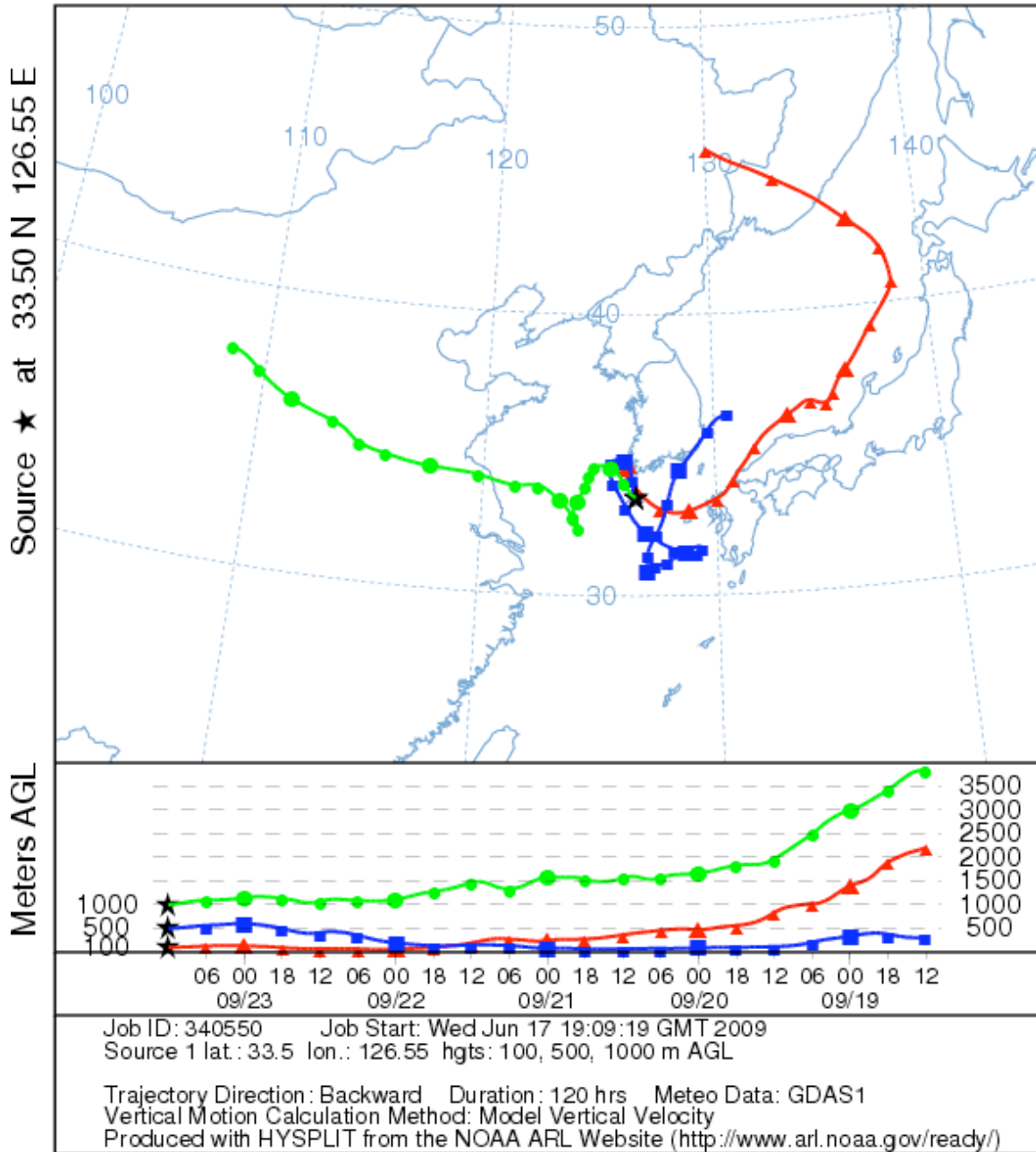




NOAA HYSPLIT MODEL  
 Backward trajectories ending at 1200 UTC 22 Sep 08  
 GDAS Meteorological Data

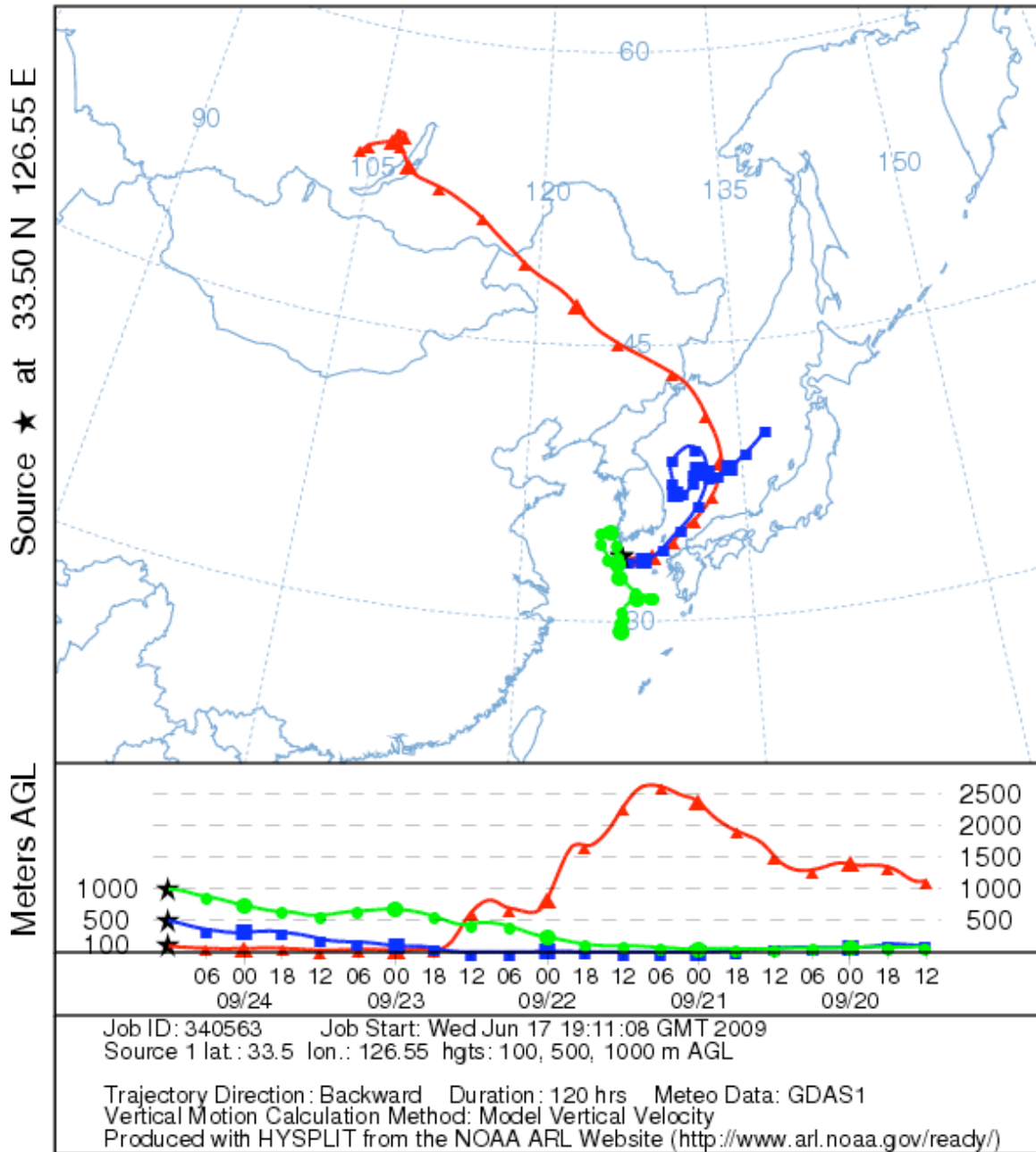


NOAA HYSPLIT MODEL  
 Backward trajectories ending at 1200 UTC 23 Sep 08  
 GDAS Meteorological Data

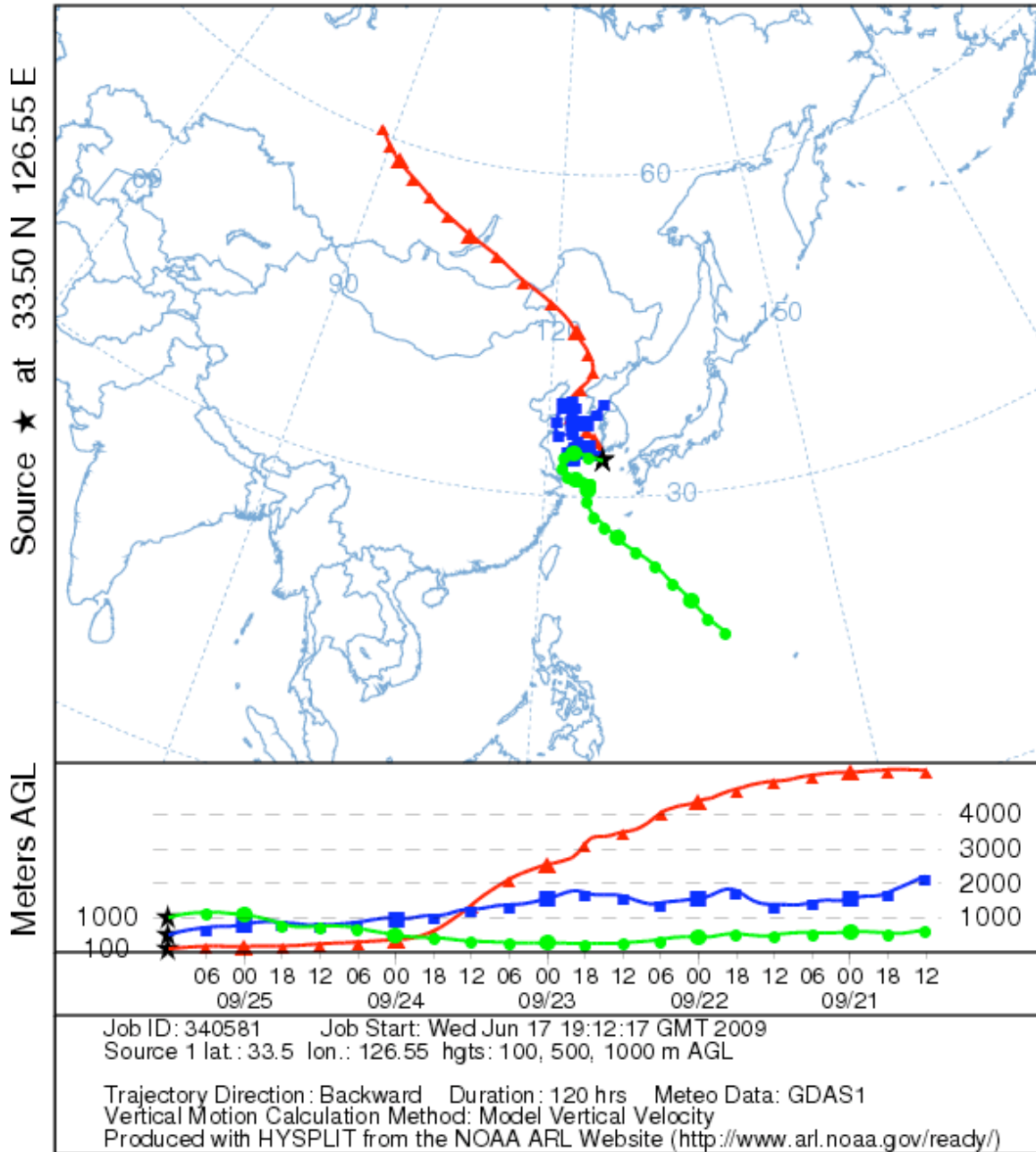


Episode 7, 22-25 September 2008.

NOAA HYSPLIT MODEL  
Backward trajectories ending at 1200 UTC 24 Sep 08  
GDAS Meteorological Data

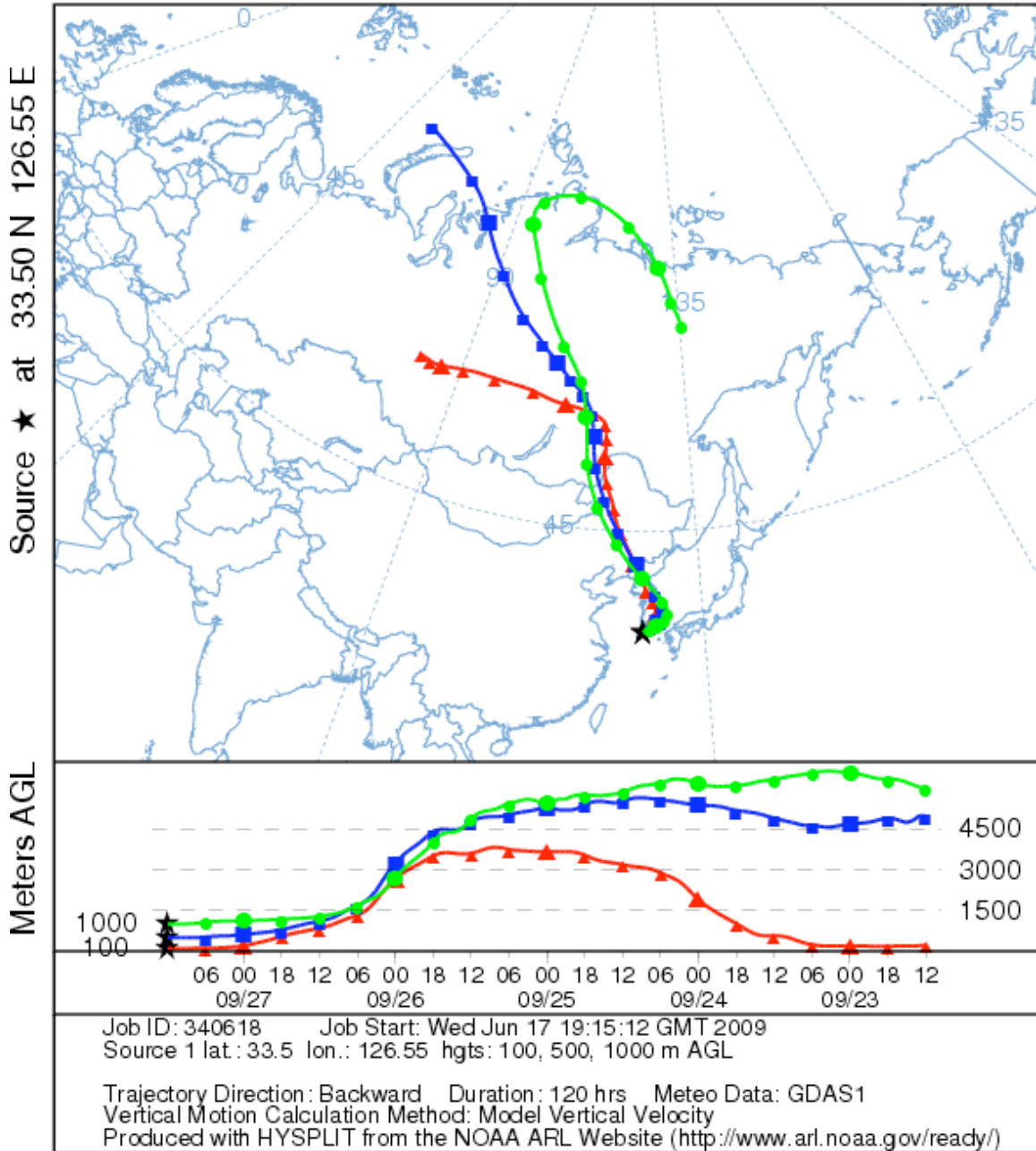


NOAA HYSPLIT MODEL  
 Backward trajectories ending at 1200 UTC 25 Sep 08  
 GDAS Meteorological Data

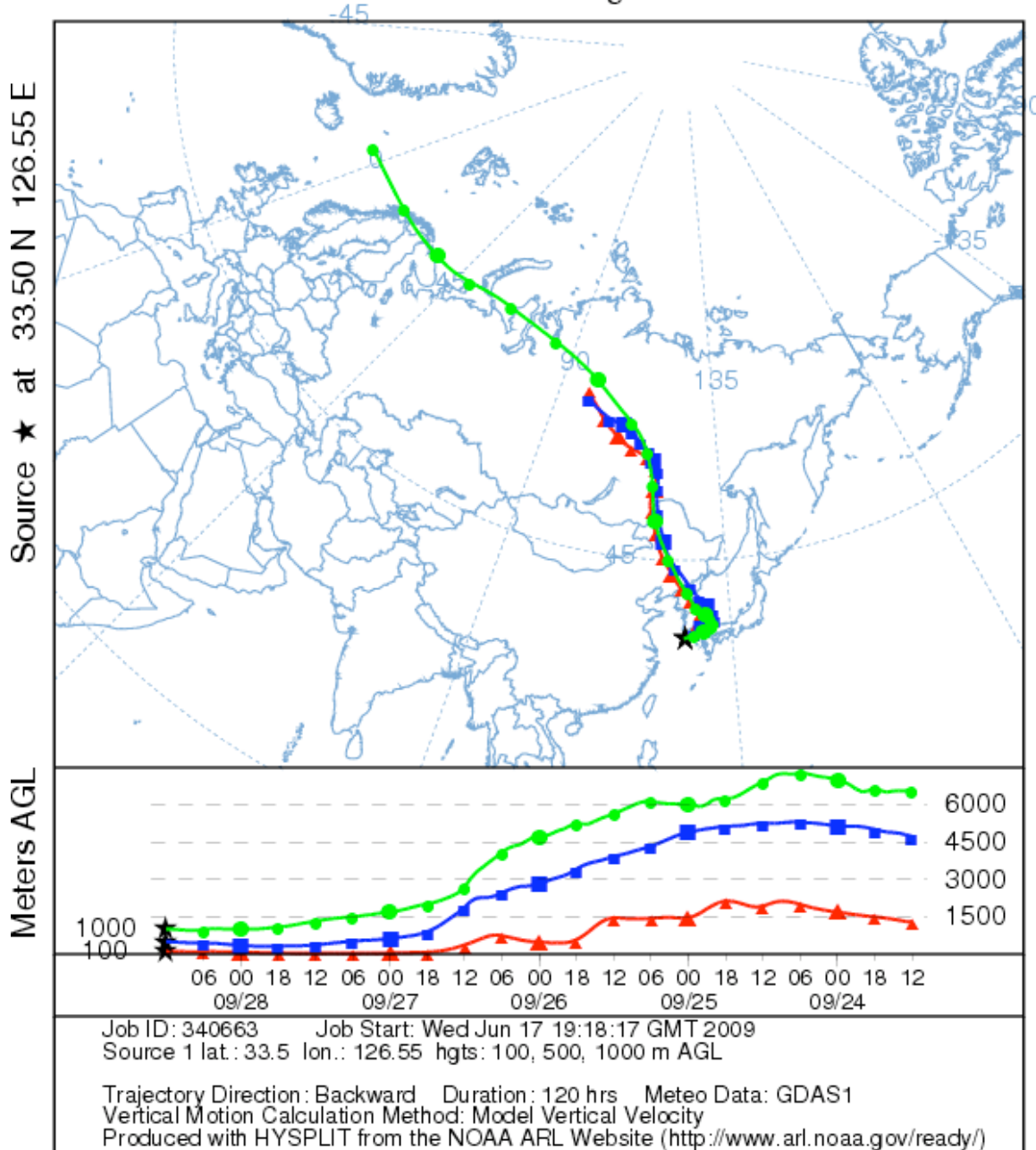


**Episode 8, 27 – 29 September 2008.**

NOAA HYSPLIT MODEL  
Backward trajectories ending at 1200 UTC 27 Sep 08  
GDAS Meteorological Data

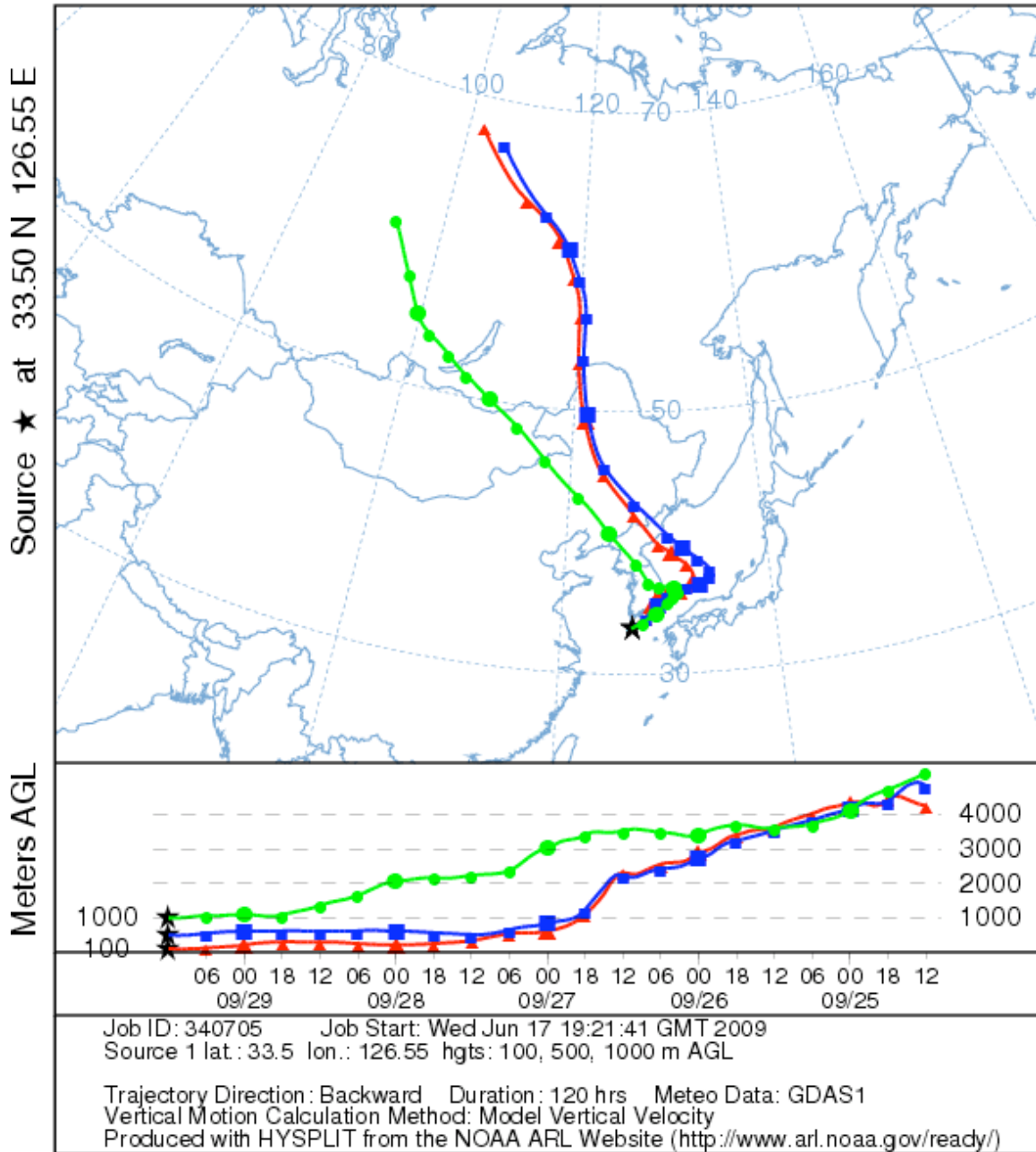


NOAA HYSPLIT MODEL  
 Backward trajectories ending at 1200 UTC 28 Sep 08  
 GDAS Meteorological Data





NOAA HYSPLIT MODEL  
 Backward trajectories ending at 1200 UTC 29 Sep 08  
 GDAS Meteorological Data





NOAA HYSPLIT MODEL  
 Backward trajectories ending at 1200 UTC 30 Aug 08  
 GDAS Meteorological Data

